RIBOFLAVIN LYASE: AN INTRIGUING FLAVOENZYME INVOLVED IN RIBOFLAVIN DEGRADATION

A Dissertation

by

YINDRILA CHAKRABARTY

Submitted to the Office of Graduate and Professional Studies of
Texas A&M University
in partial fulfillment of the requirements for the degree of

DOCTOR OF PHILOSOPHY

Chair of Committee,	Tadhg P. Begley
Committee Members,	Frank M. Raushel
	Coran M. H. Watanabe
	Margaret E. Glasner
Head of Department,	Simon W. North

August 2016

Major Subject: Chemistry

ABSTRACT

Little is known about cofactor catabolism in the literature. Pyridoxamine, thiamin, heme and nicotinic acid degradation pathways are the only well-characterized catabolic pathways. In 2012 the Begley lab isolated *Microbacterium maritypicum* G10 strain, from DSM Nutritional Products, Germany, that can degrade riboflavin (Vitamin B_2). Subsequent screening with the cosmid library made from the strain has led to the identification of the riboflavin catabolic gene cluster. One of the gene cluster products - the enzyme riboflavin lyase (RcaE), is a flavoenzyme that catalyzes the oxidative degradation of riboflavin to lumichrome and ribose. The enzymes encoded by the other genes of the cluster have been predicted by bioinformatics to include a flavokinase (RcaA), a flavin reductase (RcaB) and a ribokinase (RcaD). These enzymes have been reconstituted individually. The main focus of this work is the detailed mechanistic analysis of riboflavin lyase (RcaE).

Reconstitution of the enzyme RcaE requires reduced FMN as the cofactor with riboflavin and oxygen acting as substrates. Thus, RcaE serves as the first example where the reduced cofactor FMN catalyzes the breakdown of a second flavin molecule, riboflavin. In this degradation, the participation of a superoxide radical, derived from reduced FMN reacting with molecular oxygen at the enzyme active site**,** has been established by direct superoxide incorporation experiments. RcaE is a unique enzyme that uptakes superoxide directly and utilizes it to degrade the substrate.

Till date, there is no report in the literature of an enzyme where a superoxide radical abstracts a hydrogen atom from the substrate. Based on our results with the

radical trap cyclopropylmethylflavin, we propose that the superoxide radical mediates a one electron oxidation of the substrate riboflavin, by a hydrogen atom abstraction from the C_1' position of riboflavin to form riboflavin-C_1'-radical and hydrogen peroxide. The riboflavin-C_1'-radical in a second one electron oxidation gets converted to riboflavin-C_1'-imine. Based on the LCMS experiments showing ^{18}O incorporation into the ribose from $^{18}O_2$, we further propose that the resulting imine recombines with the hydrogen peroxide at the active site to give riboflavin-C_1'-hydroperoxide. Finally, through reduction to riboflavin-C_1'-hydroxide and subsequent hydrolysis, the riboflavin-C_1'-hydroperoxide converts to lumichrome and ribose.

DEDICATION

My thesis is devoted to my family and my friends. This journey would not have been possible without the constant support of Puchi and Kuttus in particular. My time here would have been tough without Anurina who has always provided me with the right advice in times of crisis, without Isita who has always made me feel like family both in and outside of the lab, without Piyali, Ananya, Randara and Sarah who have been my support system when I needed. I am thankful to my friends Indranil, Monojit, Anirban, Rajat and Shyamalendu for being a part of my endeavor pulling me through its highs and lows. Most importantly, I am indebted to my fiancé Piku for his love and selfless assistance in overcoming all the hurdles that I was faced with.

This thesis is dedicated to my Mother (Ma)…….

ACKNOWLEDGEMENTS

I would like to acknowledge my research advisor Dr. Tadhg P. Begley for his continuous encouragement and mentorship. This work would not have been possible without the umpteen opportunities for research that he has provided me with in the lab.

I would like to thank my committee chair, Dr. Tadhg P. Begley, and my committee members, Dr. Frank Raushel, Dr. Coran Watanabe and Dr. Margaret Glasner, for their guidance and support throughout the course of this research.

I would like to thank all the current members of the Begley group and former member Dr. Yiquan Liu and Dr. Lisa Cooper for their support and for making my time here memorable. I would also like to extend my gratitude to Indranil Malik and the former Begley lab members Dr. Dinesh Simkhada and Dr. Benjamin Philmus for their enriching suggestions and feedback on my research.

I would like to acknowledge the contributions of the former Begley Lab members Dr. Hui Xu and Dr. Benjamin Philmus in the isolation and characterization of the catabolic gene cluster of riboflavin, current lab member Dhananjay Bhandari for his riboflavin degradation studies in cell cultures, former member Dr. Angad Mehta for characterization of the sugar product from riboflavin degradation, current lab member Dr. Sameh Abdelwahed and Prem Chanani sharing with me riboflavin analogs that they have synthesized.

I am thankful to Jeremy Wood from The Sacchettini Lab for the collaboration to obtain and solve the crystal structure for the riboflavin degrading enzyme.

I am grateful for the support of my mother and father.

Finally, thanks to my fiancé for his patience and love.

NOMENCLATURE

RcaE	Riboflavin lyase
RcaA	Riboflavin kinase
RcaB	Flavin reductase
RcaD	Ribokinase
FMN	Flavin Mononucleotide
FAD	Flavin Adenine Dinucleotide

TABLE OF CONTENTS

Page

LIST OF FIGURES

Page

LIST OF TABLES

Page

CHAPTER I

INTRODUCTION

1.1 Riboflavin

Riboflavin (Vitamin B_2) **(1) (Figure 1)** is a water-soluble vitamin found in dairy products, meat, and dark-green vegetables .[1] It was originally isolated from milk in 1879 and was named lactochrome.[2] The biologically active forms of riboflavin **(1)** are flavin mononucleotide (FMN) **(2) (Figure 1)** and flavin adenine dinucleotide (FAD) **(3) (Figure 1)**, which participate in a variety of redox reactions in the cell.[3] Riboflavin **(1)** also forms a part of the glutathione redox cycle which defends the body against oxidative stress, specifically against oxidative injury and lipid peroxidation.[4] Riboflavin deficiency in humans, though rare, may cause anemia, skin disorders and preeclampsia in pregnant women. Deficiency of **1** also affects the metabolism of Vitamin B_6, folate, and niacin.[5]

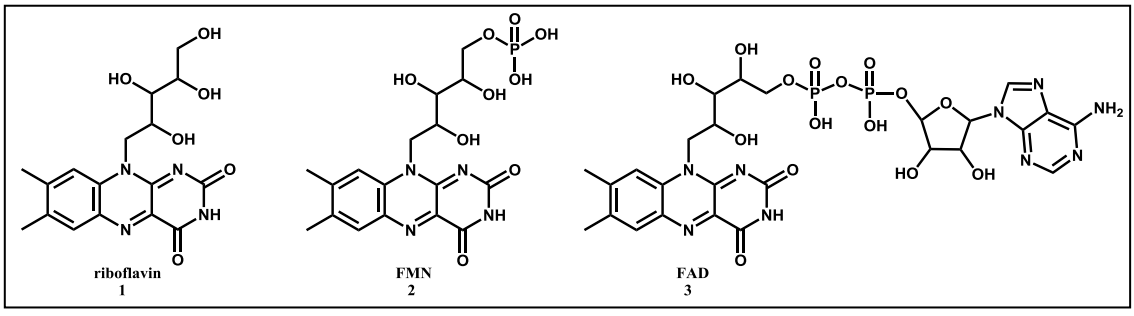

Figure 1: Structures of riboflavin and its biologically active forms FMN (2) and FAD (3)

1.2 Biosynthesis of riboflavin

Riboflavin **(1)** is biosynthesized in bacteria, fungi, yeast and plants. Humans lack riboflavin biosynthetic genes, hence uptake the vitamin from dietary sources. The

biosynthetic pathway for riboflavin is shown in Figure 2.[6] The first step in the biosynthesis of riboflavin **(1)** involves a hydrolytic ring cleavage of GTP **(4)** to form 4,5-diaminopyrimidine **(5)** with the release of formate **(6)**. Subsequent conversion of **5** to 5-amino-6-ribitylamino-2,4(1H,3H)-pyrimidinedione (**7)** is brought about by sequential side chain reduction, deamination and dephosphorylation. In fungi the reduction is followed by deamination whereas in bacteria deamination occurs first.[7] In the next step, the **7** undergoes condensation with ribulose-5-phosphate derived 3,4-dihydroxy-2-butanone-4-phosphate (**8)** through an intramolecular rearrangement accompanied by the loss of C_4 to form 6,7-dimethyl-8-ribityllumazine (**9)**.[8] The lumazine derivative then undergoes a self-disproportionation reaction giving riboflavin **(1)**.[9]

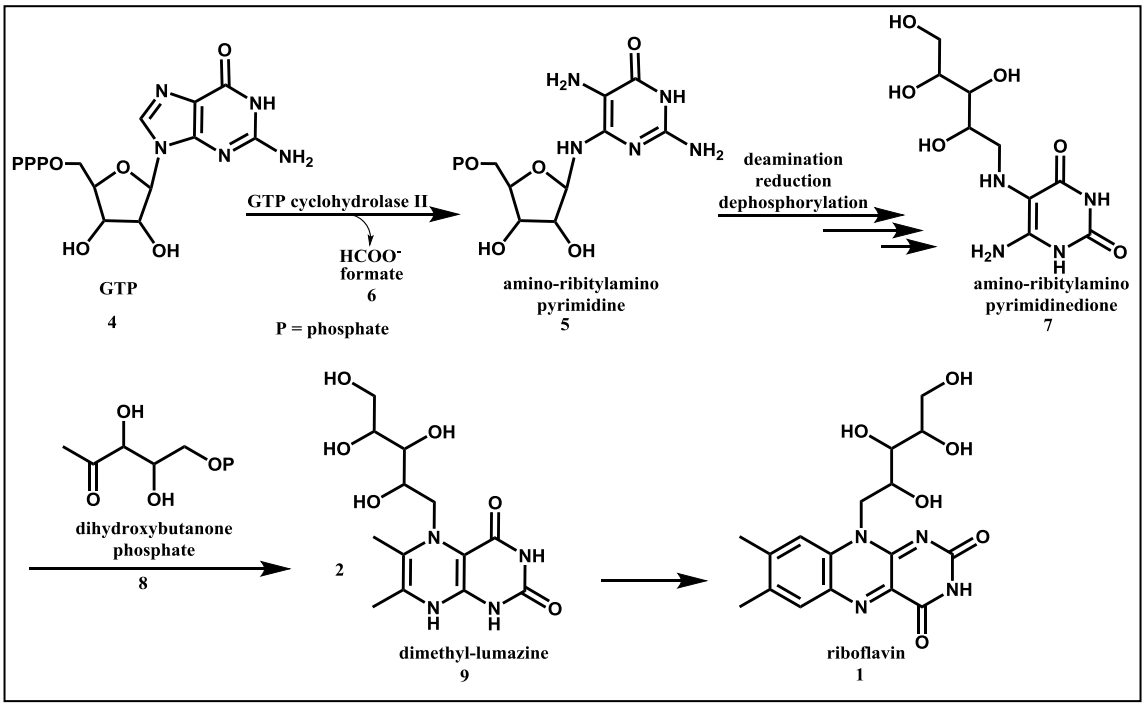

Figure 2: Biosynthetic pathway of riboflavin in microorganisms.

1.3 Riboflavin as a cofactor

After the biosynthesis or uptake of riboflavin in the cells, it is converted to its active cofactor forms FMN **(2)** and FAD **(3)** via two steps.[10] In the first step, riboflavin **(1)** is converted to FMN **(2)** by flavokinase. FMN **(2)** serves as the cofactor in some functional flavoenzymes which include NAD(P)H oxidases, chorismate synthase, alkanal monoxygenase, thymidylate synthase.[11-13] In the second step FAD synthase converts FMN **(2)** to FAD **(3)** which serves as the more common cofactor in several oxidoreductase enzymes including glucose oxidase, glutathione reductase.[14] Therefore, these two metabolically active forms of riboflavin **(1)**, serve as redox cofactors in a variety of metabolic transformations. In most of these enzymes the flavin moiety is tightly bound, non-covalently at the active site of the proteins.[15] In a few others, they are covalently attached to either the 8α-methyl group or to the C_6 atom of the flavin isoalloxazine ring with amino acid side chains of the protein.[16]

1.4 Regulation of riboflavin concentration in the cell

To complete the catalytic cycle in flavoenzymes, the reduced flavin cofactor is re-oxidized, and in some systems like the ErV family Sulfhydryl oxidases, this cycle produces superoxide as toxic reactive oxygen species.[17] Conversely, reactive oxygen species like superoxide and hydroxyl radicals can also be generated from oxidized flavin molecule non-enzymatically by exposure to light in the presence of electron donors like amino acids.[18] In order to protect the cells from these reactive species, the concentration of riboflavin **(1)** in the cells is strictly maintained under a certain threshold level. Several intestinal bacteria oxidize riboflavin **(1)** to 7α and 8α-carboxyriboflavin **(10,11)**

(Appendix A), N_{10}-hydroxyethylflavin **(85)** or lumichrome **(12) (Figure 3)**.[19] These catabolites are then excreted through the urine. The oxidative degradation pathways for riboflavin **(1)** is absent in humans and are found only in bacteria and in certain fungi.[20]

1.5 Riboflavin catabolism in bacteria

Cofactor catabolism has long been a greatly unexplored field of research.[21] Heme, nicotinamide and PLP are the only three cofactors for which the catabolic pathways are well characterized.[22-24] During 1940-1970 a number of cofactor catabolic strains were isolated including thiamin, folate, biotin and riboflavin catabolic strains.[25-28] Among these identified cofactor catabolic strains a riboflavin degrading soil bacterium *Pseudomonas riboflavina* was discovered by the Foster group in 1944 which degraded riboflavin **(1)** to lumichrome **(12)**.[29]

In 1956, riboflavin hydrolase, was identified by the same group in the crude cell-free extract of *Pseudomonas riboflavina* that could cleave riboflavin to give lumichrome **(12)** and ribitol **(13)** as the end products (Figure 3).[30] Further attempts to identify the gene encoding the enzyme and characterize the enzyme have been unsuccessful.

In 1965, the Stadtman group demonstrated the degradation of the isoalloxaxine ring of riboflavin **(1)** to 1-ribityl-2,3-diketo-1,2,3,4-tetrahydro-6,7-dimethylquinox-1,2,3,4-tetrahydro-6,7-dimethylquinoxaline **(14)** releasing ribose **(15)**, urea **(16)**, and CO_2 **(17)** with the cell-free enzyme preparations from a *Pseudomanas RF* strain (Figure 4).[28] **14** was degraded further by the same strain to the lactone **(18)** and oxalimide **(19)**.[31] Unfortunately, even this strain could not be recovered for further analysis.

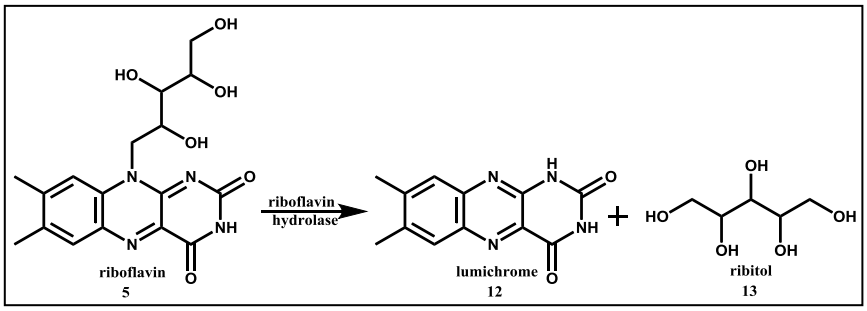

Figure 3: Riboflavin degradation by riboflavin hydrolase from *Pseudomonas riboflavina*

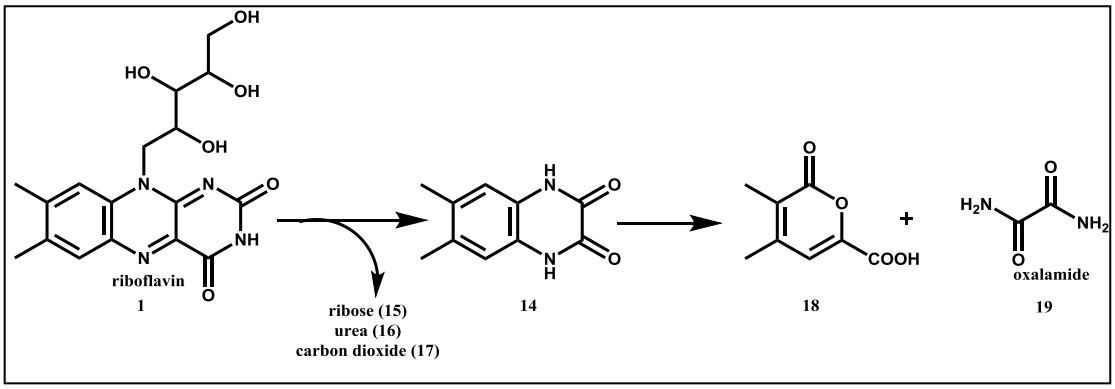

Figure 4: Isoalloxazine degradation by bacteria

1.6 Riboflavin catabolic gene cluster

In 2012, the Begley Lab discovered a riboflavin **(1)** degrading strain *Microbacterium* maritypicum G10. Successive cosmid library screening has revealed that this bacterium contains a gene cluster responsible for riboflavin catabolism. The gene cluster contains an enzyme riboflavin lyase (RcaE) that catalyzes the degradation of riboflavin **(1)** to lumichrome **(12)** and ribose **(15)** in the presence of oxygen **(20)** and reduced nicotinamide cofactor NADH **(22)**. Along with *rcaE* the other functional genes in the cluster that are involved in riboflavin catabolism encode for a flavin reductase RcaB, a flavokinase RcaA and a ribokinase RcaD. RcaA, RcaB and RcaD have been

reconstituted in our lab. Also, reconstitution of RcaE has been carried out. The proposed sequential functions of the enzymes involved in the catabolism of riboflavin are shown in Figure 5.

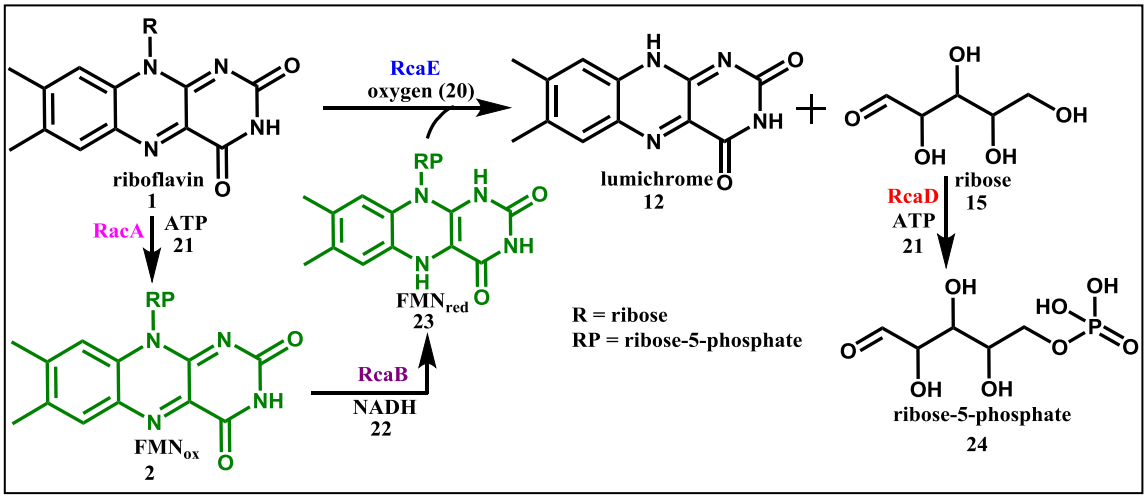

Figure 5: The proposed sequential activities of the riboflavin catabolic enzymes. Riboflavin **(1)** uptaken by cells from the environment is converted to FMN **(2)** by the flavokinase RcaA. The FMN in turn is reduced by the NADH **(22)** dependent flavoreductase RcaB. The reduced FMN **(2)** is then transferred to the riboflavin catabolizing enzyme RcaE where it assists in the degradation of riboflavin **(1)** to lumichrome **(12)** and ribose **(15)**. The ribose released by RcaE is phosphorylated by the ribokinase RcaD to form ribose-5-phosphate **(24)** which enters central metabolism.

1.7 Riboflavin Lyase (RcaE)

The riboflavin degradation pathway in *Microbacterium* maritypicum G10 is similar to the previously proposed riboflavin degradation pathway in *Pseudomonas riboflavina*.[29] The reaction catalyzed by the purified riboflavin lyase (RcaE) from the *Microbacterium* strain involves an oxidative cleavage of riboflavin **(1)** at the C_1' position

to produce lumichrome **(12)** and ribose **(15)** (Figure 6). Unlike riboflavin degradation in *Pseudomonas RF*[28,31] where further degradation of the isoalloxazine ring (lumichrome) is observed, the end product for both riboflavin hydrolase from *Pseudomonas riboflavina*[32] and RcaE from *Microbacterium* maritypicum G10 is lumichrome **(12)**.

Chemical photolytic degradation of riboflavin **(1)** to lumichrome **(12)** under alkaline conditions is well-precedented in the literature.[33] RcaE mimics this non-enzymatic transformation in absence of light under neutral conditions. Consistent with our experimental data, RcaE requires the presence of oxygen **(20)** and the flavin reductase system RcaB with the reduced nicotinamide cofactor NADH **(22)** for its activity. Since the NADH **(22)** utilizing flavin reductase RcaB is present in the same gene cluster as RcaE we propose that the oxidative transformation by RcaE is brought about by a reduced flavin cofactor received from the partner reductase RcaB.[34]

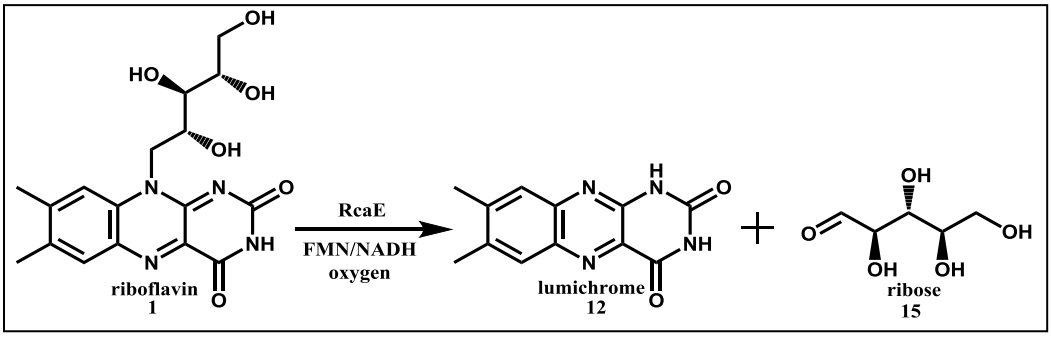

Figure 6: The degradation of riboflavin (1) to lumichrome (12) and ribose (15) catalyzed by RcaE

1.8 Riboflavin Lyase (RcaE) is a two-component flavin monooxygenase

Oxidative flavoenzymes

Thus, RcaE falls in the broad class of flavoenzyme oxygenases, which harbor a large number of interesting enzymes involved in different substrate oxidation. Oxidative flavoenzymes can be broadly classified into two classes, flavin oxidases and flavin oxygenases.[35,36] Flavin oxidases bind to oxidized flavin, which oxidizes substrates via a reductive half reaction. Examples of such oxidases include flavoenzymes that catalyze desaturations to olefins; oxidation of amines, alcohols, and thiols; and flavin-N_5 mediated oxidation of nitroalkanes.[37] Flavin oxygenases, on the other hand, bind to reduced flavin which in turn oxidizes substrates through a re-oxidative half reaction with oxygen.[38] Flavin oxygenases can be subdivided into single component and two-component flavin monoxygenases.

Single and two-component flavin oxygenases

In single component flavin oxygenases, the reduction of the bound flavin by a nicotinamide cofactor as well as the reaction of the reduced flavin with molecular oxygen to form the active oxidizing species takes place on a single protein. The extensively studied enzyme system, para-hydroxybenzoate hydrolase, which oxidizes p-hydroxybenzoate **(25)** to dihydroxybenzoate **(26)**, serves as a model for this class of monoxygenases (Appendix B).[39]

Two-component flavin oxygenases on the other hand, consist of an oxidase component that utilizes reduced flavin, generated by a separate NAD(P)H dependent

flavin reductase component, to activate oxygen for substrate oxidation.[40] Bacterial luciferase serves as the model system for this class of enzymes. This enzyme catalyzes the oxidation of reduced FMN with oxygen producing bioluminescence.[41] Apart from luciferase, this family includes flavoenzymes that catalyze $C_4\alpha$-(hydro)peroxyflavin **(27) (Appendix C)** mediated hydroxylation, epoxidation, chlorination, oxidative amide hydrolysis, Baeyer-Villiger oxidation, oxidative Favorskii rearrangement; flavin-N_5-oxide **(28) (Appendix C)** mediated oxidations and a unique transformation where the flavin molecule is destructively converted to dimethylbenzimidazole **(43)** (Figure 7).[42,43]

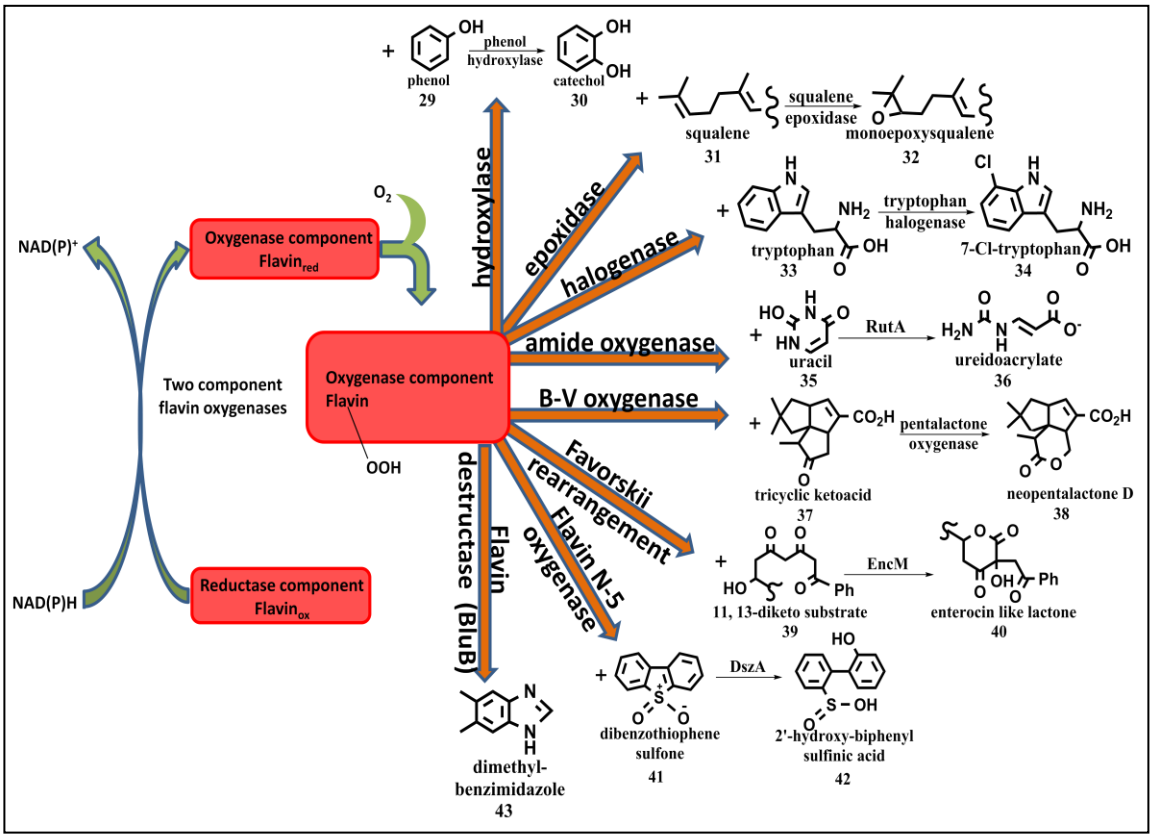

Figure 7: Reaction mechanism of two-component flavin oxygenases. The different types of oxidations catalyzed by this class of enzymes are summarized.

Flavin reducing systems for 2 ē reduction

In biological systems, flavins are reduced by the reduced nicotinamide cofactor NAD(P)H which is either bound to the same protein component as the flavin or is bound to a partner reductase component. FMN **(2)** is reduced by E.coli flavin reductase at a very fast rate with a k_{cat} of ~32 s^{-1}.[44] Though the non-enzymatic reduction of flavins with NADH in the absence of a flavin reductase proceeds at a much slower rate, this 2 ē reduction can also be achieved non-enzymatically at comparable rates by reducing agents like dithionite **(44) (Appendix A)**.[45] Here, the reduction proceeds by two single electron transfers from dithionite.[46] Flavins can also be efficiently reduced by photoreduction with single electron donors like EDTA **(45) (Appendix A)**[47] and amino acids[48] via the formation of a flavin semiquinone from the flavin in its triplet state. In monoxygenases, the formation of the 2 ē reduced flavin is necessary for its reaction with molecular oxygen to produce the active oxygenating species C_4α-(hydro)peroxyflavin **(27) (Appendix C).**

RcaE – Two-component flavin monooxygenase with RcaB as partner reductase

RcaE catalyzes an oxygen mediated oxidative degradation of riboflavin to lumichrome. This degradation requires reduced FMN which may be delivered to RcaE by the flavin reductase RcaB. Hence, RcaE is proposed to be a member of the two-component flavin oxygenases where RcaE serves as the oxidase component and RcaB as the reductase counterpart. From the experimental results obtained in the following chapters, the mechanism of riboflavin degradation by RcaE is proposed to proceed via

an unprecedented superoxide radical mediated mechanism. This makes RcaE a unique member of the two-component flavin oxygenase family.

In this work, we report the reconstitution of RcaE followed by a mechanistic description of the enzyme. Through mechanistic studies with analogs and with intermediates, we have elucidated the identity of the active oxidizing species responsible for the oxidative degradation of riboflavin by the enzyme.

CHAPTER II

ANNOTATION AND RECONSTITUTION OF THE CATABOLIC GENE CLUSTER FOR RIBOFLAVIN IN *MICROBACTERIUM MARITYPICUM G10*

2.1 Introduction

Cofactors play key roles in augmenting the limited functionality available on proteins for catalysis. As with all other metabolites, cofactors do not accumulate in the environment. This is due in part to efficient salvage of these biosynthetically expensive metabolites and in part due to cofactor catabolism. However, in contrast to the large literature which is available on the biosynthesis of cofactors[21] with relatively little information about their breakdown process.[49] Till date, only a few cofactor catabolic pathways have been identified (Figure 8). Among the characterized catabolic pathways, the most well-studied is the enzymatic degradation for Vitamin B_6 (PLP) which proceeds via two independent pathways. In one of the pathways, pyridoxine **(46)** is degraded all the way to succinic semialdehyde **(47)**, while in the second, it is degraded to 2-(hydroxymethyl)-4-oxobutanoate **(48)**.[24] The other well characterized catabolic pathway is the thiamine (Vitamin B_1) catabolism where thiaminase I and thiaminase II cleave thiamine **(49)** to generate a pyrimidine fragment **(50)** and thiazole phosphate **(51)**.[50,51] In the heme degradation pathway, heme **(52)** is degraded to biliverdin **(53)** or staphylobilin **(54)** by heme-oxygenase.[23] Another example is the catabolic pathway for nicotinic acid (Vitamin B_3) **(55)** which gets degraded aerobically to fumarate **(56),** carbon dioxide **(17),** ammonia **(57)** and formic acid **(6)** whereas the anaerobic degradation pathway generates pyruvate **(58),** propanyliumoate **(59)** and ammonia **(57)**.[22,52]

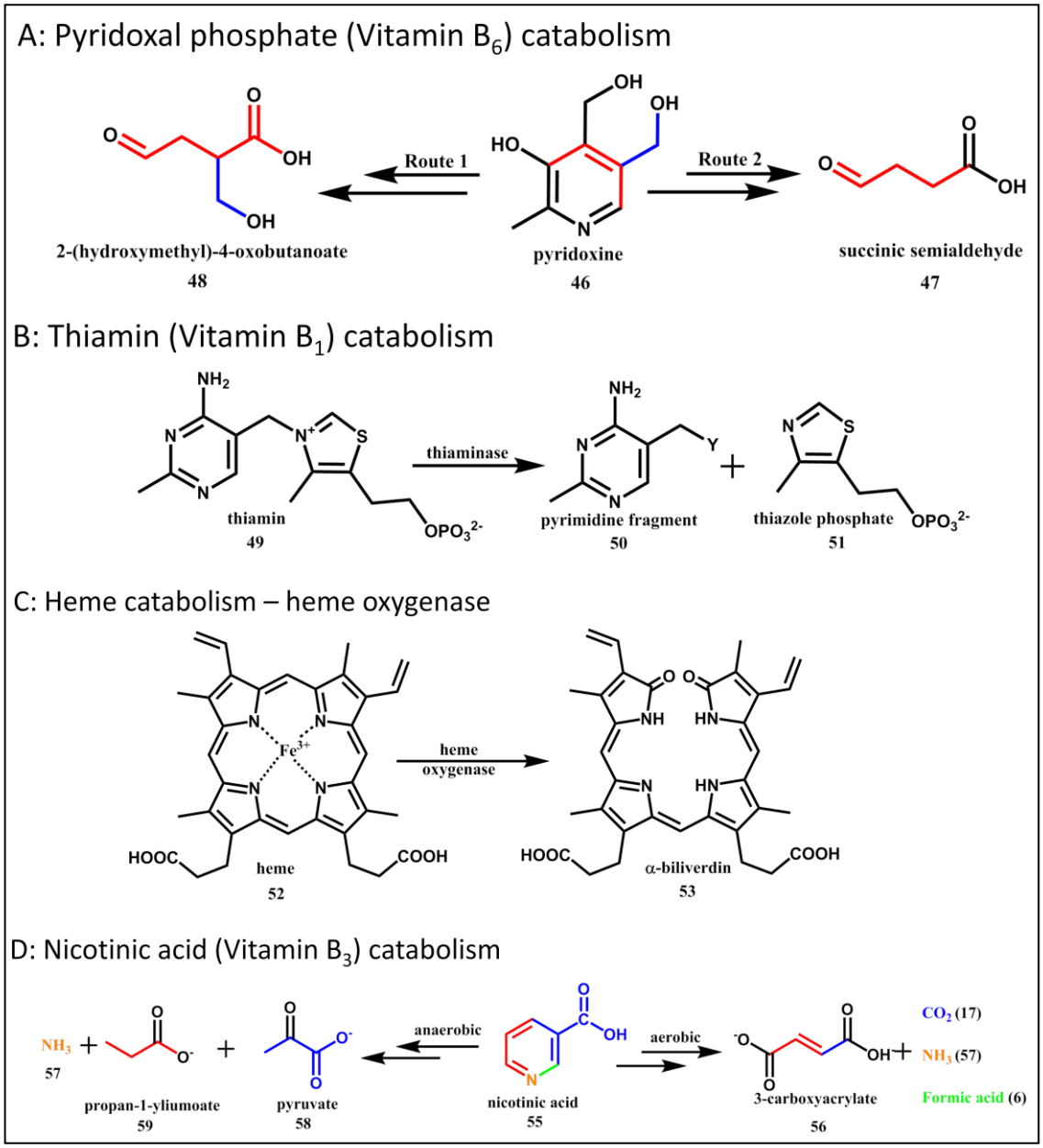

Figure 8: Catabolic pathways for Vitamin B_6, Vitamin B_1, heme and Vitamin B_3

Thiamin **(49)**, folate (Vitamin B_9) **(60) (Appendix A)**, riboflavin (Vitamin B2) **(1)**, biotin (Vitamin B_7) **(61) (Appendix A)** degrading bacteria were once isolated but have now been lost.[25-27,53-55] Analysis of culture metabolites from the reported riboflavin **(1)** catabolic strain demonstrated that this strain was capable of degrading the isoalloxazine ring of riboflavin all the way to the lactone **(63)** and oxalimide **(64)** (Figure 9).[28] None of the genes were identified and lumichrome was not an intermediate.

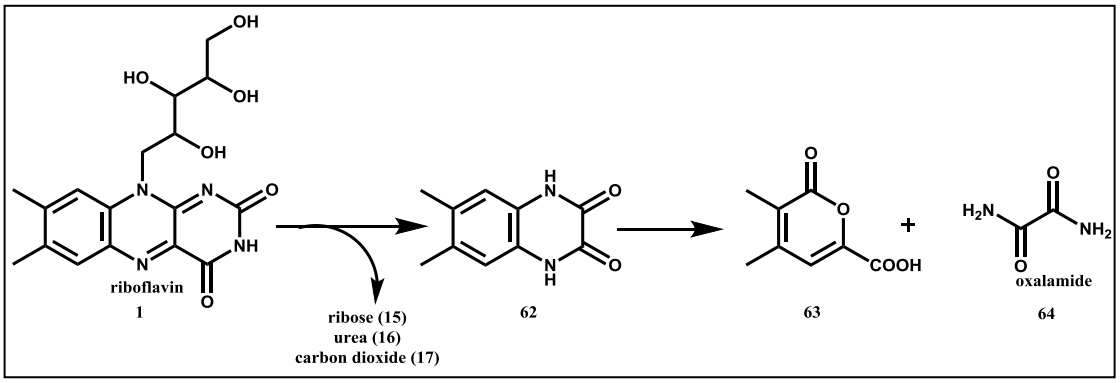

Figure 9: Riboflavin (1) degradation – breakdown of the isoalloxazine ring

RcaE, the riboflavin lyase, catalyzes the conversion of riboflavin **(1)** to lumichrome **(12)** and ribose **(15)** and has previously been identified as a potential catabolic enzyme in a second pathway identified by the Foster group in 1956.[32,56] However, despite significant effort, the gene encoding this enzyme was never identified, and the enzyme itself proved to be biochemically intractable.[57] Here we report the isolation of a riboflavin catabolizing *Microbacterium maritypicum* strain from dust samples obtained from the DSM riboflavin production plant in Germany. The catabolic

operon was identified from a cosmid library, then sequenced and annotated. Preliminary characterization of the enzymes involved suggested a riboflavin catabolic pathway.

2.2 Results and Discussions

Strain Microbacterium maritypicum G10 catabolizes riboflavin

Dust samples, collected at the DSM riboflavin production plant in Germany, were screened by culturing in M9 medium with riboflavin as the sole carbon source. Bleaching of the riboflavin **(1)** color was observed in some of the samples. The cells from these hits were grown on NB plates and single colonies were selected. Individual strains were retested for conformation on M9 medium with riboflavin as the sole carbon source. The best of these strains (Strain G10) completely bleached the yellow color of riboflavin after 12 hours of growth and was selected for further study. The 16S rRNA sequence identified this strain as *Microbacterium maritypicum*.

To identify the products generated from consumption of riboflavin **(1)**, *M. maritypicum* G10 was grown in M9 medium supplemented with 0.1% LB and 100 μg/ml (270 μM) riboflavin **(1)**. HPLC analysis of the medium showed time-dependent consumption of riboflavin **(1)** and appearance of a new signal, which co-migrated with lumichrome **(12)** (Figure 10A). Analysis after 21 hr showed complete catabolism of riboflavin, a small peak for lumichrome **(12)** and no new signals were observed on the HPLC. This result suggested that lumichrome **(12)** precipitates from the growth medium. After 30 hr, total concentration of lumichrome **(12)**, from 270 μM riboflavin **(1)**, was 260 μM. This corresponds to 96% conversion of riboflavin **(1)** to lumichrome **(12)**. When the same culture medium was filtered before basification, concentration of

lumichrome **(12)** was less than 25 μM (Figure 10B). We therefore conclude that riboflavin **(1)** catabolism in *M. maritypicum* G10 involves cleavage of the ribose **(15)** from the isoalloxazine ring. The ribose is used to sustain cell growth and the lumichrome **(12)** precipitates from the growth medium.

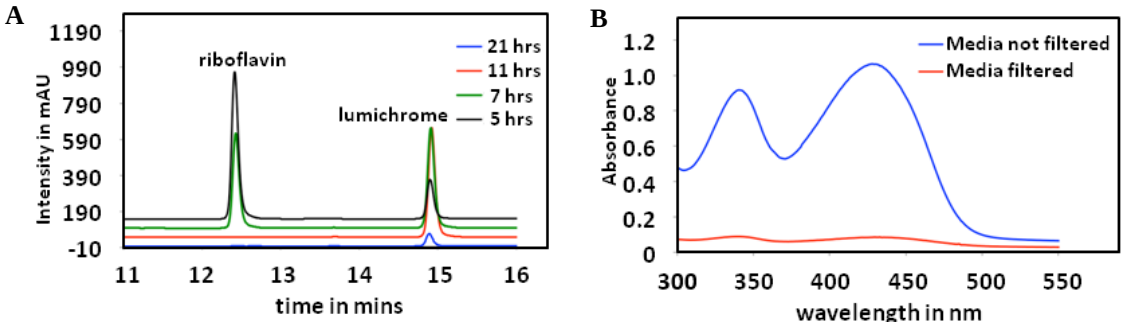

Figure 10: Analysis of riboflavin catabolism. A: HPLC analysis for the time dependent formation of lumichrome **(12)** from riboflavin **(1)** in the culture medium of *M. maritypicum* G10 at 340nm. B: UV-Vis analysis of culture medium treated with 1N KOH after ~30hours.

Identification of the riboflavin catabolic gene cluster

A cosmid library was constructed for the isolation of the riboflavin **(1)** catabolic gene cluster.[58] After failing to identify the gene cluster by screening this library in *E.coli*, *Streptomyces lividans* was chosen as the heterologous host because *Microbacterium* and *Streptomyces* both have high genomic GC content. The cosmid library was therefore reconstructed in vector pJTU2463 containing *oriT* for conjugation and integration into the *attP* site of *S. lividans*. The genome size of *Microbacterium* is 4~5 Mb. and the resulting library consisted of eight 96-well plates. This library was screened, first in batches of 12 cosmids, then individually, to yield two cosmids encoding the riboflavin

(1) catabolic pathway (1A4 and 5H7, Figure 11A). Sequence alignment of the two cosmids identified a 6.63 kb region in 1A4 showing 86% identity with 5H7 suggesting that the riboflavin catabolic genes were localized in this region. To test this, an 8.7 kb BamHI fragment from 5H7, containing the target 6.63 kb region, was cloned into pJTU2463 and introduced into *S.lividans*. This strain after the introduction of pJTU2463 consumed riboflavin **(1)**.

Functional analysis of the riboflavin catabolic (Rca) gene cluster

The genetic organization of the riboflavin catabolic gene cluster of cosmid 5H7 is shown in Figure 7B, and the gene annotations are shown in Table 1. The riboflavin **(1)** catabolic gene cluster on cosmid 1A4 was similarly annotated (Table 2). All of the genes in this cluster have high identity to those in the 5H7 cluster except for RcaH, which is replaced by a gene of unknown function (RcaJ2). Based on the sequence analysis, RcaF and RcaG are likely to be involved in riboflavin **(1)** transport and RcaC in pathway regulation. These proteins were not further studied. Cosmids 5H7 and 1A4 both contain all of the genes essential for riboflavin catabolism in *S. lividans* (Figure 11B). Since a second riboflavin kinase is available for FMN **(2)** and FAD **(3)** biosynthesis in *S.lividans*, RcaA is not an essential component of the catabolic gene cluster (see below). In addition, since *rcaH* is missing from cosmid 1A4 and *rcaJ2* is missing from cosmid 5H7, we conclude that neither of these genes are involved in riboflavin **(1)** catabolism.

Table 1: Deduced functions of ORFs in the catabolic gene cluster of 5H7.

gene	start	stop	Amino acid	Protein homolog/ **Proposed function**	Identity (%)
RcaA	1585	1193	131	Bifunctional riboflavin kinase *Arsenicicoccus bolidensis*/ **Flavokinase**	70/129 54%
RcaB	2106	1585	174	Flavin reductase *Marine actinobacterium PHSC20C1*/ **Flavin-reductase**	87/159 55%
RcaC	2209	2811	201	PadR family transcriptional regulator *Salinibacterium sp. PAMC21357*/ **Transcriptional regulator**	120/186 65%
RcaD	3671	2820	284	Ribokinase *Llyobacter polytropus DSM 2926*/ **Ribokinase**	105/287 37%
RcaE	5073	3697	459	N5,N10-methylene tetrahydromethanopterin reductase *Bacillus sp. 10403023*/ **Riboflavin lyase**	139/340 41%
RcaF	6036	5191	282	Transporter *Marine actinobacterium PHSC20C1*/ **Transporter**	202/269 75%
RcaG	6826	6032	265	ABC transporter ATP-binding protein *Marine actinobacterium PHSC20C1*/ **Transporter**	189/258 73%
RcaH	5924	6859	312	Phenol hydroxylase *Natronorubrum tibetense*/ **Unknown**	53/165 32%
RcaI	7929	6829	367	NMT1/THI5 like domain-containing protein *Salinibacterium sp. PAMC 21357*/ **Unknown**	185/245 76%

Table 2: Comparison of gene annotations between the two gene clusters.

Genes From 5H7	Genes From 1A4	Protein homolog	Identity (%)
RcaA		Flavokinase *Arsenicicoccus bolidensis*	
RcaB	RcaB2	Flavin reductase *Marine actinobacterium PHSC20C1*	132/160 83%
RcaC	RcaC2	PadR family transcriptional regulator *Salinibacterium sp. PAMC 21357*	185/194 95%
RcaD	RcaD2	Ribokinase *Llyobacter polytropus DSM 2926*	220/284 77%
RcaE	RcaE2	N5,N10-methylene tetrahydromethanopterin reductase *Bacillus sp. 10403023*	434/459 95%
RcaF	RcaF2	Transporter *Marine actinobacterium PHSC20C1*	269/282 95%
	RcaJ2	Hypothetical protein	
RcaG	RcaG2	ABC transporter ATP-binding protein *Marine actinobacterium PHSC20C1*	251/265 95%
RcaH		Phenol hydroxylase *Natronorubrum tibetense*	
RcaI	RcaI2	NMT1/THI5 like domain-containing protein *Salinibacterium sp. PAMC 21357*	344/367 94%

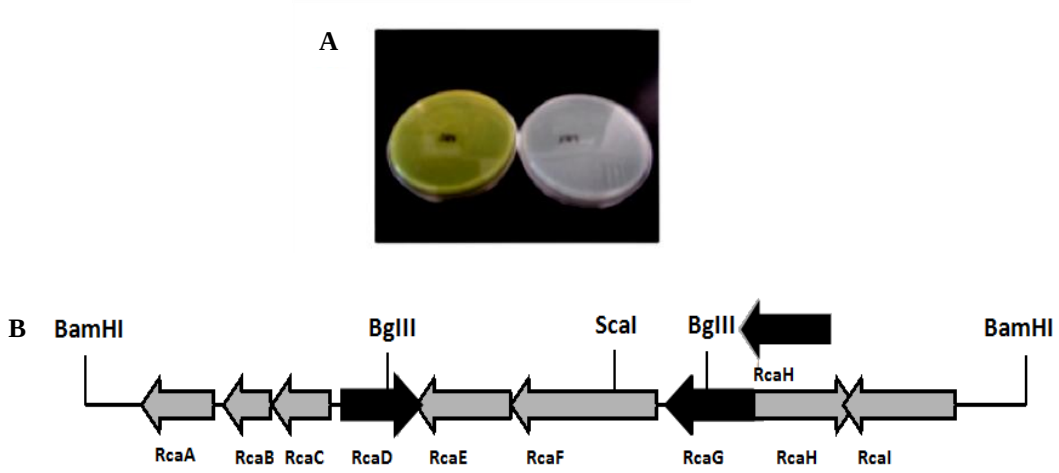

Figure 11: Cloning of the riboflavin (1) catabolic cluster. A: *S.lividans* carrying cosmid 5H7 bleached the M9 plate with riboflavin (right) compared to the mutant carrying cosmid 5H4 (left). B: Genetic organization of the riboflavin catabolic gene cluster from cosmid 5H7.

RcaA is a riboflavin kinase

RcaA was cloned into the pET28b vector and overexpressed in *E.coli* BL21 (DE3). The overexpressed enzyme was purified on a HisTrap HP column (Figure 12A). The purified enzyme was incubated with riboflavin **(1)** and ATP **(21)**, and the product was identified as FMN **(2)** by HPLC confirming RcaA as a riboflavin kinase (Figure 12B).

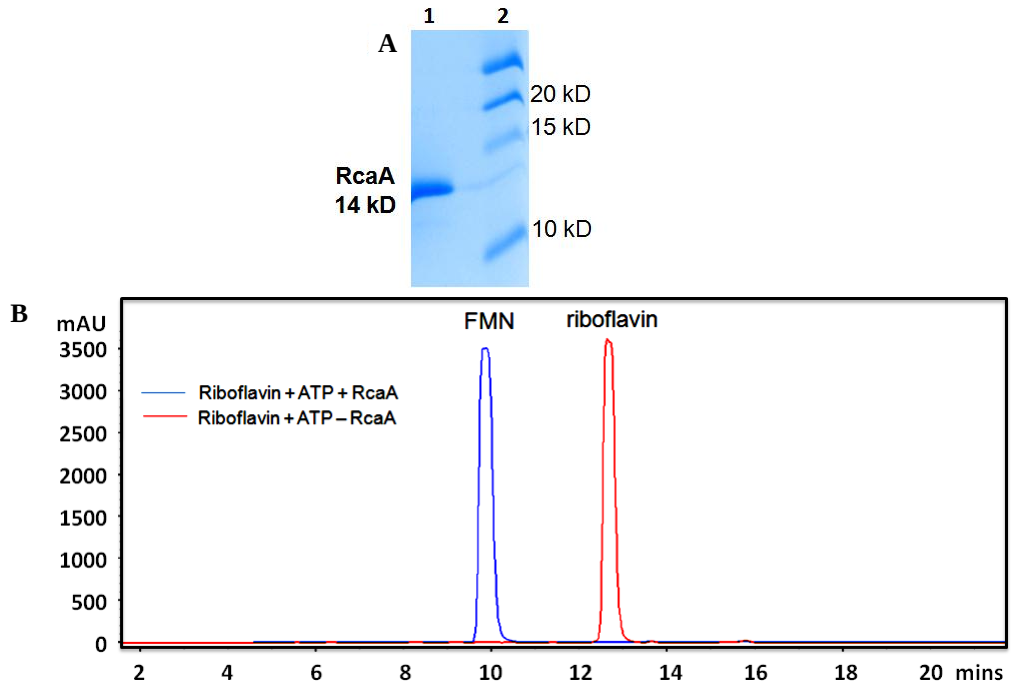

Figure 12: Biochemical characterization of RcaA. A: SDS/PAGE analysis of RcaA purified on a Ni-NTA His-Trap column. Lane 1: purified RcaA, Lane 2: molecular mass markers, **B:** HPLC trace of the RcaA catalyzed reaction of riboflavin **(1)** with ATP **(21)**. Complete conversion of riboflavin **(1)** to FMN **(2) i**n the full reaction with RcaA and ATP **(21)** (blue trace). The red trace shows the HPLC data in the reaction where the enzyme RcaA is absent.

RcaB is a riboflavin/flavin mononucleotide (FMN) reductase

RcaB was cloned into the pMAL vector and overexpressed in *E. coli* BL21(DE3). The overexpressed enzyme was purified on an amylose resin column. (Figure 13A). The purified enzyme was incubated with NADH **(22)** and riboflavin **(1)** or FMN **(2)** and a steady decrease in the absorbance at 450 nm for oxidized flavin was observed by UV-visible spectroscopy (Figure 13B). As evident from Figure 13B, a complete reduction of 80 µM FMN **(2)** was achieved in 80 secs with 100 nM RcaB in

the presence of excess NADH **(22)** whereas similar reduction of riboflavin **(1)** required 1 µM enzyme. In Figure 13C absorbance at 340 nm was monitored for NADH **(22)** consumption. Consumption of NADH **(22)** was measured for both FMN **(2)** (left panel) and riboflavin **(1)** (right panel) reduction with 100 nM RcaB. A comparison between the two panels (Figure 13F) indicates that the rate of reduction of FMN **(2)** by RcaB is much faster than the reduction of riboflavin **(1)**. No change in the absorbance for oxidized flavin at 450 nm was observed when the flavin was incubated with NADH **(22)** in the absence of the enzyme (Figure 13D). Similarly, in the absence of oxidized flavin no decrease in the absorbance for NADH **(22)** at 340 nm was observed (Figure 13E). Together these results confirmed RcaB as a flavin reductase with a modest substrate preference for FMN **(2)** over riboflavin **(1)** (Figure 13F)**.**

RcaD is a ribokinase

RcaD was cloned into the pMAL vector and overexpressed in *E.coli* BL21 (DE3). The enzyme was purified as described for RcaB above (Figure 14A). RcaD catalyzed the conversion of ribose **(15)** to ribose-5-phosphate **(24)** in the presence of ATP **(21)**. The product **24** was detected by LC-MS analysis of the reaction mixture after treatment with *O*-(2,3,4,5,6-Pentafluorobenzyl) hydroxylamine (PFBHA) **(65)** to convert the corresponding aldehyde to the ribose-5-phosphate-PFBHA oxime **(67)** (Appendix D), thus confirming RcaD as a ribokinase (Figure 14B, 14C).

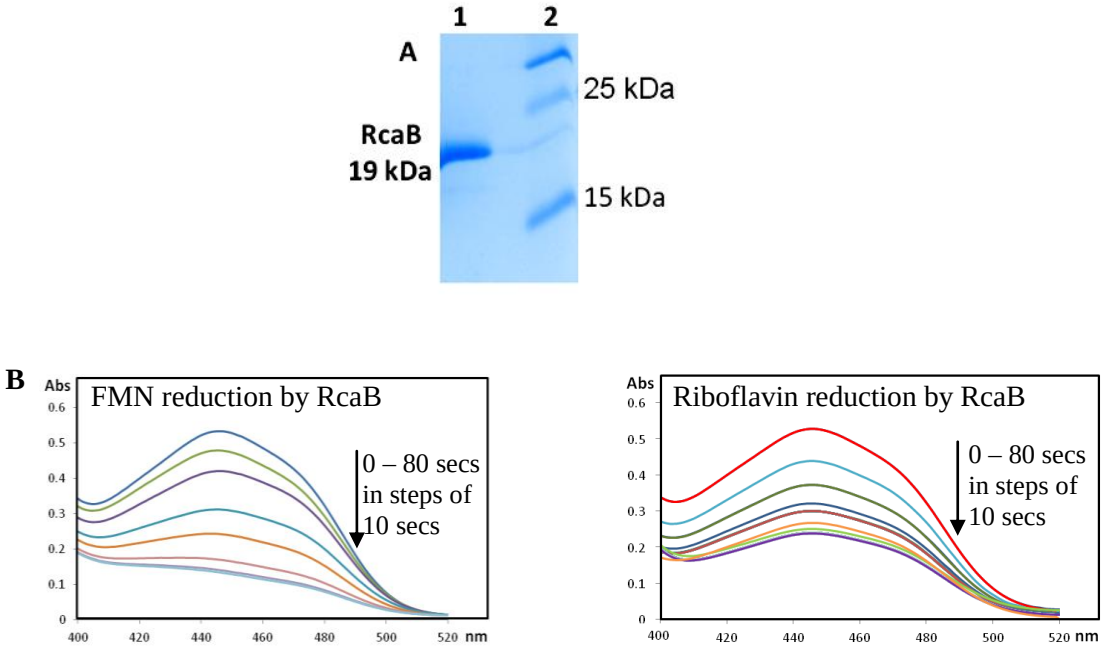

Figure 13: Biochemical characterization of RcaB. A: SDS/PAGE analysis of RcaB after purification on a Maltose-binding column followed by maltose tag cleavage. Lane 1: purified RcaB, Lane 2: molecular mass markers B: UV-visible spectra of the RcaB-catalyzed reduction of FMN **(2)** with NADH **(22)** and 100 nM RcaB (left trace), UV-visible spectra of the RcaB-catalyzed reduction of riboflavin **(1)** with NADH **(22)** and 1 µM RcaB (right trace) C: UV-visible spectra of the RcaB-catalyzed oxidation of NADH **(22)** with FMN **(11)** and 100 nm RcaB (left trace), UV-visible spectra of the RcaB-catalyzed oxidation of NADH **(22)** with riboflavin **(1)** and 100 nM RcaB (right trace). D: UV-visible spectra of non-enzymatic reduction of FMN **(11)** with NADH **(22)** E: UV-visible spectra of the RcaB-catalyzed oxidation of NADH **(22)** in the absence of flavin. F: Comparative NADH oxidation rates by FMN (blue boxes) vs. riboflavin (red boxes) in the presence of RcaB. The rate of oxidation of FMN (shown by the decrease in absorbance of NADH at 340 nm) is much faster than the rate of oxidation of NADH by riboflavin.

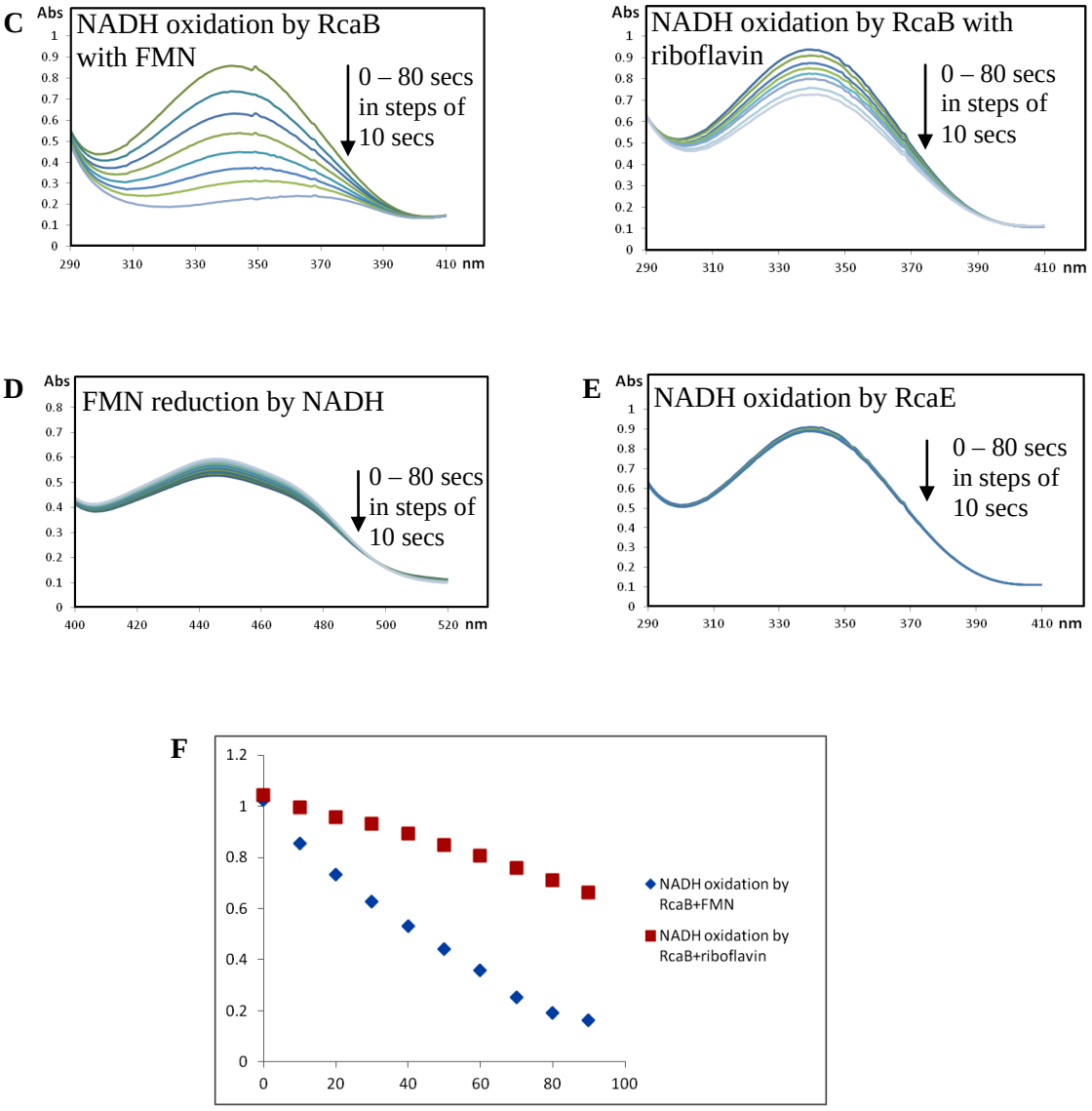

Figure 13 Continued

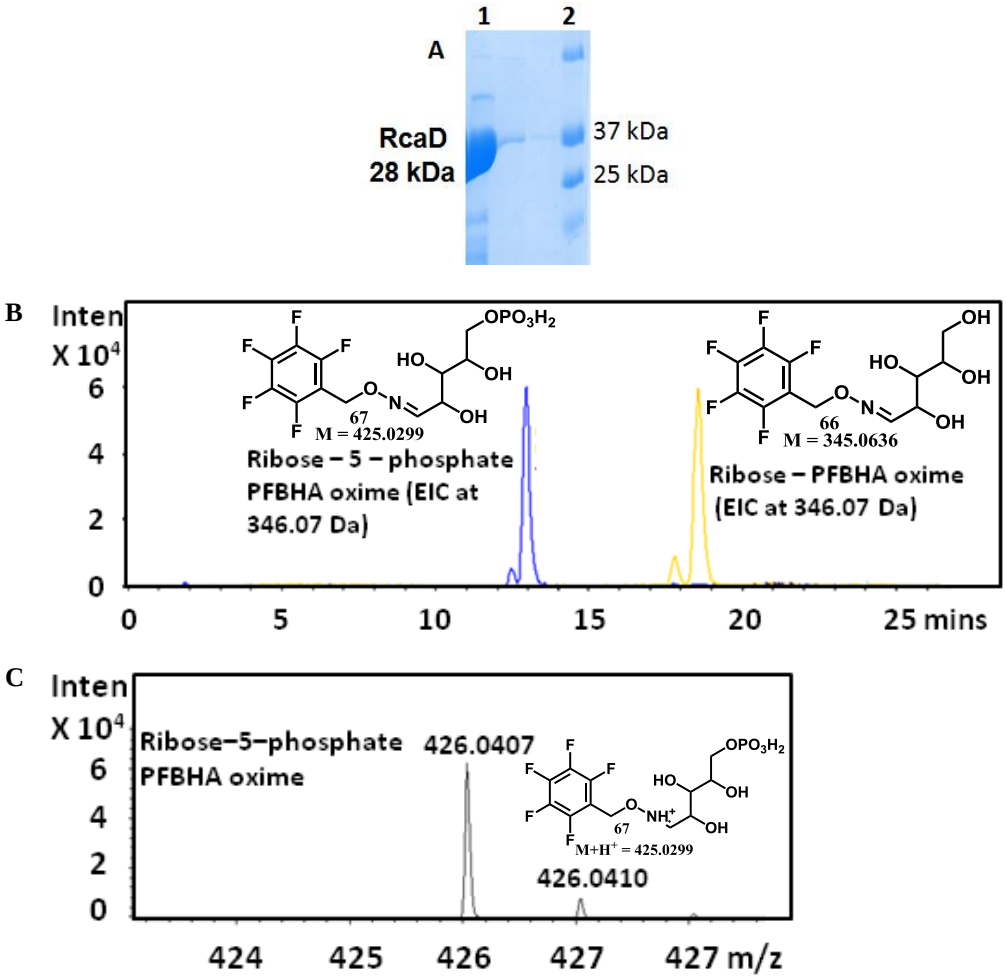

Figure 14: Biochemical characterization of RcaD. A: SDS-PAGE analysis of RcaD after purification on a Maltose-binding column followed by maltose tag cleavage. Lane 1: purified RcaD, Lane 2: molecular markers, B: Extracted Ion Chromatogram (EIC) of RcaD catalyzed a reaction of ribose **(15)** with ATP **(21)** in the presence of PFBHA **(65)**. The trace in yellow shows the no enzyme control where the PFBHA trapped substrate, ribose-PFBHA oxime **(66) (Appendix D)** ($M+H^+$ 346.0712), is detected by the EIC at 346.07 Da. The blue trace is the full reaction where the product, ribose-5-phosphate-PFBHA oxime **(67)** ($M+H^+$ 426.0417), is detected by the EIC at 426.04 Da. Ribose-PFBHA oxime **(66)** at EIC 346.07 was not detected in the full reaction demonstrating a complete conversion of ribose **(15)** to ribose-5-phosphate **(24)** by RcaD under the reaction conditions. C: ESI-Mass spectrum in the positive mode of the reaction product **67**.

RcaE catalyzes the formation of lumichrome (12)

RcaE was cloned into pET28b and overexpressed in *E.coli* BL21 (DE3). The protein was purified on a HisTrap HP column (Figure 15A). To test for RcaE activity riboflavin, NADH **(22)** and ATP **(21)** were incubated with purified RcaA, RcaB, RcaD, and RcaE and the reaction mixture was analyzed by HPLC. A time dependent formation of lumichrome **(12)** with the enzyme cocktail was observed (Figure 15B). In order to characterize the sugar product in the enzymatic degradation of riboflavin **(1)**, the reaction mixture was treated with PFBHA **(65)** and analyzed by LCMS. The full reaction revealed the formation of ribose-5-phosphate-PFBHA oxime **(67)** (Figure 15C). The above results establish that RcaE is a riboflavin lyase.

Figure 15: Biochemical characterization of RcaE. A: SDS/PAGE analysis of RcaE purified on a Ni-NTA His-Trap column. Lane 1: molecular mass markers. Lane 2: purified RcaE, B: HPLC trace of the RcaA, RcaB, RcaD, RcaE-catalyzed reaction of riboflavin with NADH (22) and ATP (21) showing time dependent formation of lumichrome (12). C: Extracted Ion Chromatogram (EIC) of the full reaction, after derivatization with PFBHA (65), showing EIC at 426.04 corresponding to the formation of ribose-**5**-phosphate-PFBHA oxime (67) (M+H+ 426.0417).

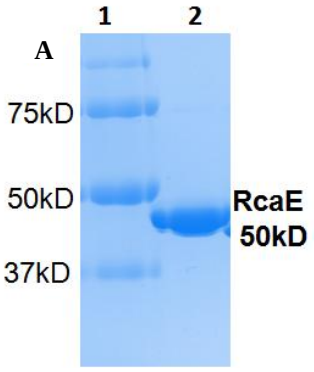

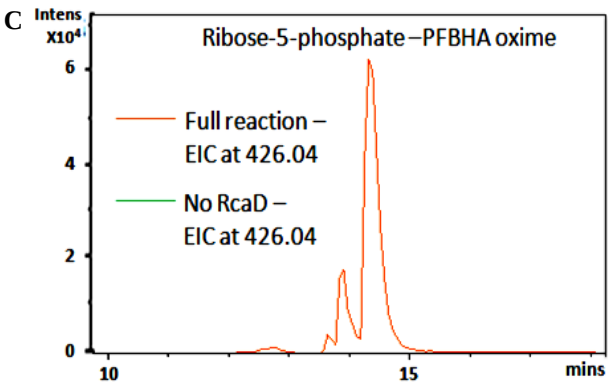

B

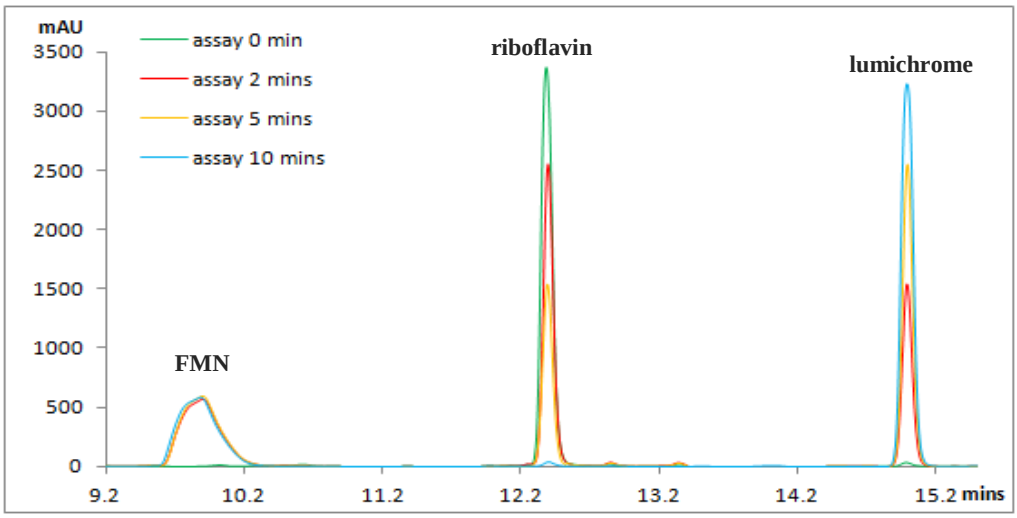

Figure 15 continued

To further define the riboflavin lyase activity, a series of reactions, lacking individual components, were run (Figure 16).

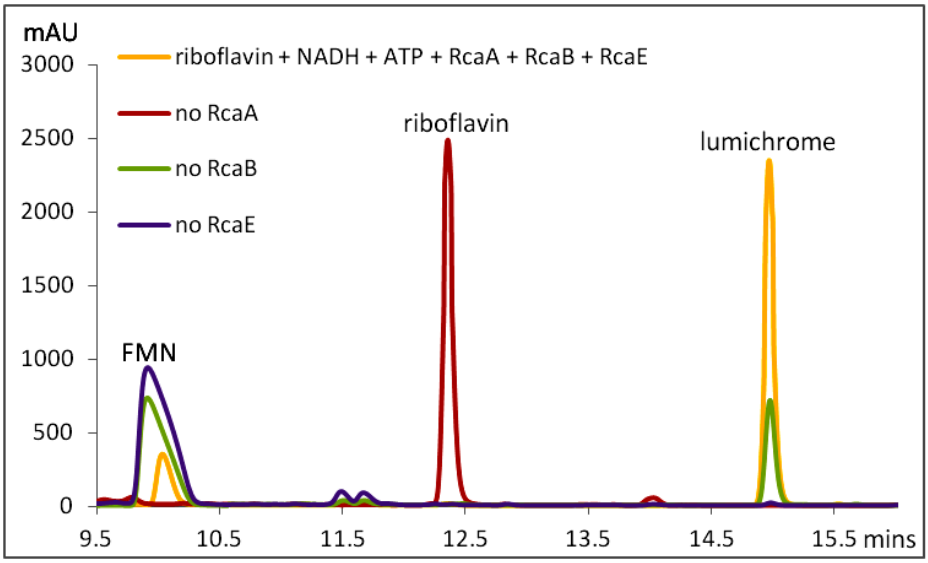

Figure 16: HPLC characterization of the enzymatic formation of lumichrome (12) in the absence of individual participating enzymes. Formation of lumichrome **(12)** is observed when riboflavin **(1)** is incubated with RcaA, RcaB, RcaE (yellow trace). No consumption of riboflavin **(1)** is observed in the absence of RcaA (red trace). Reduced lumichrome **(12)** formation is observed in the absence of RcaB (green trace). The lumichrome **(12)** formation is observed due to the slow non-enzymatic of FMN **(2)** by NADH **(22)**. The reaction stops after the formation of FMN **(2)** from riboflavin **(1)** in the absence of RcaE (purple trace).

These experiments established the following: RcaA catalyzes the first step in the catabolic pathway because in the absence of RcaA, riboflavin **(1)** is not consumed and lumichrome **(12)** is not formed. RcaB catalyzes the second step because in its absence FMN **(2)** accumulates and very little lumichrome **(12)** is formed. In the absence of RcaE, FMN **(2)** also accumulates because any reduced flavin will undergo re-oxidation during aerobic work-up. Remarkably, addition of catalytic amounts of FMN **(2)** removes the RcaA requirement thus enabling reconstitution of the riboflavin lyase using RcaB, RcaE,

NADH **(22)** and catalytic amounts of FMN **(2)** (Figure 17). The lyase reaction is oxygen-dependent and the reaction products are lumichrome and ribose (Figure 18).

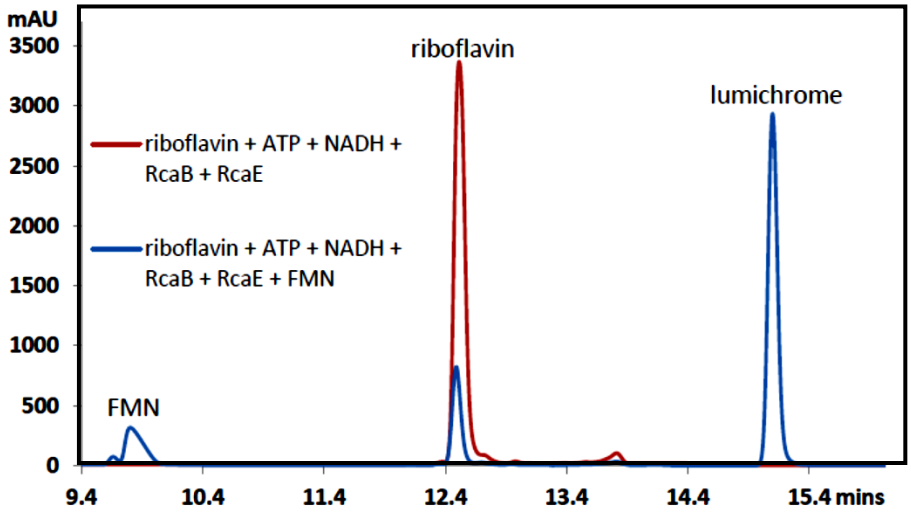

Figure 17: HPLC trace for the RcaE enzymatic reaction with RcaB and NADH (22) in the absence of the flavokinase RcaA. Formation of the product lumichrome **(12**) is not observed (red trace). Lumichrome **(12)** formation is observed when catalytic amount of FMN **(2)** is added to the enzymatic reaction (blue trace).

2.3 Experimental

Materials

Riboflavin **(1)**, FMN **(2)**, NADH **(22)**, *O*-(2,3,4,5,6-Pentafluorobenzyl) hydroxylamine (PFBHA) **(65)** and ribose-5-phosphate **(24)** were purchased from Sigma-Aldrich. The commercial FMN **(2)** comes with small amounts of riboflavin and lumichrome as impurities. The impurities could not be eliminated after a round of HPLC purification of FMN due to the spontaneous degradation of FMN **(2)**. Commercial

riboflavin **(1)** also has trace amount of lumichrome as impurity which shows up as a trace peak on the HPLC only with high concentrations (~500 µM) riboflavin **(1)**. The dehydrated form of LB broth and minimal medium salts were purchased from EMD Millipore. Kanamycin and IPTG were purchased from Lab Scientific Inc. Amicon Ultra centrifugal filter devices (10,000 MWCO) were obtained from Millipore. Histrap column was obtained from GE Healthcare. Econo-Pack 10DG desalting columns were purchased from Bio-Rad.

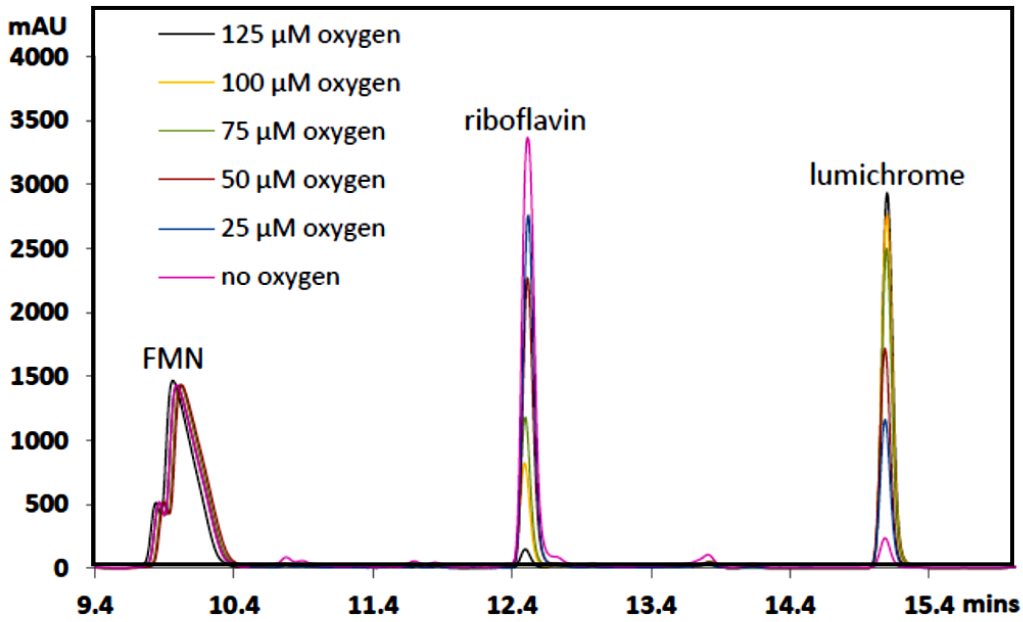

Figure 18: HPLC trace for oxygen concentration dependent enzymatic formation of lumichrome (13). The RcaE enzymatic reactions are run for 10 mins in the presence of riboflavin **(1)**, FMN **(2)**, RcaB, NADH **(22)** and oxygen **(20)** concentrations varying from 25 – 125 µM. No lumichrome **(12)** formation is observed under anaerobic conditions as indicated by the pink trace. The tiny peak of lumichrome **(12)** in the pink trace comes as a contaminant with the commercially obtained FMN **(2)** and is also present in reactions where the enzyme RcaE is absent.

General materials

All chemicals were purchased from Sigma-Aldrich. A dehydrated form of LB broth was purchased from EMD Millipore. Kanamycin and IPTG were obtained from Lab Scientific Inc. Amicon Ultra centrifugal filter devices (10,000 MWCO) were obtained from Millipore. Histrap Ni-NTA columns were obtained from GE Healthcare. Econo-Pack 10DG desalting columns were purchased from Bio-Rad. The baffled ultra yield flasks (2.5 L) for cell growth were obtained from Thomson Instrument Company. The ZORBAX Eclipse XDB-C18 column (15 cm x 4.6 mm, 5 μm particles) was purchased from Agilent Technologies.

Bacterial strains and plasmids, culture conditions, general techniques

Streptomyces lividans 1326 was used as the heterologous host for cosmid library screening for the riboflavin **(1)** catabolic gene cluster. *S.lividans* 1326 and its derivatives were grown at 30°C on soy flour-mannitol (SFM) agar plates for sporulation and conjugation. *E. coli* DH5α was used for plasmid construction, and S17-1 was used for *E.coli-Streptomyces* conjugation. BL21 (DE3) was used for protein overexpression and Epi100^{TM} from Epicentre was used for cosmid library construction. The cosmid library was constructed with vector pJTU2463,[59] which is a derivative of pOJ446 with the SCP2 replicon replaced by *int* and *attp* from pSET152.[60] Plasmid pXH1 was cloned by inserting an 8.7 kb BamHI fragment from cosmid 5H7 into BamHI/CIP treated pJTU2463. The strains and plasmids used are listed in Table 3.

Isolation of a riboflavin (1) catabolizing strain

Riboflavin **(1)** catabolic strains were isolated from the dust at the DSM riboflavin-producing plant (Germany). Bacteria from dust samples were cultured in modified M9 medium (no glucose, 0.1 mM of $FeCl_3$, 0.1% LB, 100 μg/ml of riboflavin) for several days. The growing cells were plated on NB plates and single colonies were selected to make a collection. Individual strains were then inoculated into 5 ml of NB and cultured at 30°C overnight. 1% of each starter culture was inoculated into 50 ml of modified M9 medium. The best strain catabolized riboflavin **(1)** within 12 hours and was selected for further study. 16s rRNA was amplified by PCR with primers FD1 (5'-CCGAATTCGTCGACAACAGAGTTTGA-3') and RP2 (5'-CCCGGGATCCAAGCTTACGGCTACCT-3').[61] The sequence results suggested that this riboflavin catabolic strain had high homology with *M. maritypicum* strain DSM12512, and it was named *M. maritypicum* G10.

Table 3: Strains and plasmids used.

Strain/plasmid	Relevant characteristics	Reference or source
Actinomyces		
Microbacterium maritypicum G10	Wild-type strain catabolizing riboflavin	This study
Streptomyces lividans 1326	Heterologous host for screening riboflavin catabolic gene cluster	1
E.coli		
Epi100^{TM}	Host cell for construction of genomic library	Epicentre
S17-1	TpR SmR *recA, thi, pro, hsd*R-M+RP4: 2-Tc:Mu: Km Tn7 λpir	3
DH5α	F- *endA1 glnV44 thi-1 recA1 relA1 gyrA96 deoR nupG* Φ80d*lacZ*ΔM15 Δ(*lacZYA-argF*)U169, *hsdR17*(r_K^- m_K^+), λ–	Invitrogen
BL21(DE3)	F– *ompT gal dcm lon hsdS$_B$*(r_B^- m_B^-) λ(DE3 [*lacI lacUV5-T7 gene 1 ind1 sam7 nin5*])	Novagen
plasmid		
pOJ446	*aac(3)IV*, SCP2, *rep*^{pMB1*}, attΦC31, *ori*T	1
pSET152	*aac(3)IV*, *lacZ*, *rep*^{pMB1*},attΦC31, *ori*T	1
pJTU2463	For construction of genomic library. A derivative of pOJ446 with SCP2 replicon replaced by *int* and *attp* from pSET152	Yao et al. unpublished
pXH-1	pJTU2463 carrying 8.7 kb BamHI from 5H7	This study
pET28b	*Kan*, *rep*^{pBR322}, T7 promoter	Novagen
pXH-2	pET28b carrying ORF24	This study
cosmid		
5H7	pJTU2463 derived comid containing riboflavin catabolic gene cluster	This work
1A4	pJTU2463 derived comid containing	This work

Identification of the products of riboflavin (1) catabolism

M.maritypicum G10 was inoculated into 5 ml NB and grown overnight. The starter culture (1%) was inoculated into 50 ml of fresh M9 medium with riboflavin **(1)** as the only carbon source. The cultures were grown in the dark at 30°C for ~4 days. For HPLC analysis, 200 ul of culture medium was filtered at various time points using 10 kDa filters and 100 ul of the filtrate was injected onto the HPLC column. To determine total lumichrome **(12)** produced, 500ul of culture medium was mixed with 500ul of 1N KOH and the UV-Visible spectrum of the resulting mixture was recorded.[62] The concentration of lumichrome **(12)** was determined using a calibration curve constructed using known quantities of lumichrome **(12)** (2 μg/ml to 80 μg/ml) dissolved in a basic growth medium.

Cosmid library screening for the riboflavin catabolic gene cluster

The cosmid library was constructed in vector pJTU2463 containing *oriT* for conjugation and integration into the *attP* site of *S. lividans*. The genome size of *Microbacterium* is 4~5 Mb. and the resulting library consisted of eight 96-well plates. The cosmid mixture from combining each row (12 samples) of the 96-well plates was transformed into *E.coli* S17-1 and then introduced into *S.lividans* by conjugation (https://www.elabprotocols.com/viewer/?id=504)[63] to give the corresponding *S.lividans* mutant mixture. Sixty four conjugations were carried out and all the spores of the conjugants from each plate were collected to make one glycerol stock. Each mixture was tested on an M9 riboflavin plate for color bleach. After 7 days at 30 °C, plates with mutants carrying cosmid mixtures from Plate 1, row A (1A) and Plate 5, row H (5H)

bleached the riboflavin. Each of the 24 cosmids from rows 1A and 5H was then individually introduced into *S.lividans* and tested on modified M9 agar plates at 30°C for a week. The bottom layer of the modified plates was M9 medium (no glucose) with 1.6% of agar. The top layer was M9 medium (no glucose), 1.6% agar, 100 μg/ml of riboflavin **(1)** and 40 μl of spore stock. Two mutants (1A well 4 and 5H well 7) consumed riboflavin **(1)** (Figure 11A).

Sequencing and annotation of the riboflavin catabolic gene cluster

Next generation sequencing of cosmids 1A4 and 5H7 was performed by AgriLife Genomics and Bioinformatics Services at Texas A&M University using an Illumina HiSeq 2**1**00 instrument. The raw sequence data was analyzed with FramePlot 4.0 Beta and annotated using the BLAST algorithm (http://blast.ncbi.nlm.nih.gov/Blast.cgi) and the SEED (http://theSEED.org).

Cloning and overproduction of recombined His-tagged RcaE and RcaA

The *rcaE* gene was amplified by PCR using cosmid 5H7 as the template (F primer: 5'-AAAA *CATATG* ACCGATCAGAACACCGT-3', R primer: 5'-AAAA *GAATTC* AGA CACGCGACATCGTC-3', engineered NdeI and EcoRI site are in italics). The PCR product was digested with NdeI and EcoRI and ligated into pET28b (NdeI/EcoRI) to generate plasmid pXH-2. This was transformed into BL21 (DE3). The transformants were grown in 3 L of LB medium with 40 μg/mL of kanamycin at 37°C to an OD_{600} of 0.5. IPTG was added to a final concentration of 0.4 mM and incubation was continued at 15 °C for 18 hours. The His-tagged RcaE was purified on a HisTrap HP

column (GE) and buffer-exchanged into 50 mM KH_2PO_4, 300 mM NaCl, 10% glycerol, pH 7.5 by passing through an Econo-Pac 10DG desalting column (Bio-rad). The protein was frozen in liquid nitrogen and stored at -80 °C. RcaA cloned into the pTHT vector and purchased from Genscript. The His-tagged RcaA was overexpressed and purified using the same procedure used for RcaE.

Cloning and overproduction of RcaB and RcaD

The *rcaB* gene was amplified by PCR using cosmid 5H7 as the template (F primer: 5'-AAAA *CATATG* ACGACTGTCGTGACCGA-3', R primer: 5'-AAAA *CTCGAG* TTA CGCGCTCTCGGGAGC-3', engineered NdeI and XhoI site are in italics). The PCR product was digested with NdeI and XhoI and ligated into pMAL (NdeI/XhoI) to generate plasmid pXH-3. The plasmid was transformed into BL21 (DE3). The transformants were grown in 3 L of LB medium with 100 μg/mL of ampicillin and 0.5% glucose at 37°C to an OD_{600} of 0.6. IPTG was added to a final concentration of 0.4 mM and the incubation was continued at 15 °C for 18 hours. RcaA was purified on an amylose resin column followed by cleavage of the maltose tag with Factor Xa protease. The solution was then passed through an amylose resin column where the maltose tag was retained in the column, and the pure protein was recovered as the flow-through. The purified protein was then exchanged into 50 mM KH_2PO_4, 300 mM NaCl, 10% glycerol, pH 7.5 by passing through an Econo-Pac 10DG desalting column (Bio-rad). The protein was frozen in liquid nitrogen and stored at -80 °C. RcaD was similarly overexpressed and purified.

Reconstitution of the RcaA-catalyzed reaction

A reaction mixture (100 μL) of 20 μM RcaA, 250 μM riboflavin **(1)**, 5 mM ATP **(21)**, 5 mM $MgCl_2$ **(68)** was incubated in potassium phosphate buffer at pH 7.5 at 37 °C for 15 mins. After the incubation period, the enzyme was removed by ultrafiltration (10 kDa cut-off filter) and the reaction mixture was analyzed by HPLC followed by LC-MS.

Reconstitution of the RcaB-catalyzed reaction

RcaB was cloned into the pMAL vector and overexpressed in *E. coli* BL21(DE3). The overexpressed enzyme was purified on an amylose resin column. A reaction mixture (1 mL) containing 100 nM RcaB, 250 μM NADH **(22)**, 80 μM FMN **(2)** (Figure 13B – left trace) OR 1 μM RcaB, 250 μM NADH **(22)**, 80 μM riboflavin **(1)** (Figure 13B – right trace) was placed in a quartz cuvette and the reaction was monitored by following the reduction in the spectrum of oxidized flavin between 400 and 510 nm by UV-visible spectroscopy. Similarly 20 nM RcaB was incubated with 50 μM NADH **(22)** and 20 μM riboflavin **(1)** (or FMN **(2)**) to monitor the relative rates for the consumption of NADH **(22)** (Figure 13C) in the enzymatic reaction between 290 and 410 nm for FMN **(2)** (left trace) versus riboflavin **(1)** (right trace). As negative controls the non-enzymatic reduction of FMN **(2)** was monitored between 400 and 510 nm (Figure 13D). Also the oxidation of NADH **(22)** by RcaB in the absence of flavins was monitored between 290 and 410 nm (Figure 13E).

Reconstitution of the RcaD-catalyzed reaction

A reaction mixture (100 μL) containing 20 μM RcaD, 10 mM ATP **(21)**, 5 mM $MgCl_2$ **(68)**, 250 μM ribose **(15)** was incubated in potassium phosphate buffer at pH 7.5 at 37 °C for 10 mins. Protein was removed by ultrafiltration (10 kDa cut-off) and the product was converted to the corresponding oxime by treatment with PFBHA **(65)** at 65 °C for 1 hour and analyzed by LC-MS.

Analysis of the reaction mixture of RcaE

A reaction mixture (100 μL) containing 10 μM RcaE, 100 nM RcaA, 1 μM RcaB, 10 μM RcaD, 500 μM riboflavin **(1),** 5 mM NADH **(22),** 5 mM ATP **(21)** and 5 mM $MgCl_2$ **(68)** was incubated in potassium phosphate buffer at pH 7.5 at 37 °C for 0, 1, 2, 5 and 10 mins. Protein was removed by ultrafiltration (10 kDa cut-off filter) and the reaction mixture from each time point was analyzed by HPLC.

Requirement for FMN in the RcaE reaction

A reaction mixture (100 μL) containing 4 μM RcaE, 400 nM RcaB, 200 μM riboflavin **(1)**, 5 mM NADH **(22)**, 5 mM $MgCl_2$ **(68)** and 5 mM ATP **(21)** in the absence of RcaA was incubated at 37 °C for 10 mins. In a second reaction mixture, 20 μM FMN **(2)** was added to the mixture (100 μL) with 20 μM RcaE, 4 μM RcaB, 200 μM riboflavin **(1)**, 5 mM NADH **(22)**, 5 mM $MgCl_2$ **(68)** and 5 mM ATP **(21)**. Protein was removed by ultrafiltration (10 kDa cut-off filter) and the two reaction mixtures (with and without catalytic amounts of FMN) were analyzed by HPLC (Figure 17).

Oxygen requirement for RcaE reaction

In the glove box, a reaction mixture (100 µL) containing 10 µM RcaE, 1 µM RcaB, 200 µM FMN, 500 µM riboflavin **(1),** 5 mM NADH **(22)**, 5 mM $MgCl_2$ **(68)** and 5 mM ATP **(21)** was incubated at 37 °C for 10 mins with 25, 50, 100, 125 uM oxygen **(20)** prepared by appropriately diluting aerobic buffer containing 260 µM oxygen with anaerobic buffer. A reaction with identical conditions was set up in the presence of anaerobic buffer. Protein was removed by ultrafiltration (10 kDa cut-off filter) and the reaction mixture from each oxygen concentration was analyzed by HPLC.

Analysis of the ribose-phosphate

The reaction mixture after incubation for 10 mins with the enzyme cocktail was treated with PFBHA **(65)** at 65 °C for 1 hour and the corresponding oxime was analyzed by LC-MS (Figure 15C).

2.4 Conclusion

Gene cluster identification for riboflavin degradation in Microbacterium maritypicum G10

Initial screenings for riboflavin catabolic organisms in soil and sewage samples from various locations were unsuccessful. This suggested that it was necessary to screen from environments richer in riboflavin **(1)**. With this in mind, riboflavin **(1)** catabolic microorganisms were readily isolated from dust samples obtained at the DSM riboflavin production plant in Germany. From these *M. maritypicum* G10, capable of growth on riboflavin **(1)** as the sole carbon source, was isolated. HPLC analysis of the growth

medium from this strain demonstrated the conversion of riboflavin **(1)** to lumichrome **(12)** (Figure 10A). Recently another strain of *M. maritypicum* was isolated from soil samples in Japan and optimized for lumichrome **(12)** production. The catabolic operon in this strain was not characterized.[64]

A cosmid library, prepared from *M. maritypicum* G10, was screened in *S.lividans* and two cosmids encoding a riboflavin catabolic cluster were identified. Sequence analysis revealed that the two gene clusters (86% identity, Tables 1 and 2) were on different locations in the genome. Derived on sequence similarity and in vivo screening of the BamHI fragments of one of the cosmids, the gene cluster was localized to a 6.63kb DNA fragment. This DNA segment had 8 open reading frames (Figure 11A and Table 1). Biochemical studies were focused on identifying the reactions catalyzed by four open reading frames encoding for RcaA, RcaB, RcaD, and RcaE. Derived on the sequence analysis it was inferred that RcaF, and RcaG were likely to be involved in riboflavin **(1)** transport and RcaC in pathway regulation. RcaH was not studied further because it is not present in the second catabolic cosmid (1A4).

Role of individual genes in the riboflavin catabolic gene cluster

RcaA, RcaB, and RcaD were overexpressed and their predicted activities as riboflavin kinase, riboflavin reductase and ribokinase, respectively, were confirmed. Sequence analysis of RcaE identified this enzyme as a possible riboflavin dependent N_5,N_{10}-methylene-tetrahydromethanopterin reductase. As this was the only remaining unassigned riboflavin binding protein in the catabolic cluster, it seemed reasonable that RcaE might function as a riboflavin lyase. In support of this hypothesis, it was possible

to demonstrate that a reaction mixture containing purified RcaA, RcaB, RcaD and RcaE catalyzed the conversion of riboflavin **(1)** to lumichrome **(12)** and ribose-5-phosphate **(24)** (Figure 15). Further simplification of the reaction mixture demonstrated that RcaB and RcaE were sufficient to cleave riboflavin **(1)** to give lumichrome **(12)** and ribose **(15)** using FMN **(2)** as the RcaE cofactor (Figure 17).

A proposal for riboflavin catabolism in *M. maritypicum* G10 is shown in Figure 19. In this proposal, RcaF and RcaG transport riboflavin into the cell (not shown). RcaA phosphorylates riboflavin and RcaB reduces the resulting FMN **(2)** to generate the active form of the riboflavin lyase (RcaE) cofactor. Cleavage of FMN **(2)** to lumichrome **(12)** and ribose **(15)** is an oxygen requiring reaction. The final step of riboflavin catabolism involves ribose phosphorylation. The mechanism of riboflavin lyase does not follow any of the canonical motifs in flavoenzymology. One possibility is that reduced FMN **(23)** generates superoxide, which then triggers the ribose **(15)** cleavage reaction by hydrogen atom abstraction from C_1' of the riboflavin ribose. The *M. maritypicum* G10 pathway is considerably simpler than a previously reported pathway in which culture medium metabolites indicated complete isoalloxazine degradation.[31] It is likely that cleavage of the ribose from riboflavin terminates the *M. maritypicum* G10 catabolic pathway because of lumichrome **(12)** insolubility and that more extensive catabolism requires that the ribose **(15)** remains bound to the heterocycle throughout the early stages of the isoalloxazine degradation.

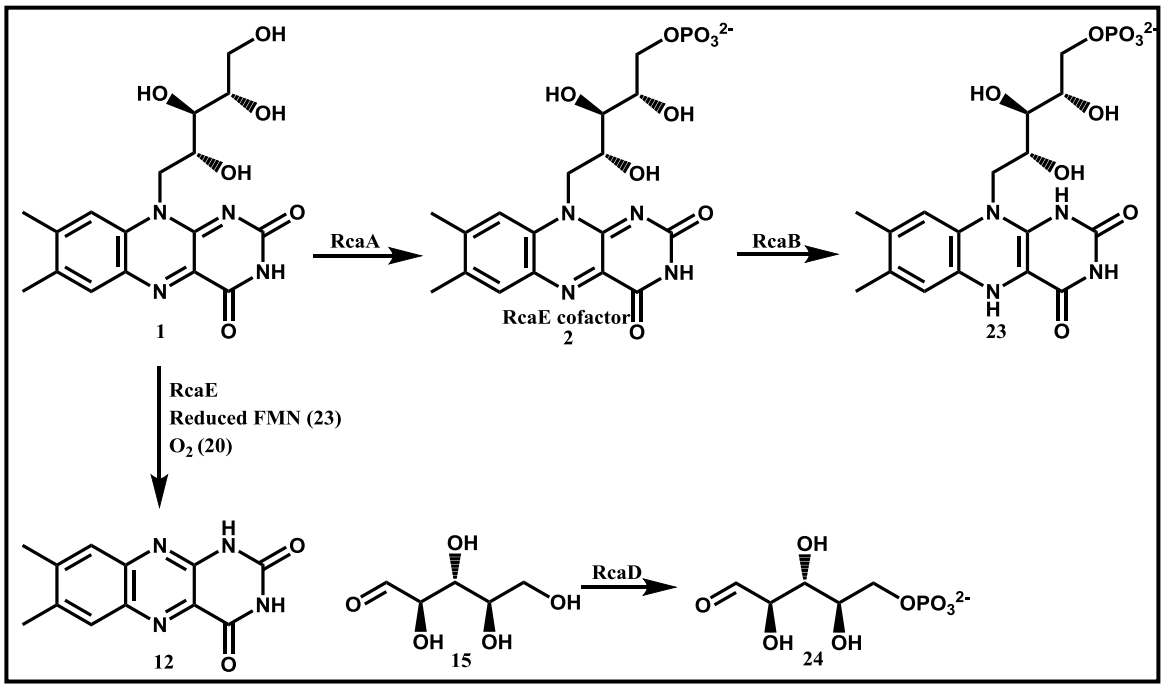

Figure 19: Proposed riboflavin catabolic pathway in *M. maritypicum* G10

Phylogenetic distribution of RcaE

A phylogenetic tree constructed for RcaE using the Fast Minimum Evolution Method is shown in Figure 20 and suggests that RcaE is narrowly distributed in bacteria. In addition to its intermediacy in riboflavin **(1)** catabolism, lumichrome **(12)** has been suggested as a generally important signaling molecule in plant microbe interactions. Lumichrome **(12)** activates the LasR bacterial quorum sensing receptor[65] and lumichrome **(12)** produced by *Sinorhizobium* is an enhancer of alfalfa root respiration and shoot growth.[66] The orthologs marked in red in the phylogenectic tree of RcaE (Figure 20), show that RcaE is well distributed among rhizosphere bacteria like *Azorhizobium caulinodans,* several *Bradyrhizobium species* and root endophytes like *Microbacteium sp. Root322, Leifsonia sp. Root4.* The RcaE orthologs in these species

are likely to be involved in signaling rather than catabolism. Riboflavin catabolism in these species is likely to play an additional signaling role.

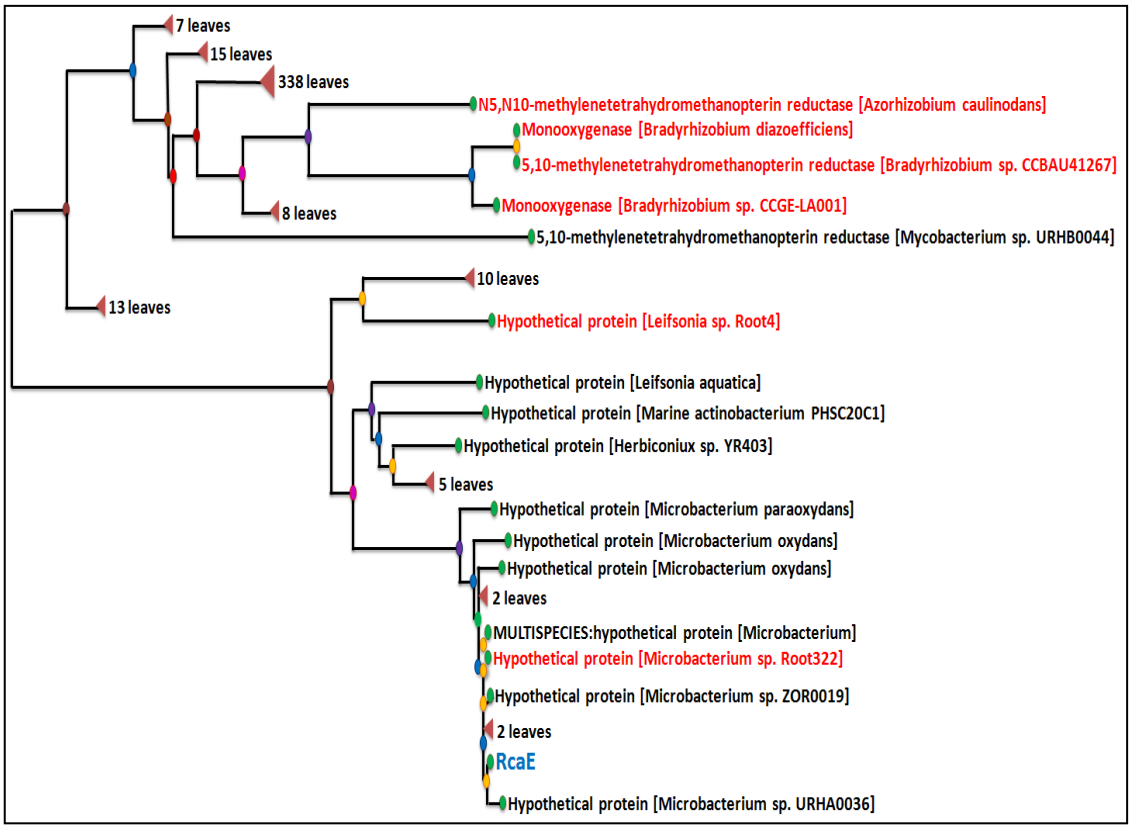

Figure 20: Phylogenetic tree for RcaE. All orthologs with a 38% sequence identity or higher with RcaE have been included in the phylogenetic tree construction.

CHAPTER III

RECONSTITUTION OF RcaE, IDENTIFICATION OF THE COFACTOR AND KINETIC STUDIES FOR THE ENZYME

3.1 Introduction

As described in Chapter II, the conversion of riboflavin **(1)** to lumichrome **(12)** and ribose-5-phosphate **(24)** requires a cocktail of enzymes RcaA, RcaB, RcaD, and RcaE. This result suggested the need for de-convoluting the system to figure out the minimal set of components in the reaction required for the degradation. Ribose-5-phosphate **(24)**, and not the corresponding ribitol-5-phosphate **(70) (Appendix A)** is formed as one of the reaction products. This observation clearly suggests the degradation is not a simple hydrolysis but proceeds via an oxidation followed by cleavage of the sugar side chain on the flavin. This observation is supported by the fact that oxygen is a necessary component for the transformation (Figure 18). Also, the requirement of RcaA as one of the components of the reaction point towards the fact that FMN **(2)** might play an essential role in the activity of the enzyme. Previous attempts to reconstitute the enzyme have failed. So far, all the biochemical studies with this enzyme have been carried out with the crude cell-free extract containing the enzyme.[32]

In this chapter, we report the reconstitution of RcaE followed by elucidation of the individual roles of all the components required for the reaction. The steady-state kinetics for the enzyme has also been reported.

3.2 Results and Discussions

Reconstitution of RcaE (RcaE)

RcaE was incubated with riboflavin **(1)** as the substrate in the presence of excess NADH **(22)** under aerobic conditions. The reaction mixture was analyzed by HPLC (Figure 21). A new peak appeared in the full reaction (green trace) with same retention time as lumichrome **(12)**.

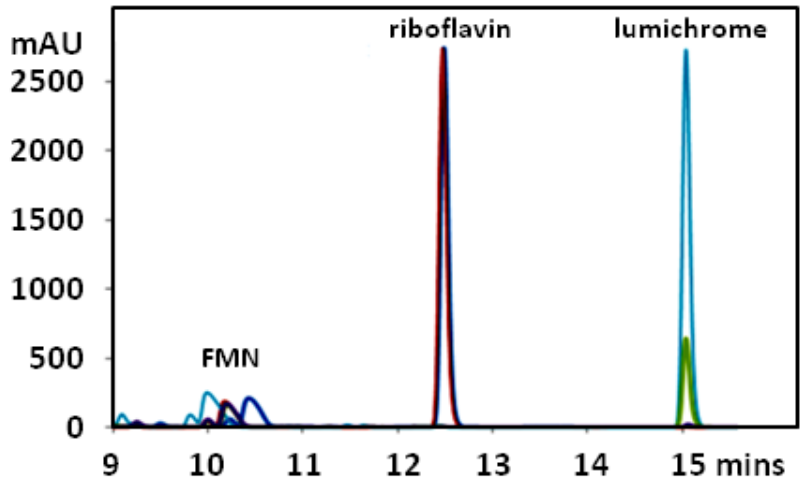

Figure 21: HPLC trace for the reconstitution of RcaE with riboflavin (1) as the substrate, FMN (2) as the cofactor and NADH (22) as the reducing agent. Slight formation of lumichrome **(12)** from riboflavin was observed in the full reaction (**1**, **22** and RcaE) in the absence of FMN **(2)** in the reaction (green trace). Full conversion of riboflavin **(1)** to lumichrome **(12)** occured in the full reaction when FMN **(2)** was present in the reaction (cyan trace). The control reactions include no oxygen **(20)** control (red trace), no RcaE control (blue trace) and no substrate control (purple trace). In all the three controls minute levels (a blip in the chromatogram) of lumichrome **(12)** was observed due to contamination of lumichrome **(12)** in the FMN **(2)** obtained from a commercial source.

The product was further characterized as lumichrome **(12)** with LC-MS where peak with mass $M+H^+$ of 243 Da corresponding to lumichrome **(12)** was observed only in the full reaction (Figure 22). Due to the inefficient conversion of riboflavin **(1)** to lumichrome **(12)** with the above conditions, the reaction was further optimized for maximum activity. A complete reconstitution of the enzyme was achieved with the introduction of catalytic amounts of FMN **(2)** in the reaction (Figure 21 cyan trace). FMN **(1)** did not act as a substrate for the enzyme and was regenerated at the end of the reaction. This indicated that FMN **(1)** acted as the cofactor assisting the cleavage of riboflavin **(1)** to lumichrome **(12)** and ribose **(15)**.

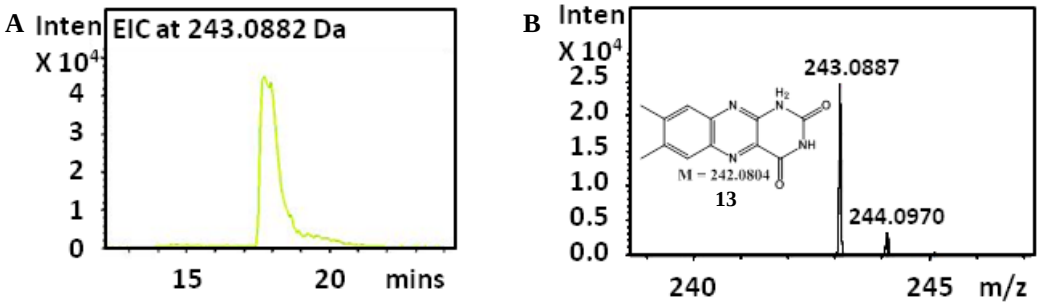

Figure 22: LCMS characterization of lumichrome (12) formed from the RcaE reaction. A: EIC at 243.0822 Da corresponding to the $M+H^+$ of lumichrome **(12)** from the reaction (yellow trace) and for standard lumichrome **(12)** (green trace). B: ESI-MS in the positive mode for the EIC in A showing the formation of lumichrome **(12)**.

Characterization of ribose (15)

The ribityl chain derived product released from the reaction was detected by LCMS after derivatization with PFBHA **(65) (Appendix A)** (Figure 23A). The product

was identified as ribose-PFBHA oxime **(66) (Appendix A)** ($M+H^+$ 346.0711) by co-elution with the standard (Figure 23B).

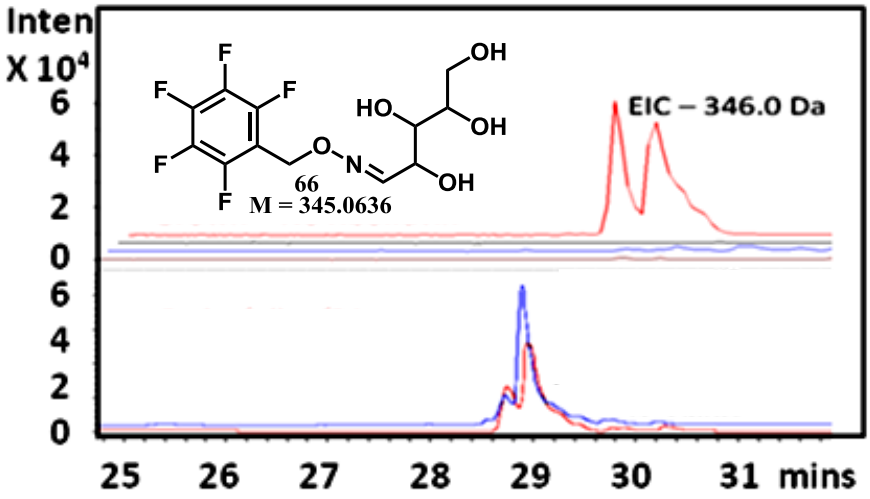

Figure 23: Characterization of ribose as ribose-PFBHA oxime (66) from the RcaE reaction treated with PFBHA by LCMS. A: Extracted Ion Chromatogram (EIC) at m/z 346 Da for detection of ribose-PFBHA oxime **(66)** ($M+H^+$ 346.0711) in the full reaction with riboflavin **(1)**, FMN **(2)**, NADH **(22)** and RcaE (red trace). The control reactions include no oxygen **(20)** control (black trace), no RcaE control (blue trace) and no substrate control (brown trace) where the formation of the oxime is not observed. B: Characterization of the EIC at 346 Da for ribose-PFBHA oxime **(66)** released from the reaction (red trace) by co-elution with EIC at 346 Da for the synthesized standard of **66** (blue trace).

Binding studies with RcaE

The as-isolated enzyme did not show any UV-visible absorbance at 450 nm indicating that the protein did not come bound with either the substrate riboflavin **(1)** or the cofactor FMN **(2).** Binding studies in the glove box revealed that the enzyme initially

binds to the reduced form of FMN **(23)**, which then activates the enzyme to bind with the oxidized form of the substrate riboflavin **(1)**. A weak binding of riboflavin **(1)** in the oxidized to the protein is obtained in the absence of reduced FMN **(23)**.

Synthesis of deazaflavins

An in-vitro reconstitution of the enzyme reinforces the fact that the enzyme binds riboflavin **(1)** and FMN **(2)** simultaneously in the two distinct binding sites. Oxygen **(20)** being one of the substrates for the enzyme, it was necessary to figure out which one of the flavins reacted with triplet di-oxygen to produce the active oxidizing agent in the reaction. In the past, 5-deaza analogs of flavins have been extensively used in flavin-chemistry to shut down SET mechanisms with single electron acceptors like oxygen **(20)** (Fig. 24A).[67] The 5-deaza analogs for both riboflavin **(1)** and FMN **(2)** were synthesized from 5-deazaFAD **(71)** (Appendix E). 5-deazaFMN **(72)** was prepared by phosphodiesterase treatment of 5-deazaFAD **(71)**, whereas 5-deazariboflavin **(73)** was prepared by the treatment of 5-deazaFMN **(72)** with phosphatase (Figure 24B).

Role of FMN as the cofactor

Both 5-deazaFMN **(72)** and 5-deazariboflavin **(73)** were used in enzymatic reactions to probe the role of the individual flavins in molecular oxygen **(20)** activation (Figure 25A). No product formation was observed when the enzyme is incubated with 5-deazaFMN **(72)** instead of FMN **(2)** in the presence of riboflavin **(1)** and dithionite **(44)**. On the contrary, complete conversion of 5-deazariboflavin **(73)** to 5-deaza-lumichrome **(74)** was observed when 5-deazariboflavin **(73)** was used as the substrate instead of

riboflavin **(1)** in a reaction containing FMN **(2)**, dithionite **(44)**, and the enzyme. 5-deaza-lumichrome **(74)** was characterized by LCMS (Figure 25B). The above experimental results establish the role of FMN **(2)** as the cofactor involved in the chemistry with molecular oxygen **(20)**. Riboflavin **(1)**, on the other hand, does not participate in dioxygen chemistry and only serves as the substrate.

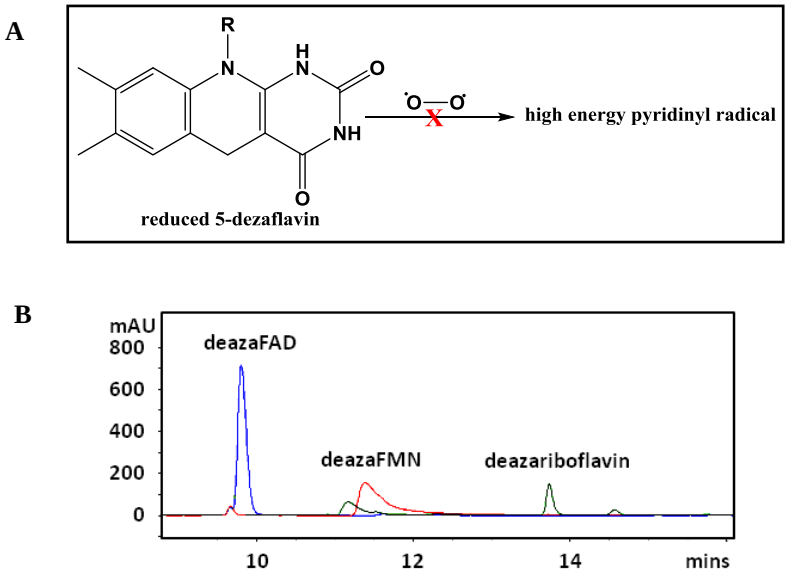

Figure 24: Oxygen chemistry with deazaflavin analogs. A: Scheme indicating no 5-deazaflavin semiquinone radical formation (high energy pyridinyl system) on treatment of 5-deazaflavin with triplet oxygen **(20)**. B: HPLC chromatogram for the enzymatic synthesis of 5-deazaFMN **(72)** from 5-deazaFAD **(71)** on treatment with phosphodiesterase (red trace). The green trace shows the formation of 5-deazariboflavin **(73)** when 5-deazaFMN **(72)** is treated with CIP. Standard 5-deazaFAD **(71)** (blue trace).

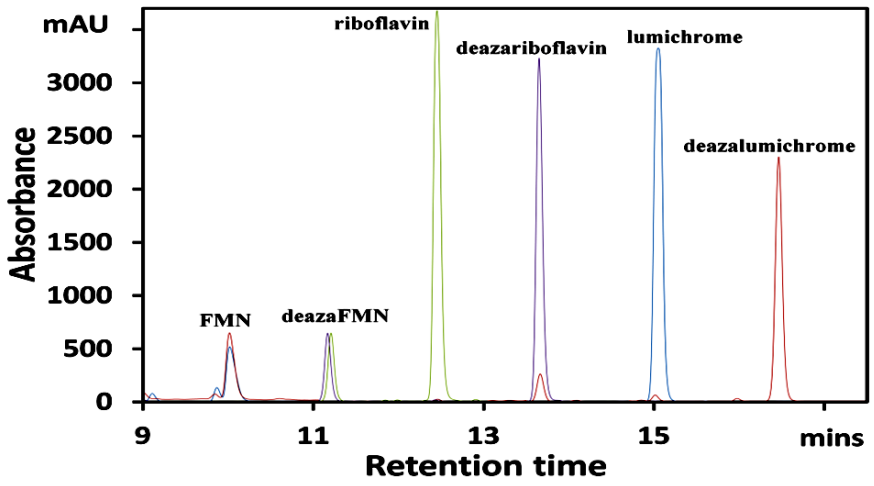

Figure 25: RcaE enzymatic reaction with 5-deazaFMN (72) and 5-deazariboflavin (73). A: HPLC Chromatogram for the reactions with riboflavin **(1)** and FMN **(2)** showing the complete conversion of riboflavin to lumichrome **(12)** (blue trace). When FMN **(2)** and 5-deazariboflavin **(73)** are incubated with the enzyme a complete conversion to 5-deazalumichrome **(74)** is observed (red trace). No lumichrome **(12)** formation is observed in the reaction with 5-deazaFMN **(72)** and riboflavin **(1) (**green trace). No formation of 5-deazalumichrome **(74)** is observed when 5-deazaFMN **(72)** and 5-deazariboflavin **(73)** are incubated with the enzyme (purple trace).

Kinetics of RcaE

To figure out intermediates in the course of the reaction, a kinetic analysis of RcaE was required. Initial rate plots were produced for varying concentrations of riboflavin in the presence of excess in the presence of FRE reducing system containing FMN **(2)** and NADH **(22)** and RcaB. From the slopes of the rate plots, a Michaelis-Menten plot was generated using KaleidaGraph to determine the k_{cat} and the K_m. From the steady-state kinetic data analysis, the enzyme turns out to be a fast enzyme with a k_{cat}

of 4.56 $^{+}$ 0.06 s^{-1} and a K_m of 53.46 $^{+}$ 4.5 µM for riboflavin (Figure 26). This indicated a catalytic efficiency, k_{cat}/K_m, of (8.53 $^{+}$ 0.73) × 10^4 M^{-1} s^{-1}.

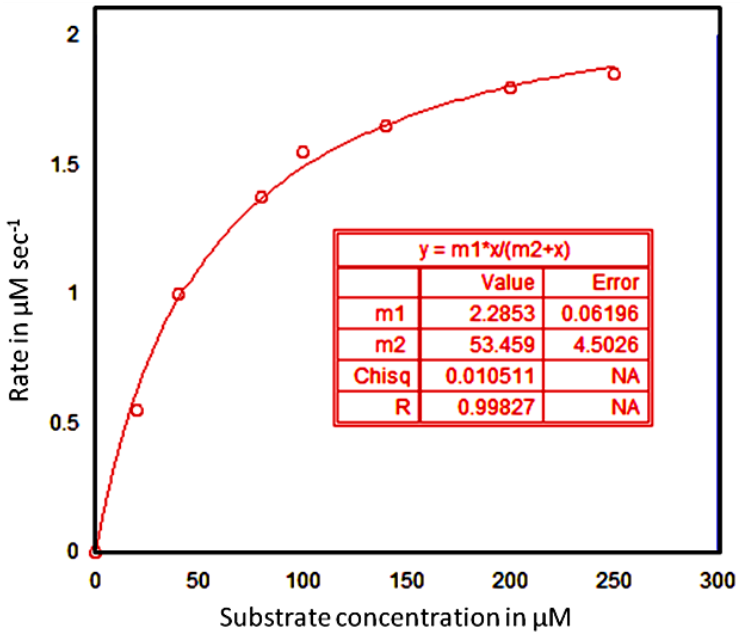

Figure 26: Michaelis-Menten plot for RcaE with riboflavin. The k_{cat} and K_m values have been calculated for riboflavin as the substrate.

3.3 Experimental

Enzymatic reactions and HPLC parameters

All enzymatic reactions were carried out in potassium phosphate buffer at pH 7.5. An Agilent 1260 HPLC equipped with a quaternary pump was used. The system included a diode array UV-Vis detector and products were detected using absorbance at 260 nm and 450 nm. The analysis was performed on a ZORBAX Eclipse XDB-C18 column (15 cm x 4.6 mm, 5 µm particles, Agilent Technologies).

HPLC conditions (for C18 column)

A-Water

B-10 mM ammonium acetate buffer, pH 6.6

C-Methanol

HPLC method

0 min- 0% A 100% B, 4 min- 10% A 90% B, 10 min-25% A 60% B 15% C, 25 min-20% A 30% B 50% C, 28 min-18% A 20% B, 62% C, 30 min-15% A 10% B 75% C, 32 min- 25% A, 75% B, 35 min- 0% A 100% B, 40 min- 0% A 100% B.

LC-MS parameters

LC-ESI-TOF-MS was performed using an Agilent 1260 HPLC system equipped with a binary pump and a 1200 series diode array detector followed by a MicroToF-Q II mass spectrometer (Bruker Daltonics) using an ESI source either in negative or positive mode. The analysis was performed on an LC-18-T column (15 cm x 3 mm, 3 μm particles, Supelco).

LC conditions

A – 5 mM Ammonium acetate buffer, pH 6.6

B – 75 % Methanol and 25 % Water.

LC method: (for positive and negative mode on MS)

0 min-100% A, 2 min-100% A, 12 min-

30% A 70% B, 20 min-30% A 70% B, 25 min-100% A, 35 min-100% A.

Reconstitution of RcaE

A reaction mixture (100 μL) containing 5 μM RcaE, 10 μM FMN **(2),** 5 mM NADH **(22)** and 250 μM riboflavin **(1)** was incubated at 37 °C for 10 mins. Protein was removed by ultrafiltration (10 kDa cut-off filter) and the reaction mixture was analyzed by HPLC followed by LC-MS.

Binding studies with RcaE

Aerobic binding reactions were done with 250 μM RcaE, 500 μM each of FMN **(2)** and riboflavin **(1)** in both oxidized and reduced states. The enzyme was incubated with FMN **(2)** and/or riboflavin **(1)** in phosphate buffer at pH 7.5 for 1 hour at room temperature. The enzyme solution was then buffer exchanged to fresh phosphate buffer at pH 7.5 to get rid of any excess unbound flavin. The enzyme was then denatured by heating at 100 °C for 2 mins. The enzyme was removed by centrifugation, and the remaining solution was then analyzed by HPLC to look for flavin bound to the enzyme. Similar binding experiments were carried out in the glove box with reduced flavins. The enzyme was buffer exchanged with anaerobic phosphate buffer to get rid of all the oxygen **(20)** in the solution before incubation with the reduced flavins.

Enzymatic synthesis of deazaFMN and deazariboflavin

5-deazaFAD was a gift from the Liu lab at the University of Texas at Austin. For the enzymatic synthesis of 5-deazaFMN **(72)**, an reaction volume of 100 uL reaction 10 units of snake venom pyrophosphatase was incubated with 500 μM 5-deazaFAD **(71)** and 5 mM $MgCl_2$ **(68)** for 2 hours at 37^oC to achieve complete conversion. In order to

convert 5-deazaFMN **(72)** to 5-deazariboflavin **(73)** 500 µM of 5-deazaFMN **(72)** was incubated with 10 units of CIP for 1 hour at 37^{o}C.

Reactions with 5-deazaFMN (72) and 5-deazariboflavin (73)

Three separate 100 uL reactions were set up. The first reaction contained 20 µM enzyme with 20 µM FMN **(2)** as the cofactor, 250 µM of riboflavin **(1)** as the substrate and 5 mM dithionite **(44)** as the reducing agent. The second reaction was similar to the first one except 20 µM of FMN **(2)** was used as the cofactor and 250 µM 5-deazariboflavin **(73)** was added as the substrate. The third reaction had 20 µM of 5-deazaFMN **(72)** as the cofactor and 250 µM of riboflavin **(1)** as the substrate. The forth reaction had 20 µM of 5-deazaFMN **(72)** as the cofactor and 250 µM of 5-deazariboflavin **(73)** as the substrate. The reactions were incubated at 37^{o}C for 15 mins followed by filtration of the reactions using a 10 kDa cut-off filter. The filtrates were then analyzed by HPLC and LCMS.

Kinetics of RcaE

FMN **(2)** concentration was 50 µM and NADH **(22)** concentration was kept at saturation (5 mM) in the presence of 100 nM RcaB. The concentration of riboflavin **(1)** was varied from 20 – 500 µM in initial rate determination reactions with 500 nM enzyme. The formation of lumichrome **(12)** was quantified by HPLC using standard concentration curves. Reactions were carried out in 100 µL aliquots. The reactions were quenched at 3 s, 6 s, 10 s, 15 s, 20 s time points by denaturing the enzyme with 0.1 N HCl. Each time-point reaction was repeated in triplicates. The amount of lumichrome

(12) formed was plotted against the time points for each set of substrate concentrations. The initial slopes from each set of substrate concentrations were then plotted against the substrate concentration and fit to the Michaelis−Menten equation using KaleidaGraph (Synergy Software).

3.4 Conclusion

Till date, all of the characterized flavoenzymes have been known to contain one flavin binding site. In contrast, RcaE, has two distinct flavin-binding sites. This has been shown by our experimental evidence for the requirement of two flavins for enzyme activity.

In this chapter, we have elucidated the individual roles of all the reaction components required by RcaE for the conversion of riboflavin **(1)** to lumichrome **(12)**. This enzyme serves as the first example where the reduced cofactor FMN **(23)** is required to catalyze the breakdown of a second flavin molecule, riboflavin **(1)**. Binding studies along with deazaflavin enzymatic reactions have established that the enzyme binds FMN **(2)** in the reduced state and activates it towards an SET chemistry with molecular oxygen **(20)**.

CHAPTER IV

MECHANISTIC HYPOTHESIS FOR AN ACID-BASE MEDIATED DEGRADATION OF RIBOFLAVIN TO LUMICHROME BY RcaE

4.1 Redox chemistry leading to the formation of lumichrome (12)

Under initial reconstitution conditions, RcaE was treated with riboflavin in the presence of reduced nicotinamide cofactor NADH **(22)** to yield lumichrome **(12)** and ribose **(15)** (Figure 21 green trace). As a preliminary mechanistic hypothesis for riboflavin degradation by the enzyme, the oxidized form of the nicotinamide cofactor NAD^+ **(75)** was proposed to act as the cofactor (Figure 27). The source of NAD^+ **(75)** was assumed to be the commercial NADH **(22)** samples where the oxidized cofactor is a contaminant due to aerial oxidation. The limited availability of NAD^+ **(75)** in the reaction mixture explained the inefficient conversion of riboflavin to lumichrome **(12)** under the reaction conditions.

In order to test the mechanistic hypothesis, further experiments were performed with externally added NAD^+ **(75)**. Interestingly, no lumichrome **(12)** formation was observed in the reaction, indicating that the cofactor required for the transformation is probably NADH **(22)** itself. Also, as discussed in Chapter 2 (Figure 18), the enzyme was found to be oxygen **(20)** dependent with no conversion in reactions carried out in the glove box. This requirement for oxygen **(20)** was not supported by the mechanistic proposal. Hence, both the experimental facts invalidated the plausibility of the initial mechanistic hypothesis.

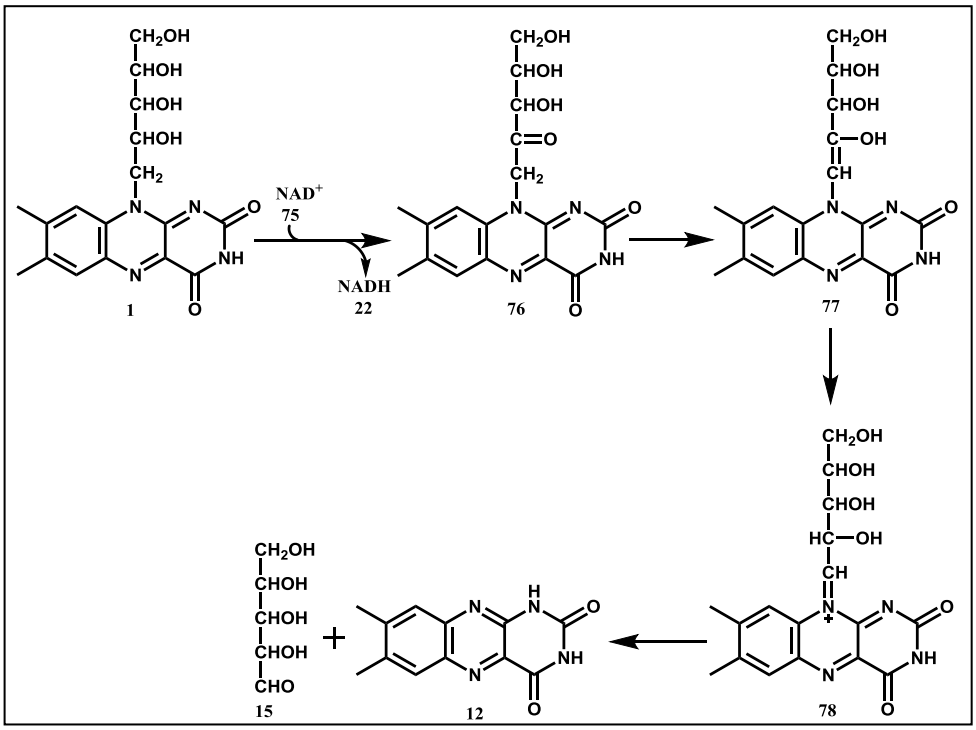

Figure 27: Mechanistic proposal for RcaE. Oxidation of the C_2'-hydroxy group of riboflavin to ketone **76** by the oxidized nicotinamide cofactor **75** followed by the base catalyzed formation of **77** which then tautomerizes to the corresponding imine **78**. This is followed by the subsequent imine bond hydrolysis to give lumichrome **(12)** and ribose **(15)**.

4.2 Acid-base catalyzed mechanism leading to the formation of lumichrome (12)

Having established the roles of the individual flavins in the enzymatic transformation a preliminary investigation into the mechanism indicated that the reaction may proceed via acid-base catalysis at the C_1' of riboflavin with the assistance of the 2' or the 3' hydroxyl groups. It was postulated that the glycosidic bond cleavage in riboflavin was brought about by initial redox chemistry with the cofactor NADH **(22)** and the sugar side chain (Figure 28).

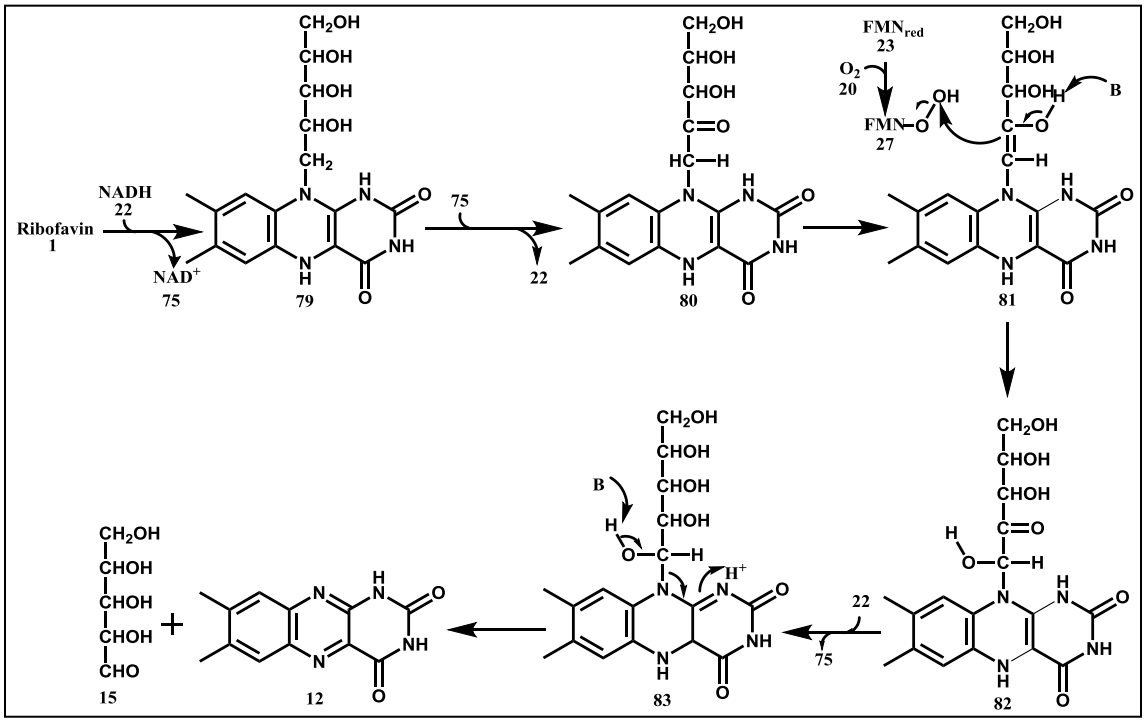

Figure 28: Mechanistic proposal for RcaE involving initial reduction of riboflavin (1) to reduced flavin (79) by NADH (22). In the next step, oxidation of the C_2'-hydroxy group of riboflavin to ketone **80** is carried out by the oxidized nicotinamide cofactor NAD^+ **(75)**. The corresponding enol **81** then adds to a hydroxyl group by nucleophilic attack on the cofactor flavin-hydroperoxide **(27)** to give intermediate **82** which then degrades to lumichrome **(12)** and ribose **(15)** via the formation of intermediate **83.**

The mechanistic proposal as outlined in Figure 28 involves a masked redox reaction with the nicotinamide cofactor. This did not agree with our observations where dithionite **(44)** was able to replace NADH **(22)** in the reactions indicating that the only role of the nicotinamide cofactor was the reduction of the flavin. Also, with the proposed mechanism operating, the enzyme would most likely be a metal dependant enzyme where the metal would be required to stabilize the ketone formed at C_2'. However, no

metal was required in the reaction. Moreover, an ICP-MS [68] analysis of the protein also revealed no metal ions bound to the enzyme. No deuterium incorporation was observed as well in the ribose **(15)** released from the reactions carried out in deuterated buffer (Figure 29). This suggested that no exchangeable protons were formed on the ribose chain during the transformation. Furthermore, the role of the hydroxyl groups of the sugar chain in the mechanism was conclusively ruled out by analog studies where 2'-deoxyriboflavin **(84) (Figure 30)** and hydroxyethylriboflavin **(85) (Figure 30)** served as the substrates (Figure 31). The key evidence that ruled out the possibility of an ionic mechanism operating was obtained when lumiflavin **(86) (Figure 30)** was found to be a substrate for the enzyme (Figure 32). The above results clearly indicated that a radical mechanism was operating in the enzymatic transformation.

4.3 Results

Reaction in deuterated buffer and with substrate analogs

No deuterium incorporation was observed in the ribose-PFBHA oxime **(66)** when the reactions were carried out with riboflavin **(1)** in deuterated buffer in the presence of PFBHA **(65)** suggesting the absence of exchangeable protons in the ribose side chain of riboflavin **(1)** (Fig 29). 2'-deoxyriboflavin **(84)** lacking the 2'-hydroxy group and hydroxyethylflavin **(85)** lacking the 3'-hydroxy were tested as substrates for the enzyme. Lumichrome **(12)** was identified as the product for both the reactions (Figure 31). Also, the conversion of lumiflavin **(86)** to lumichrome **(12)** was observed by HPLC analysis (Figure 32). These observations eliminated the possibility that the hydroxyl groups on the ribose played any role in the mechanism.

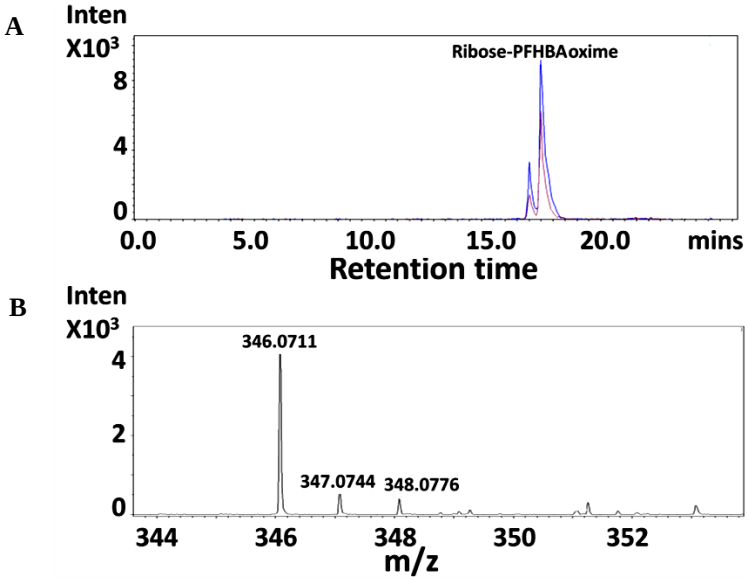

Figure 29: LCMS analysis of RcaE reaction with riboflavin (1) as the substrate and reduced FMN (23) as the cofactor in the presence of PFBHA (65) in deuterated buffer. A: Extracted Ion Chromatogram (EIC) at m/z 346.07 Da to show the formation of ribose-PFBHA oxime **(66)** ($M+H^+$ 346.0712) in the reaction (blue trace). **66** released from the reaction is co-eluted with a synthesized standard of **66** (brown trace). B: ESI-MS trace in the positive mode of the EIC peak in A (blue trace) showing no deuterium incorporation (no enhancement in $M+2^+$ peak) in the PFBHA trapped ribose **(15)** that is released from the reaction.

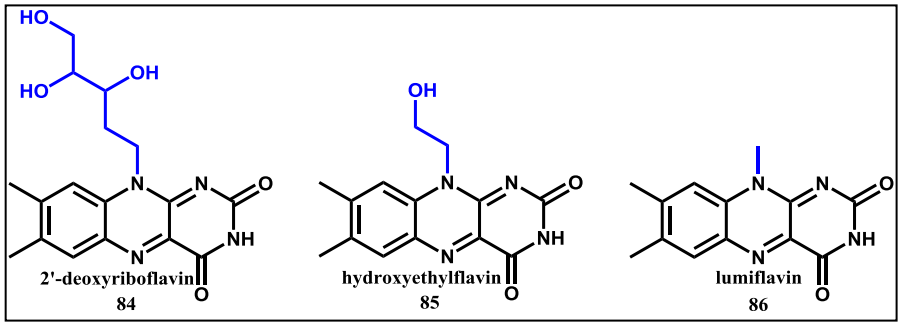

Figure 30: Structures of the flavin analogs tested as substrates for RcaE.

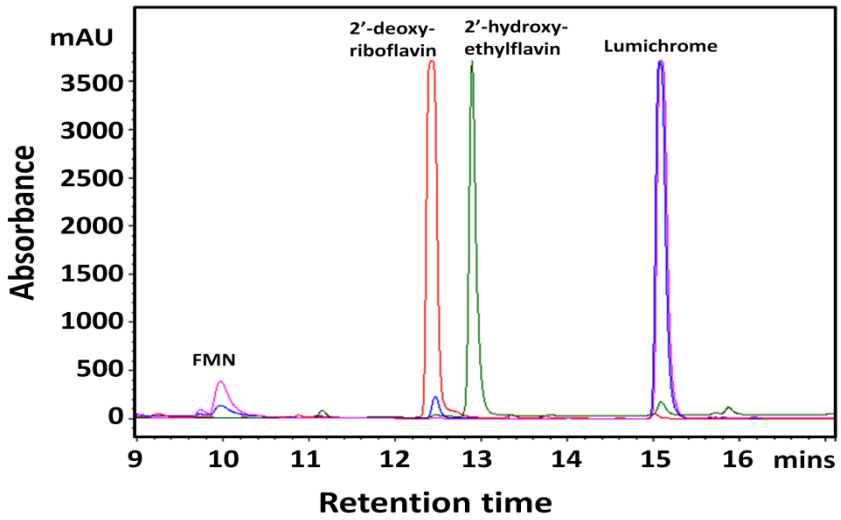

Figure 31: RcaE reactions with 2'-deoxyriboflavin (84) and 2'-hydroxyethylriboflavin (85). HPLC chromatogram of RcaE reaction with substrates **84** (blue trace) and **85** (pink trace), showing the complete conversion of both the analogs to lumichrome **(12)**. In both the reactions reduced FMN **(23)** serves as the cofactor. The red trace corresponds to the synthesized standard **84** and the green trace to synthesized standard **85**.

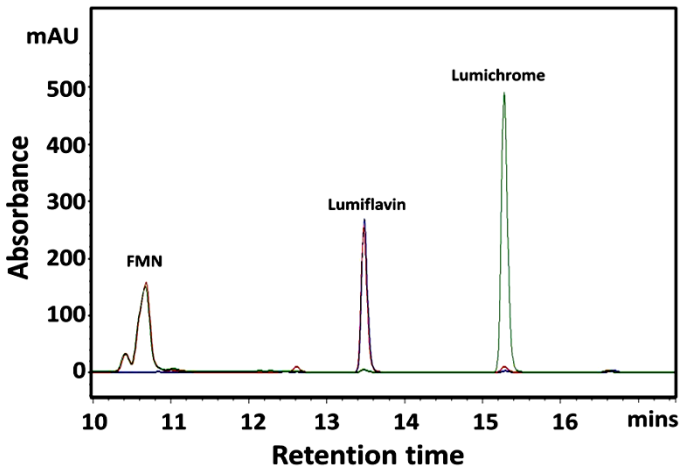

Figure 32: RcaE reaction with lumiflavin (86). HPLC chromatogram of RcaE reaction with **86** as the substrate and reduced FMN **(23)** as the cofactor shows the complete conversion of **86** to lumichrome **(12)** (green trace). The red trace is the no enzyme control and the blue trace is the synthesized standard **86**.

4.4 Experimental

Synthesis of 2'-deoxyriboflavin (84)

Procedure for the synthesis of **84** is similar to the procedure followed for the synthesis of cyclopropylmethylflavin **(115)**. The NMR of the reaction intermediates are shown in Appendix F.

Synthesis of N-hydroxyethylflavin (85)

The synthetic route to the substrate analog is given in Figure 33.

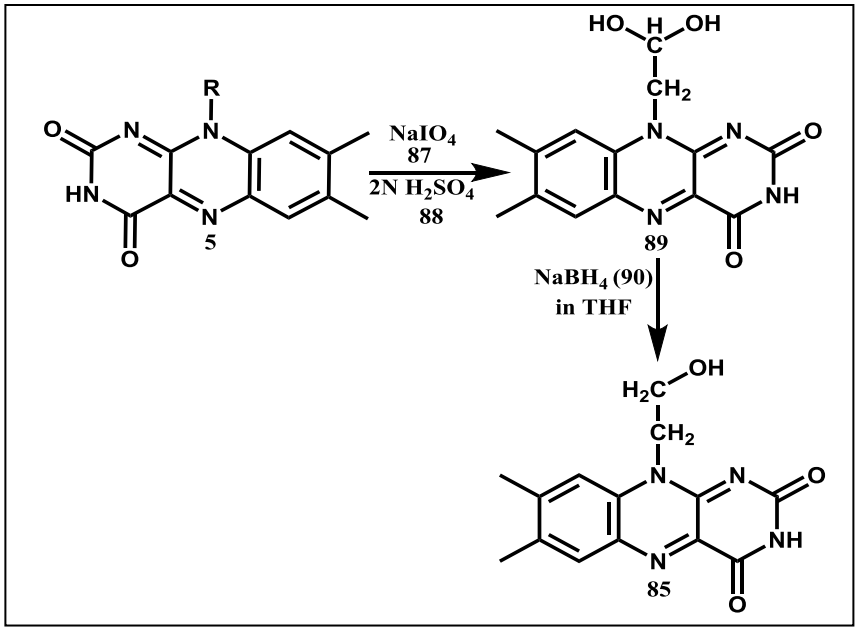

Figure 33: Synthetic scheme for N-hydroxyethylflavin (85) synthesis.

Procedure

*Synthesis of flavin-N_1-carbaldehyde **(89)***[69]

To a suspension of riboflavin (5 grams, 1.35 mmoles) in 2N aqueous sulfuric acid **(88)** (130.5 mL) cooled to 0 °C in a flask covered with tin foil, sodium

orthoperiodate **(87)** (10.4 grams, 48.5 mmoles) dissolved in 120 mL of water was added. The reaction was carried out on ice for 30 mins. Then the ice was removed, and the reaction was brought to room temperature. When the reaction became clear, the pH was adjusted to 3.8 – 3.9 by adding solid sodium bicarbonate. The precipitate obtained was washed with cold water, ethanol and diethyl ether to yield the product. Yield was 2.8 grams (75%). Figure 34 shows the NMR of purified **89** as compared to the starting material riboflavin.

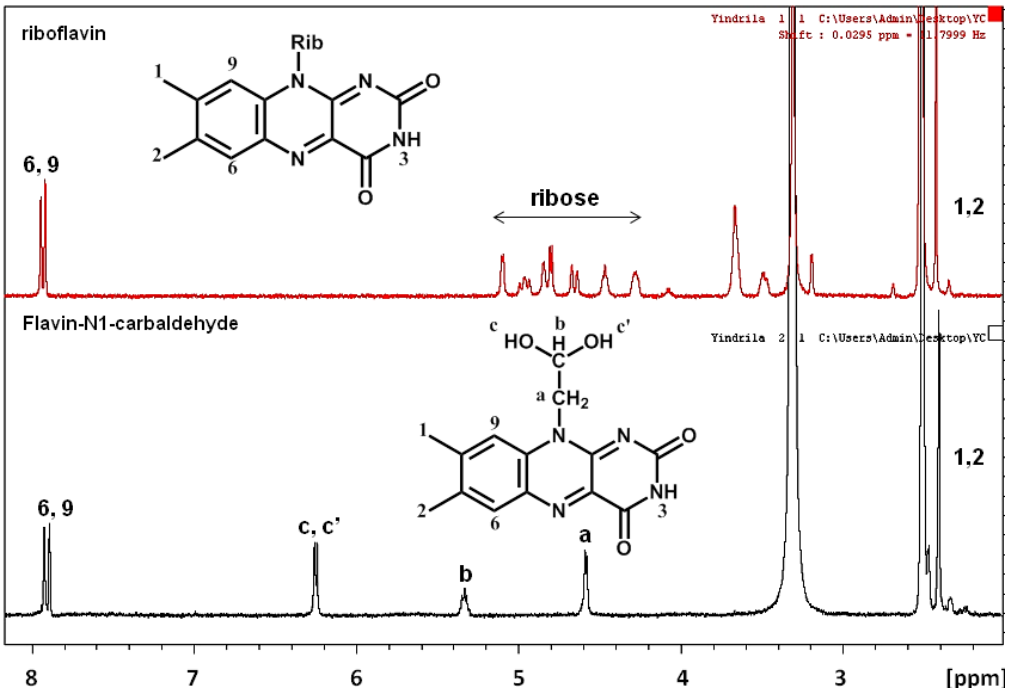

Figure 34: Proton NMR of starting material riboflavin (1) (top). Proton NMR of the diol form of flavin-N_1-carbaldehyde (89) (bottom).

Synthesis of N-hydroxyethylflavin (85)

89 (1 gram, 2.82 mmoles) was dissolved in 10 mL of dry THF in a round bottom flask under an inert atmosphere. Sodium borohydride **(90)** (189 mg, 5 mmoles) was added to the mixture and the reaction was stirred at room temperature for 6 hours. The reaction product **85** was purified by HPLC and characterized by LCMS (Figure 35). **85** was obtained in 50% yield.

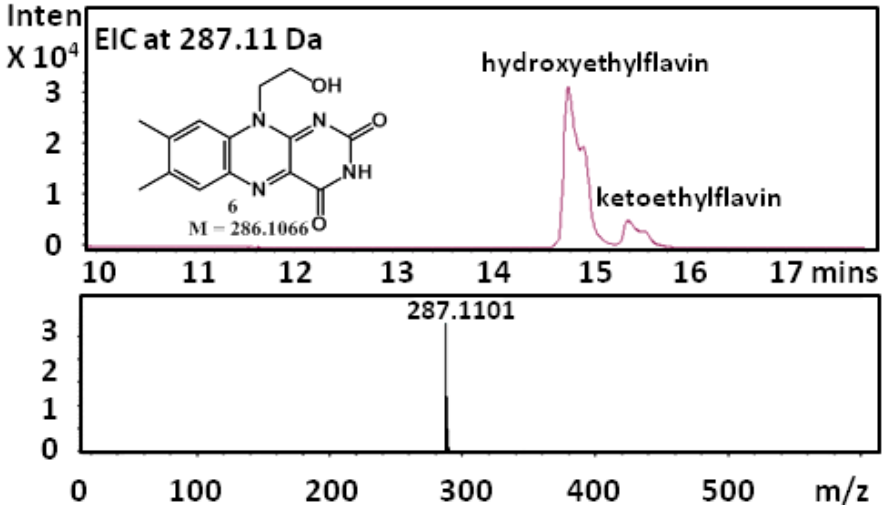

Figure 35: LCMS trace for purified hydroxyethylflavin (85).

Synthesis of Lumiflavin

Lumiflavin was synthesized via following route (Figure 36). [71]

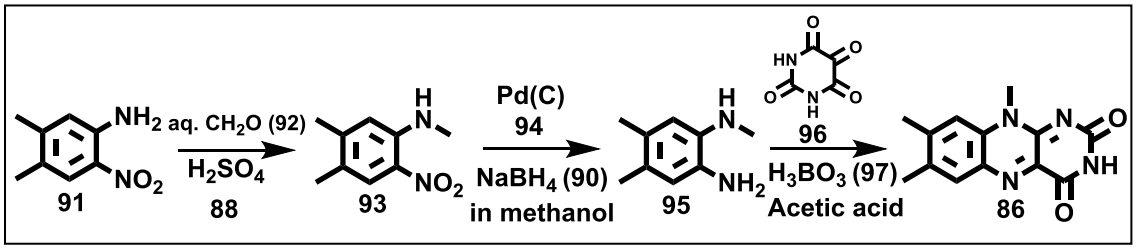

Figure 36: Scheme for synthesis of lumiflavin (86).

Procedure

*Synthesis of N-4,5-trimethyl-2-nitoaniline **(93)***

Aqueous formaldehyde **(92)** (37%; 20 ml) was added dropwise over a period of 3 hours to a stirred mixture of 4,5-dimethyl-2-nitroaniline **(91)** (500 mg; 2.7 mmol) and (0.01 H_2SO_4 **(88)**; 20 mL). The reaction mixture was heated at 65^oC for 3 hours, then cooled to room temperature and poured into ice water (400 mL). The solid product was collected by filtration and dissolved in ethyl acetate. The solution was washed with saturated aqueous $NaHCO_3$, dried over $MgSO_4$, filtered, and evaporated to obtain the product **93** (yield 90%) as a red-orange solid. This compound was used in the next step without further purification.

*Synthesis of N-1,4,*5*-trimethylbenzene-1,2-diamine **(95)***

Catalytic reduction of **93** was carried out with Pd/C **(94)** (10% Pd/C, 4% Pd w/w) and $NaBH_4$ **(90)** (3 eqv.) in MeOH at r.t. under argon. After 40 mins the reaction mixture was filtered through celite using methanol as eluent. The solvent was evaporated to give the product **95** (Yield > 90%) which is used for the next step without further purification.

*Synthesis of lumiflavin **(86)***

95 (195 mg; 1.3 mmol), alloxan monohydrate **(96)** (3 eqv.) and H_3BO_3 **(97)** (2 eqv.) in 20 ml acetic acid were stirred under argon for 12 h. The fluorescent yellow precipitate obtained was collected by filtration and washed with acetic acid (30 ml) followed by ether to get the final product lumiflavin **(86)** in 40% yield. The proton NMR for **86** is shown in Figure 37.

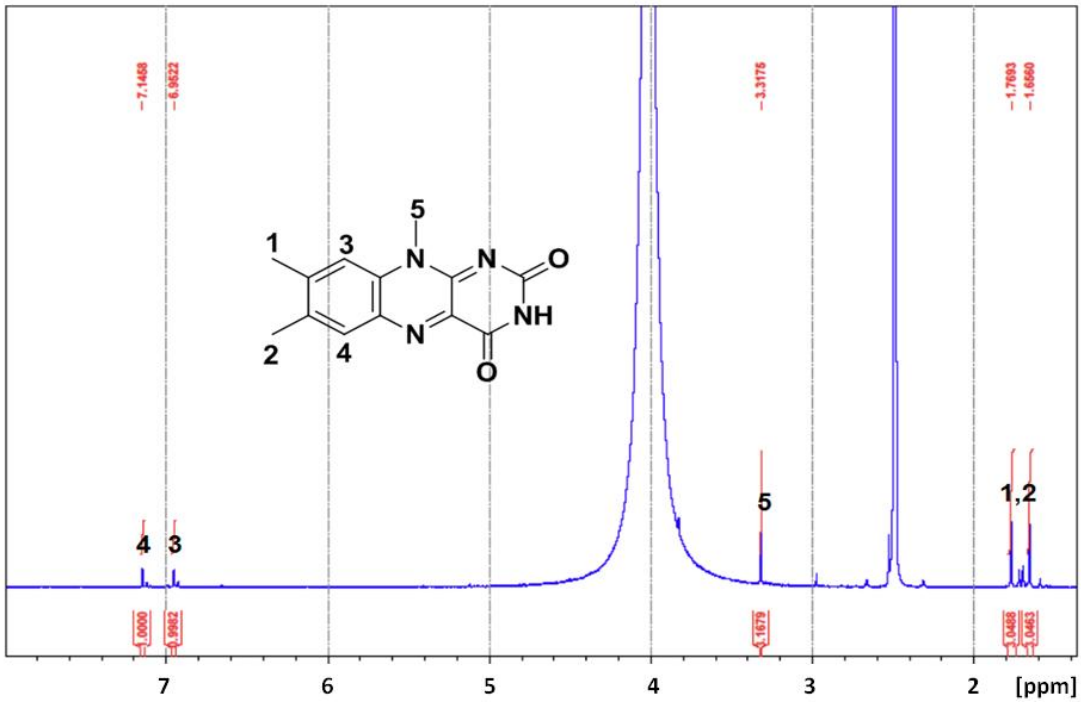

Figure 37: Proton NMR of lumiflavin (86).

Enzymatic reactions with 2'-deoxyriboflavin (84), N-hydroxyethylriboflavin (85) and lumiflavin (86)

2'-deoxyriboflavin **(84)**, N_{10}-hydroxyethylriboflavin **(85)** and lumiflavin **(86)** were synthesized using the reported literature procedure. Reactions were carried out with 250 µM of the three analogs in individual reactions with 20 µM enzyme, 20 µM FMN **(2)** and NADH **(22)** as the reducing agent. The reactions were incubated at 37 $^{\circ}$C for 15 mins followed by filtration of the reactions using a 10 kDa cut-off filter. For 2'-deoxyriboflavin **(84)** and N_{10}-hydroxyethylriboflavin **(85),** the filtrate was divided into two parts. The first part was analyzed by HPLC to look for the formation of lumichrome **(12)**. The second part was treated with pentafluorobenzylhydroxylamine (PFBHA) **(65)** at 65 $^{\circ}$C for 1 hour to trap the corresponding sugars released. The solution was then

analyzed by LCMS to look for the trapped sugar-oxime. The identities of the sugar-oximes were confirmed by co-elution experiments with the standard oximes (Appendix D) which were synthesized by incubation of 2'-deoxyribose **(98)** and 3-hydroxypropanol **(99)** with PFBHA **(65)** (Figures 38, 39).

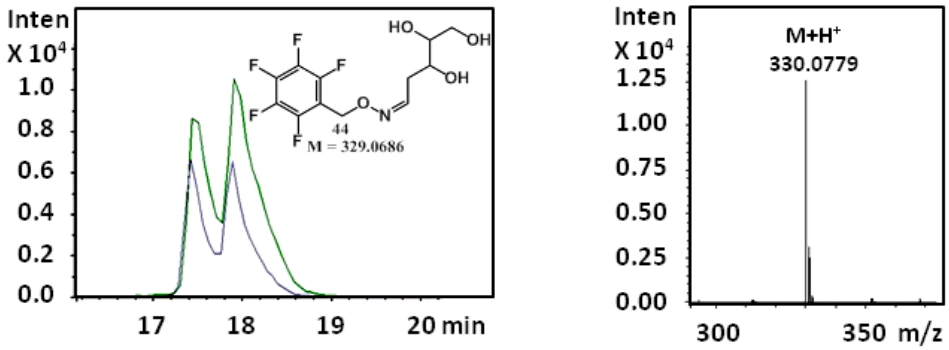

Figure 38: LCMS characterization of the sugar products released from 2'-deoxyriboflavin (84) after treatment with PFBHA. Left trace – EIC at 330.07 Da corresponding to the $M+H^+$ of 2'-deoxyribose-PFBHA oxime **(100)** from the reaction (blue trace) co-eluted with synthesized standard of **100** (brown trace). Right trace – ESI-MS in the positive mode for the EIC trace in A showing the mass for **100**.

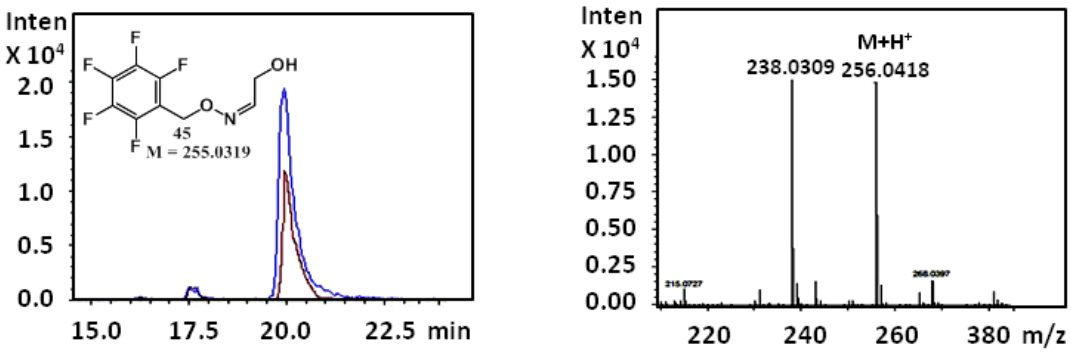

Figure 39: LCMS characterization of the sugar products released from hydroxyethylflavin (85) after treatment with PFBHA. EIC at 316.04 Da corresponding to the $M+H^+$ of N-hydroxyethylflavin-PFBHA oxime **(101)** from the reaction (green trace) co-eluted with synthesized standard of **101** (blue trace). Right trace – ESI-MS in the positive mode for the EIC trace in A showing the mass for **101**.

CHAPTER V

FLAVIN DERIVED SUPEROXIDE RADICAL MECHANISM FOR RIBOFLAVIN DEGRADATION BY RcaE

5.1 Introduction

Substrate analog studies have ruled out the possibility of an acid-base mediated cleavage of the ribose chain of riboflavin **(1)** to give lumichrome **(12)**. Here we report the mechanistic key points of the interesting degradation reaction. We have probed into the possible intermediacy of a flavin-semiquinone superoxide radical pair **(Appendix C)** in the formation of lumichrome **(12)** from riboflavin **(1)**.[73]

It is well known in flavin dependent oxidases and oxygenases that reduced flavin **(23)** reacts with molecular oxygen **(20)** to form a flavinsemiquinone-superoxide radical pair in a fast step.[15] While in oxygenases, this radical pair then rapidly collapses to give $C_4\alpha$-hydroperoxy-flavin adduct **(27) (Appendix C)** which participates in the oxidation of the substrate; in oxidases, oxidized flavin is formed directly from the $C_4\alpha$-hydroperoxy-flavin adduct **(27)**. In cryptochromes, the flavin semiquinone-superoxide radical pair formed during the dark re-oxidation of protein-bound flavin is responsible for cryptochrome derived magnetoreception.[74] CPO-coproporphyrinogen oxidase is the only example of cofactor-independent oxygenase where a substrate derived superoxide radical anion **(104)** abstracts hydrogen atom from the substrate **(102)** to undergo further chemistry (Figure 40).[75] So far, the only example of a flavin derived superoxide radical **(104)** abstracting a hydrogen atom from a primary amine substrate **(108)** is the mixed function amine oxidase (MFAO) where the superoxide radical **(104)** is proposed to

oxidize hydroxylamines to nitroxides [76] In this case the superoxide **(104)** abstracts a hydrogen atom from the N-H bond resulting in a one-electron oxidation. But, the participation of the superoxide **(104)** in these systems have been proposed but have not been experimentally verified.[77] Till date, there is no report in the literature of a flavin derived superoxide radical anion **(104)** abstracting hydrogen from a relatively stable C-H bond of the substrate. For RcaE, superoxide incorporation experiments along with substrate analog studies support an unanticipated mechanism for a radical derived cleavage of riboflavin **(1)** to form lumichrome **(12)**.

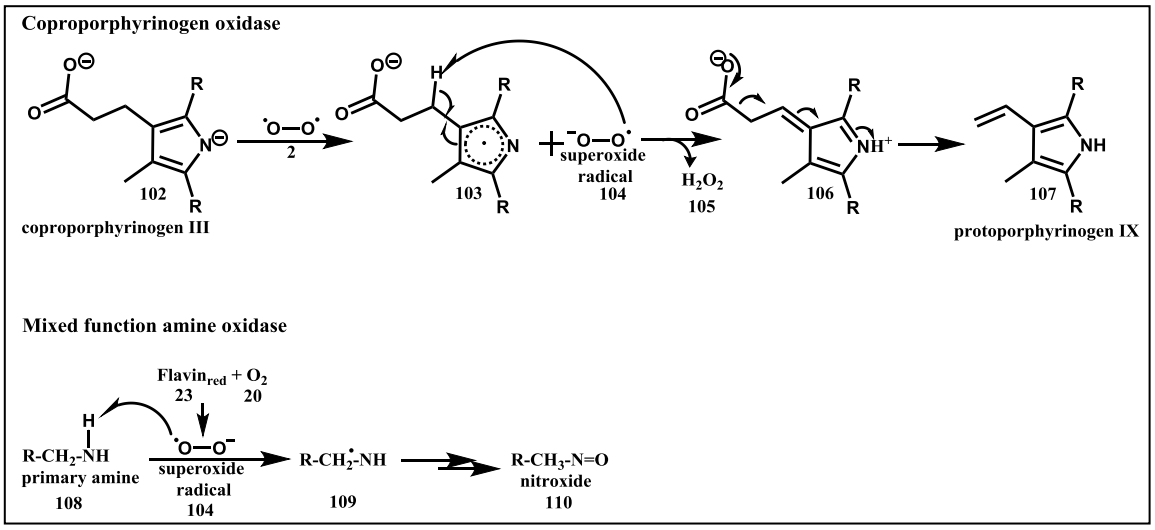

Figure 40: Mechanistic proposal for the intermediacy of superoxide radical anion in coproporphyrin oxidase and mixed amine oxidase.

5.2 Results and Discussions

Non-enzymatic degradation of riboflavin by superoxide

With the possibility of a radical mechanism operating in the enzymatic

transformation, the most plausible hypothesis for a radical initiator was a flavin derived superoxide radical anion **(104)**. It is widely known in the literature that superoxide radical anion **(104)** is generated from oxygen **(20)** in the presence of riboflavin **(1)** undergoing photodegradation in air.[33,78] This suggests that superoxide radical anion **(104)** might be generated as an intermediate by the enzyme when the reduced cofactor FMN **(23)** reacts with molecular oxygen **(20)**. superoxide radical anion **(104)** may then initiate a subsequent radical reaction by H-atom abstraction at the C_1' of the substrate riboflavin eventually forming lumichrome **(12)**. In order to validate the hypothesis, it was necessary to test the non-enzymatic degradation products of riboflavin **(1)** when treated with potassium **(111)** superoxide.[79] When riboflavin **(1)** was heated with excess of potassium superoxide **(111)** (Appendix G), lumichrome **(12)** was detected as one of the degradation products by HPLC (Figure 41)

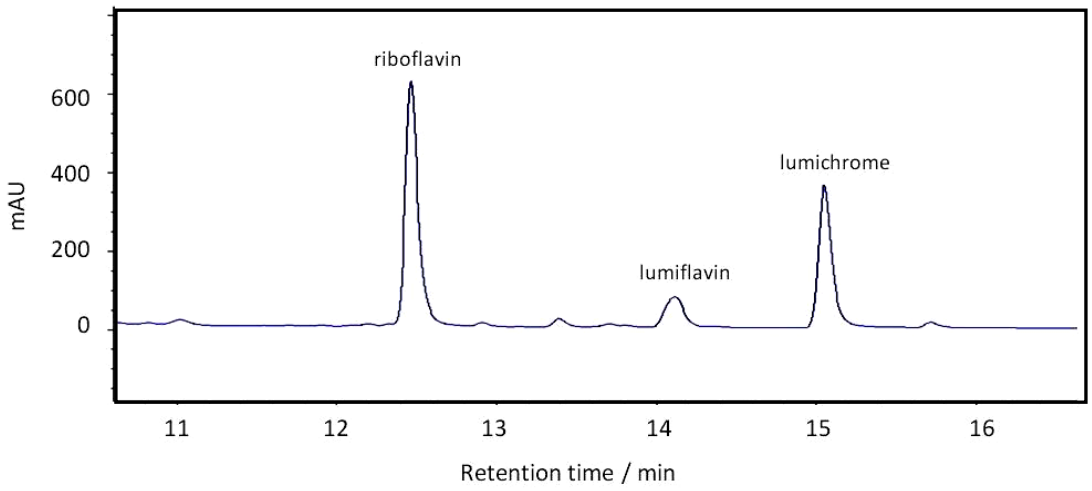

Figure 41: Non-enzymatic degradation of riboflavin (1) to lumichrome (13) and trace amounts of lumiflavin (86) when treated with excess potassium superoxide (111).

Enzymatic reaction with superoxide

Extending the observations of the non-enzymatic break-down of riboflavin **(1)** by superoxide **(104)** to the enzymatic degradation of riboflavin by RcaE, we proposed that the superoxide radical anion **(104)**, formed by riboflavin **(1)** reacting with molecular oxygen **(20)** at the active site, further reacted with the substrate riboflavin **(1)** to give lumichrome **(12)**. When RcaE was incubated with riboflavin **(1)** in the presence of limiting concentrations of potassium superoxide **(111)**, formation of lumichrome **(12)** was observed in proportional amounts to the added superoxide **(111)**. The no enzyme control under similar conditions generated minimal amounts of lumichrome **(12)** (Figure 42A). A proportional increase in the formation of lumichrome **(12)** was observed with increasing concentrations of added potassium superoxide **(111)** in the presence of the enzyme, whereas no change in the amounts of lumichrome **(12)** formed was observed with increasing concentrations of added potassium superoxide **(111)** in the absence of the enzyme (Figure 42B). When superoxide dismutase was used as one of the components of the enzymatic reaction reduced amounts of the formation of lumichrome **(12)** was observed. Also, pre-incubation of the **111** with superoxide dismutase abolished the enzyme activity (Figure 42C). These results clearly suggested that superoxide **(104)** was an intermediate in the enzymatic degradation pathway of riboflavin **(1)** to lumichrome **(12)** and ribose **(15)** by RcaE. The above experiments pointed to the fact that superoxide **(104)** could also be used as the substrate by the enzyme.

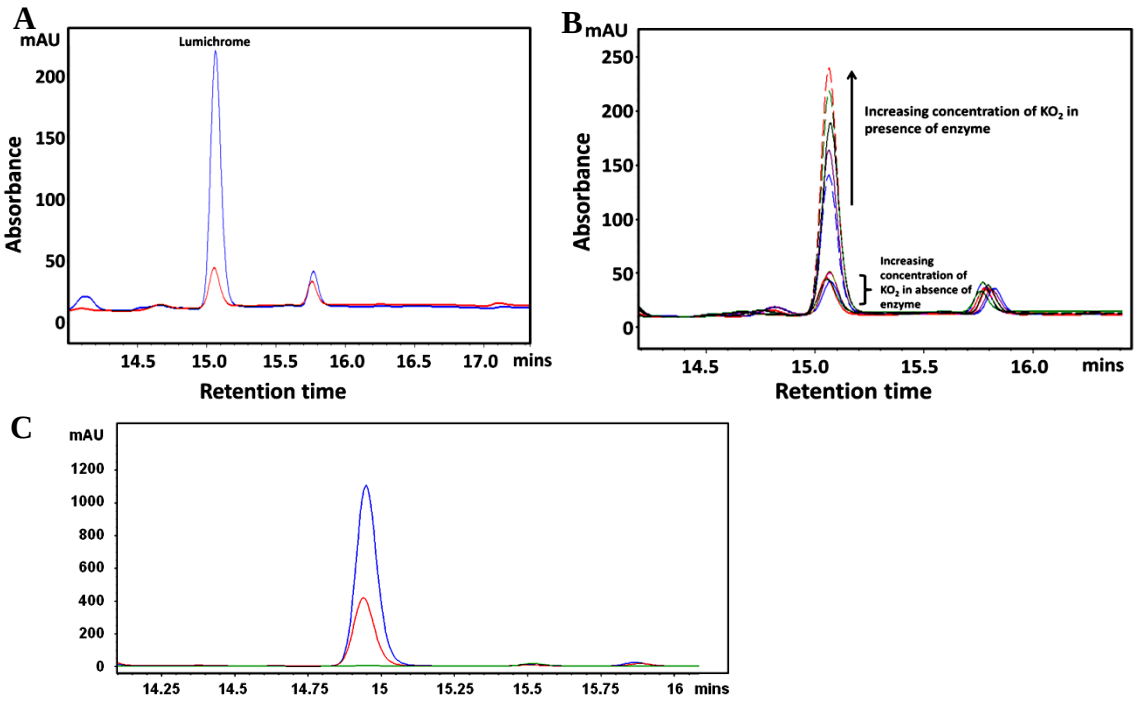

Figure 42: RcaE reaction with Superoxide. A: HPLC trace for the formation of lumichrome **(12)** in the RcaE reaction with riboflavin **(1)** as the substrate in the presence of limiting concentrations of external potassium superoxide **(111)**. FMN **(2)** and reducing agents are absent in the reaction (blue trace). Slight formation of lumichrome **(12)** in the no enzyme control (red trace) B: HPLC the chromatogram showing superoxide concentration dependent formation of lumichrome **(12)** in the presence of RcaE. The increase in the formation of lumichrome **(12)** corresponds to the increase in the concentration of potassium superoxide **(111)** (upper set of traces) from (20 – 200) µM (20, 40, 80, 160, 200 µM). No such increase in the formation of lumichrome **(12)** (lower set of traces) is observed with the increasing concentrations of potassium superoxide **(111)** in the absence of enzyme. C: HPLC trace for the formation of lumichrome **(12)** by enzymatic reaction with riboflavin **(1)** and potassium superoxide **(111)** only (blue trace). The red trace shows reduced formation of lumichrome **(12)** due to the addition of superoxide dismutase in the reaction. Preincubation of potassium superoxide **(111)** with superoxide dismutase followed by incubation with RcaE and riboflavin (green trace) shows no formation of lumichrome **(12).**

Cyclopropylflavin (115) as a radical trap to detect the formation of riboflavin-C_1' radical as an intermediate

In the case of oxidases and oxygenases the FMN-semiquinone superoxide radical pair formed recombines to give flavin hydroperoxide **(27)** (Appendix C). However, in the case of RcaE, we propose that instead of recombining, the superoxide radical **(104)** in the radical pair proceeds to abstract H-atom from the C_1' of the ribose chain of substrate riboflavin to give riboflavin-C_1' substrate radical **(114)** (Figure 43).

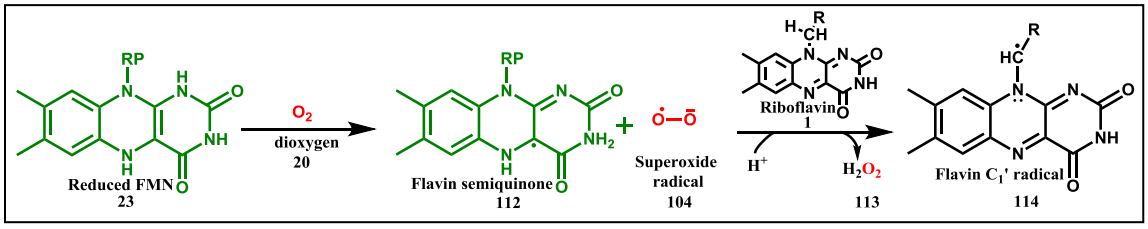

Figure 43: Formation of riboflavin C_1'-radical (114)

In order to test this hypothesis, riboflavin analog cyclopropylflavin **(115)** was designed to be used as a radical trap. In case of cyclopropylflavin **(115)**, lumichrome **(12)** formation may proceed by two routes. In the normal route (Figure 44, Route 1) **115** may cleave to give lumichromne **(12)** and cyclopropylcarboxaldehyde **(116)**. The other route by which **115** can be degraded by the enzyme is given by Route 2 in Figure 44. Here, a radical at C_1' position would initiate a β-bond scission to open the cyclopropyl ring eventually leading to either the tagging of the side chain to the enzyme or the release of butanal **(117)** as the final product.

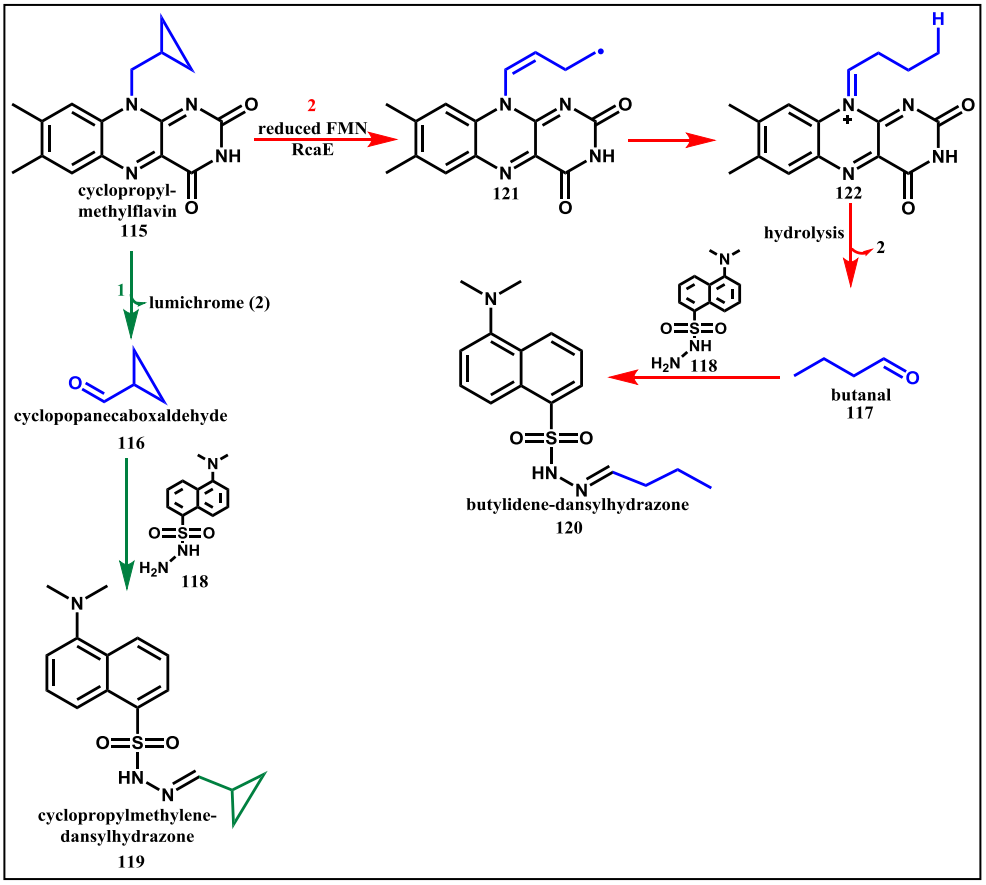

Figure 44: Scheme for the formation of lumichrome (2) from cyclopropylflavin (115) by two routes. Route1 (green) shows the formation of lumichrome **(2)** along with the release of cyclopropylcarboxaldehyde **(116)** as the other product which can be converted to the corresponding hydrazone **(119)** by dansylhydrazine **(118)**. Route 2 (red) shows the formation of flavin C_1' radical **121** followed by a β-bond scission to give **122** which then can release butanal **(117)**. The butanal is detected after trapping with **118** to form the corresponding hydrazone **120**.

Reactions were carried out with synthesized cyclopropylmethylflavin **(115)** as the substrate where formation of lumichrome **(12)** was observed (Figure 45A). No modification in the molecular weight of the enzyme was observed by whole protein mass spectrometry (Appendix H) indicating that no covalent adduct with the enzyme was

formed. Hence, to characterize the corresponding side chain released, the reaction was treated with dansylhydrazine **(118)** where the side chain released was trapped as the hydrazone and detected by HPLC (Figure 45B). No cyclopropyl-dansylhydrazone **(119) (Appendix A)** was detected in the reactions (Appendix I) whereas the two E and Z isomers of butanal-dansylhydrazone **(120)** were detected by HPLC (Figure 45B). The identity of **120** was confirmed by LCMS (Figure 45C) followed by co-elution with a synthesized standard (Figure 45D).

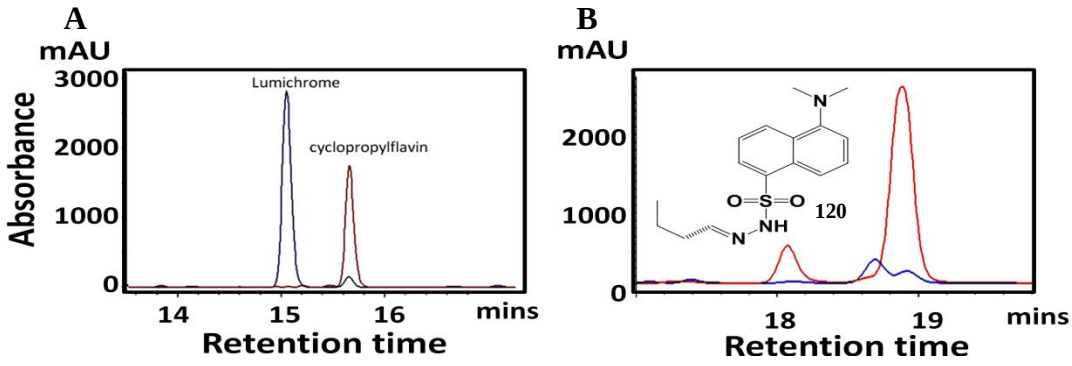

Figure 45: RcaE reaction with cyclopropylflavin (115). A: HPLC chromatogram for the reaction of RcaE with **115** as the substrate and reduced FMN **(23)** as the cofactor, showing the complete conversion of **115** to lumichrome **(12)** in the full reaction (blue trace). The synthesized standard of **115** is shown in the red trace. B: HPLC trace for the formation of the two E and Z isomers of butanal-dansylhydrazone **(120)** in the reaction with **115** as the substrate, reduced FMN **(23)** as the cofactor in the presence of **118** (red trace). The blue trace corresponds to the no enzyme control. C: ESI-MS characterization of the **120** ($M+H^+$) 320.14 in the positive mode. D: Co-elution of **120** generated from the reaction with synthesized standard of **120.**

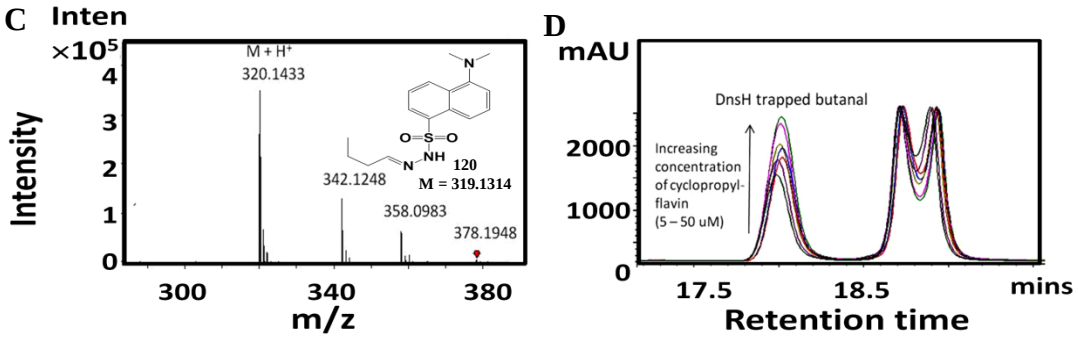

Figure 45 continued

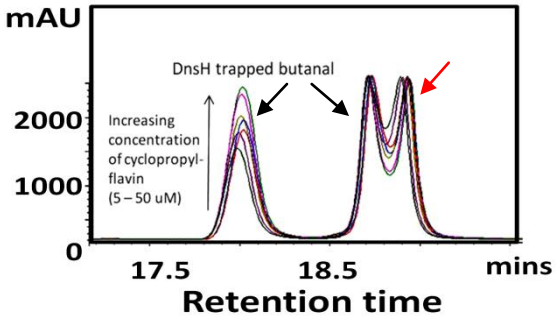

Figure 46: HPLC trace for the proportional increase in the formation of butanal-dansylhydrazone (120) with increasing concentrations (5, 10, 11, 20, 40, 10 uM) of cyclopropylmethylflavin (115) in the reaction. The two E and Z isomers of **120** are marked by the arrows. The isomer (right) of **120** comes with a saturated signal and hence its corresponding increase cannot be detected. The third peak (red arrow) is derived from the other enzyme reaction components and is not related to the dansylhydrazine **(118)** derivatization.

A proportional increase in the formation of butanal-dansylhydrazone **(120)** was observed with increasing concentrations of cyclopropylflavin **(115)** in the reaction

(Figure 46). The release of butanal **(117)** as a product from cyclopropylflavin **(115)** provided a clear evidence for the formation of a radical at C_1' of the substrate flavin by superoxide radical anion **(104)** and in the course, the superoxide **(104)** was converted to a hydrogen peroxide **(113)**.

Comparison of the steady-state kinetic parameters of RcaE for lumiflavin (86) vs. cyclopropylmethylflavin (115)

To figure out the relative rate constants for lumiflavin **(86)** and cyclopropylmethylflavin **(115)**, initial rate plots were produced for varying concentrations of lumiflavin **(86)** and cyclopropylmethylflavin **(115)** in the presence of FRE reducing system containing FMN **(2)** and NADH **(22)** and RcaB. From the slopes of the initial rate plots, Michaelis-Menten plots were generated using KaleidaGraph to determine the k_{cat} and the K_m both for lumiflavin **(86)** (Figure 47) and cyclopropylmethylflavin **(115)** (Figure 48). From the steady-state kinetic data analysis the corresponding kinetic constants calculated are: k_{cat} of 0.27 s^{-1} $\pm$ 0.003 and a K_m of 38.57 $\pm$ 3.55 µM with respect to cyclopropylmethylflavin **(115)** and k_{cat} of 1.3 s^{-1} $\pm$ 0.02 and a K_m of 94.61 $\pm$ 19.22 µM with respect to lumiflavin **(86)**. Though the K_m of cyclopropylmethylflavin **(115)** is ~2.5 time that of lumiflavin **(86)**, the enzyme is ~ 6 times slower with the degradation of cyclopropylmethylflavin **(115)** with respect to lumiflavin **(86)**. The rate plots in Figure 49 gives a comparative analysis of rates of enzymatic lumichrome **(12)** formation from the same concentrations (100 µM) of lumiflavin **(86)** and cyclopropylmethylflavin **(115)**. Rate of lumichrome **(12)** formation

is faster for lumiflavin **(86)** as compared to cyclopropylmethylflavin **(115)**. Compared to the native substrate riboflavin **(1)** the enzyme is ~3.5 times slower for lumiflavin **(86)** and ~17 times slower for cyclopropylmethylflavin **(115)**.

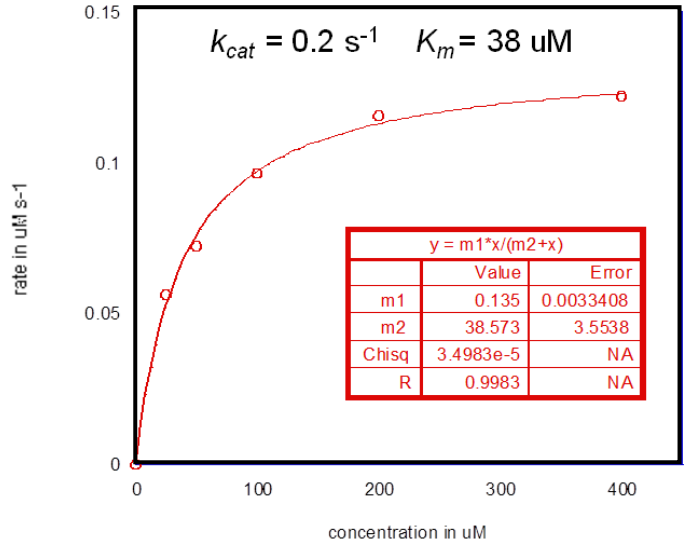

Figure 47: Michaelis-Menten plot for RcaE with cyclopropylmethylflavin (115).

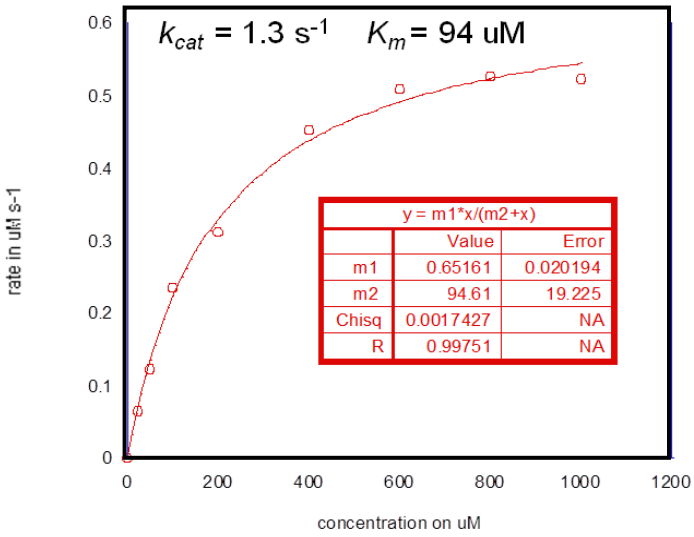

Figure 48: Michaelis-Menten plot for RcaE with lumiflavin (86).

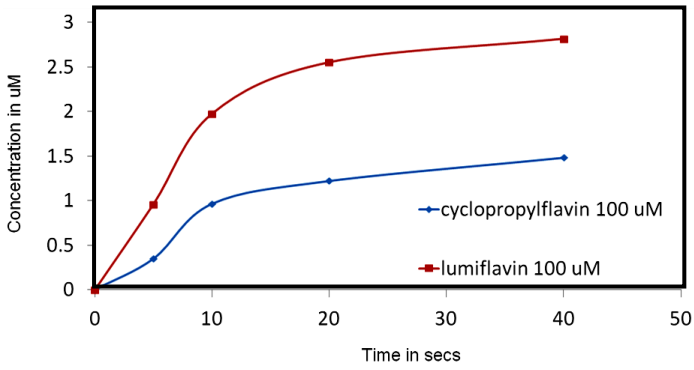

Figure 49: Comparative rates of formation of lumichrome (12) by RcaE from lumiflavin (86) and cyclopropylmethylflavin (115).

5.3 Experimental

Non-enzymatic degradation of riboflavin with superoxide

1 mM riboflavin **(1)** was dissolved in 5 % DMSO and was reacted with an excess of potassium superoxide **(111)**. The reaction mixture was heated at 60 ^{o}C for 1 hour. The resulting solution was treated with dithionite to reduce the remaining potassium superoxide **(111)** in the mixture. The solution was then analyzed by HPLC to identify the reaction products.

Enzymatic degradation of riboflavin with superoxide

50 µM of RcaE was incubated with 250 µM riboflavin **(1)** and ~100 µM potassium superoxide **(111)** in an reaction volume of 100 µL. Due to solubility problems the exact concentration of potassium superoxide **(111)** could not be determined. A similar reaction with no enzyme added was used as the control. The reactions were incubated for 15 mins at 37 ^{o}C. The reactions were filtered through a 10 kDa cut-off

filter and analyzed by HPLC for the formation of lumichrome **(12)**. In order to test the dependence of the formation of lumichrome **(12)** with increasing concentrations of potassium superoxide, five individual reactions were set up each with 250 µM riboflavin **(1)** and 50 µM RcaE. The concentration of the potassium superoxide **(111)** added in the reactions ranged from 20 – 150 µM. The resulting reactions were analyzed by HPLC to look for a proportional increase in the formation of lumichrome **(12)** with the increasing concentrations of potassium superoxide **(111)** in the presence of the enzyme. As controls five exact reactions were set up in the absence of the enzyme and analyzed by HPLC.

Enzyme reactions with cyclopropylflavin (115)

250 µM of cyclopropylmethylflavin **(115)** dissolved in 100 mM phosphate buffer at pH 7.5 with 5 % acetonitrile was treated with 20 µM enzyme in the presence of 50 µM FMN **(2)** and 5 mM NADH **(22)** and 5 mM dansylhydrazine **(118)**. The reaction was incubated for 30 mins at 37 ^{o}C, filtered and then divided into two parts. The first part was analyzed by HPLC to detect lumichrome **(12)** as one of the products. The second part was heated at 40 ^{o}C for 1 hour followed by analysis by LCMS to look for the corresponding hydrazone **(120)** with dansylhydrazine **(118)** and butanal **(117)**. The hydrazone **(120)** was separated as E and Z isomers on HPLC as confirmed by running a standard of **120** synthesized by incubating the two components in 5 % acetonitrile for 1 hour at 40 ^{o}C. In order to test if the formation of the hydrazone is substrate dependent, 20, 50, 100, 200, 300, 500 µM cyclopropylflavin **(115)** were used as substrates for separate reactions following the above conditions. The corresponding hydrazone formed was analyzed by HPLC.

Synthesis of cyclopropylmethylflavin (115)

The scheme for the synthesis of **115** is given below (Figure 50)

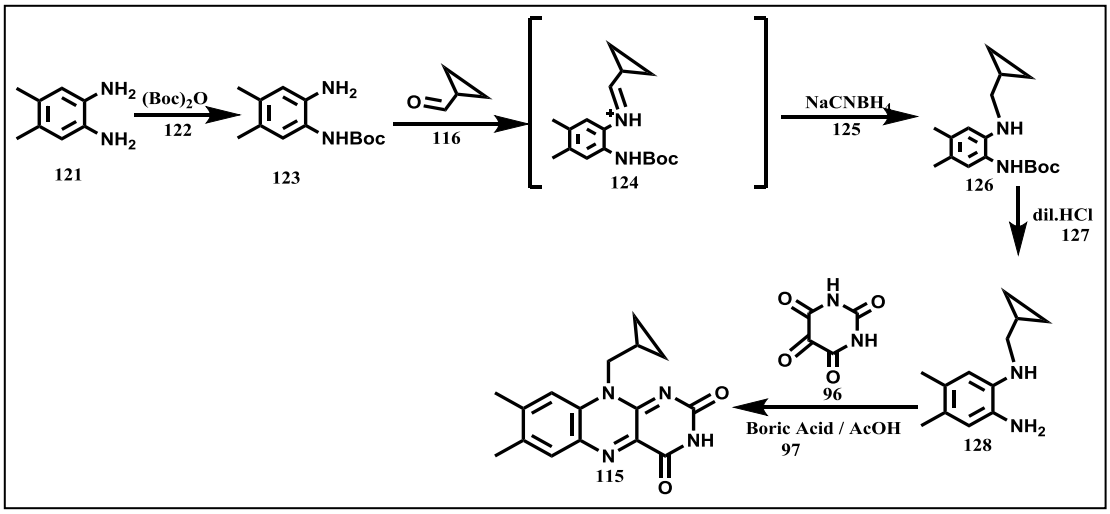

Figure 50: Scheme for the synthesis of cyclopropylmethylflavin (115).

Synthesis of tert-butyl (2-amino-4,5-dimethylphenyl)carbamate (123)

Sodium bicarbonate (1.04 grams) was slowly added to a solution of 4,5-dimethylbenzene-1,2-diamine **(121)** (680 mg; 2.8 mmoles) in 40 mL of distilled water resulting in a gas evolution followed by formation of a suspension. After stirring for 10 mins, di-tert-butyl dicarbonate **(122)** (dissolved in 30 mL of THF) was added to the aqueous suspension. The resulting two phase system was stirred vigorously for 12 hours. The organic layer was extracted with dichloromethane and the solvent was removed by a rotovap. The compound obtained was purified using a silica gel column chromatography using chloroform/methanol as the mobile phase. The compound eluted with 4%

methanol in chloroform. Yield of **123** was 72 %. The proton NMR of **123** in D_6-DMSO is presented in Figure 51.

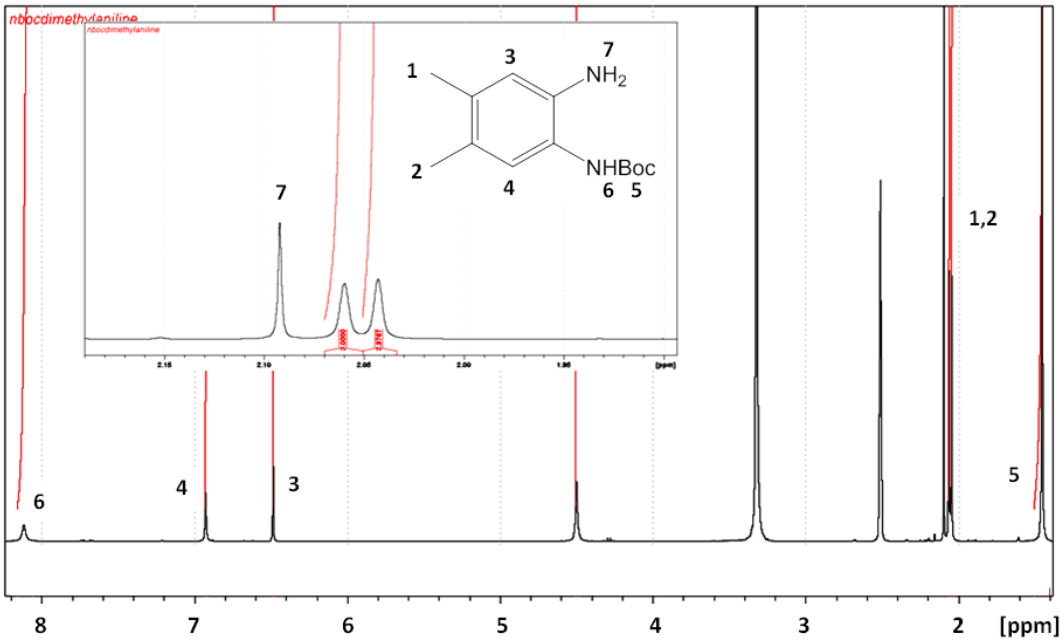

Figure 51: Proton NMR for 123 in D_6-DMSO.

Synthesis of tert-butyl (2-((cyclopropylmethyl)amino)-4,5-dimethylphenyl) carbamate (126)

370.26 mg (1.57 mmoles) of **123**, 326.6 mg (6.2 mmoles) of cyclopropylcaboaldehyde **(116)** and 198 mg (3.1 mmoles) of sodium cyanoborohydride **(125)** were dissolved in 15 mL of dry methanol under stirring. The resulting solution was refluxed at 70 °C for 48-64 hours. The solvent was removed under reduced pressure. The compound was obtained in pure form by silica column chromatography with hexane/ethylacetate gradient as the mobile phase. The compound was eluted with 15%

ethyl acetate in hexane. The proton NMR for **126** in D_6-DMSO is given below (Figure 52)

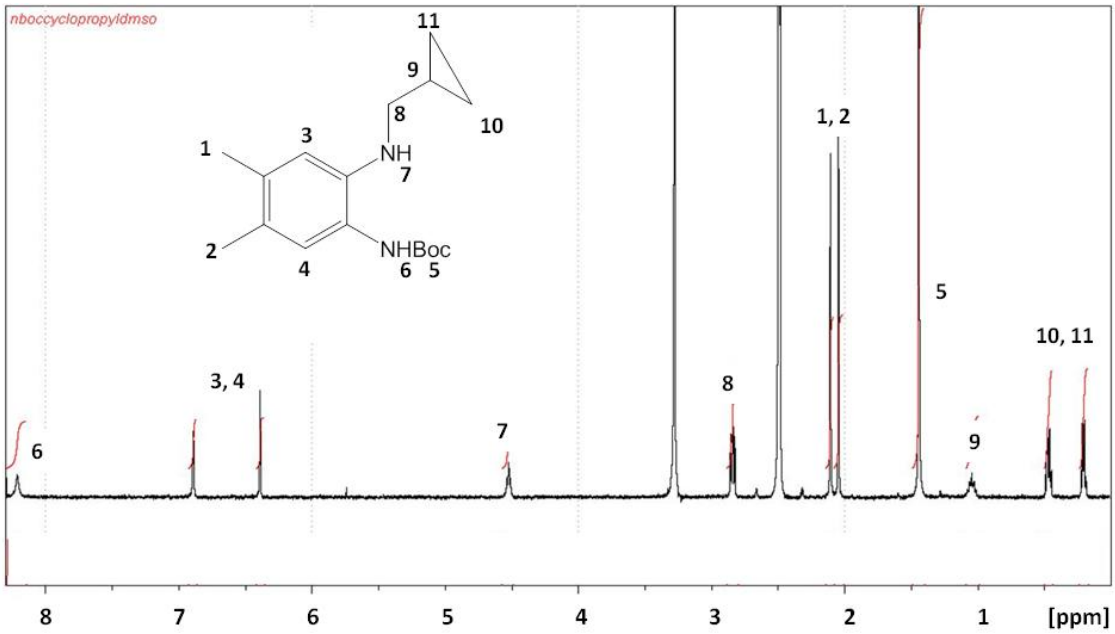

Figure 52: Proton NMR for 126 in D_6-DMSO.

Synthesis of (2-((cyclopropylmethyl)amino)-4,5-dimethylphenyl) carbamate (128)

200 mg (0.68 mmoles) of **126** was dissolved in 2 mL of ethanol. 200 uL of HCl **(127)** was added to the reaction mixture and stirred for 4 hours at room temperature. The reaction mixture was then evaporated to dryness and neutralized with saturated sodium bicarbonate solution. The mixture was then extracted with ethylacetate. The product **128** obtained was further purified by a flash column chromatography with 100% chloroform. The NMR of **128** in deuterated methanol is given in Figure 53.

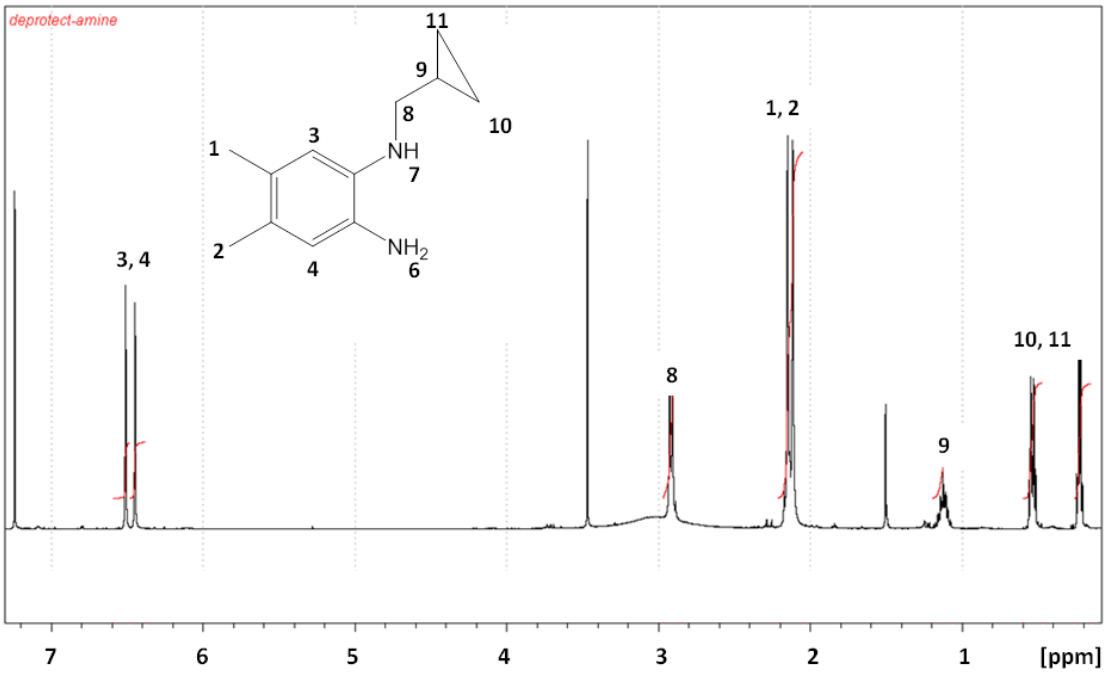

Figure 53: Proton NMR for 128 in deuterated methanol.

Synthesis of cyclopropylmethylflavin (115)

100 mg (0.52 mmoles) of **128** and 142 mg (1 mmoles) of alloxan monohydrate **(96)** was treated with 20 mg of boric acid **(97)** in 20 mL acetic acid. The reaction mixture was stirred under argon for 12 hours until a fluorescent yellow precipitate was obtained. The solid precipitate was collected by filtration and washed with 30 mL acetic acid followed by washing with 30 mL diethylether. The resulting product **115** was further purified by silica column chromatography with chloroform/methanol as the mobile phase. The compound eluted with 30% methanol in chloroform. The proton NMR in D_6-DMSO for **115** is given in Figure 54.

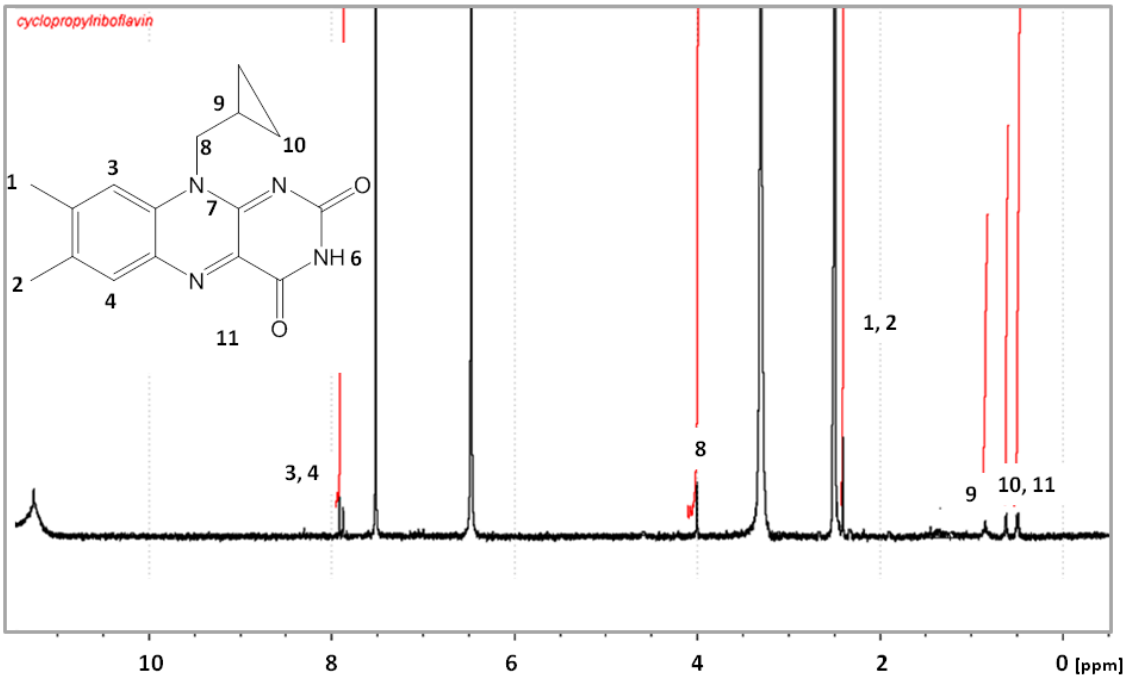

Figure 54: Proton NMR characterization of 115 in D_6-DMSO.

Kinetics of RcaE for lumiflavin (86) and cyclopropylmethylflavin (115)

FMN **(2)** concentration was 50 µM and NADH **(22)** concentration was kept at saturation (5 mM) in the presence of 100 nM RcaB. The concentration of both the substrates was varied from 20 – 500 µM in initial rate determination reactions with 500 nM enzyme. The formation of lumichrome **(2)** was quantified by HPLC using standard concentration curves. Reactions were carried out in 100 µL aliquots. The reactions were quenched at 5s, 10 s, 20 s, 30 s, 40 s, 1 min time points by denaturing the enzyme with 0.1 N HCl. Each time-point reaction was repeated in triplicates. The amount of lumichrome **(2)** formed was plotted against the time points for each set of substrate concentrations. The initial slopes from each set of substrate concentrations were then

plotted against the substrate concentration and fit to the Michaelis−Menten equation using KaleidaGraph (Synergy Software).

5.4 Conclusion

Hint of a flavin derived superoxide radical anion mediated mechanism

It is widely known that superoxide radical anion **(104)** is generated from oxygen **(20)** by SET chemistry with reduced flavins. In oxygenases the superoxide **(104)** is then quenched by recombination with the flavin semiquinone **(112)** to give a flavin hydroperoxide **(27)**. Very few examples of enzymes are known where the superoxide radical **(104)** participates in further chemistry.[73]

In this chapter, we propose that in RcaE, the superoxide radical anion **(104)**, formed by reduced FMN **(23)** reacting with molecular oxygen **(20)** at the active site, further reacts with the substrate riboflavin **(1)** to give lumichrome **(12)**. According to the mechanistic proposal (Figure 55) the superoxide radical anion **(104)** after its formation, initiates a subsequent radical reaction by H-atom abstraction at the C_1' of the substrate riboflavin to give the riboflavin C_1'-radical intermediate **(114)**. The results in this chapter clearly suggest that not only is superoxide **(104)** an intermediate in the transformation but the enzyme can also use it as the substrate.

This is extremely atypical as superoxide **(104)** is toxic to cells.[80] The ErV family Sulfhydryl oxidases are the only examples of enzymes releasing superoxide **(104)** into the cell in the extra-mitochondria locations.[17] superoxide **(104)** is released during the re-oxidation of the reduced flavin cofactor **(23)** generated after the oxidation of dithiol substrates (Figure 56). This released superoxide is proposed to act as a signaling

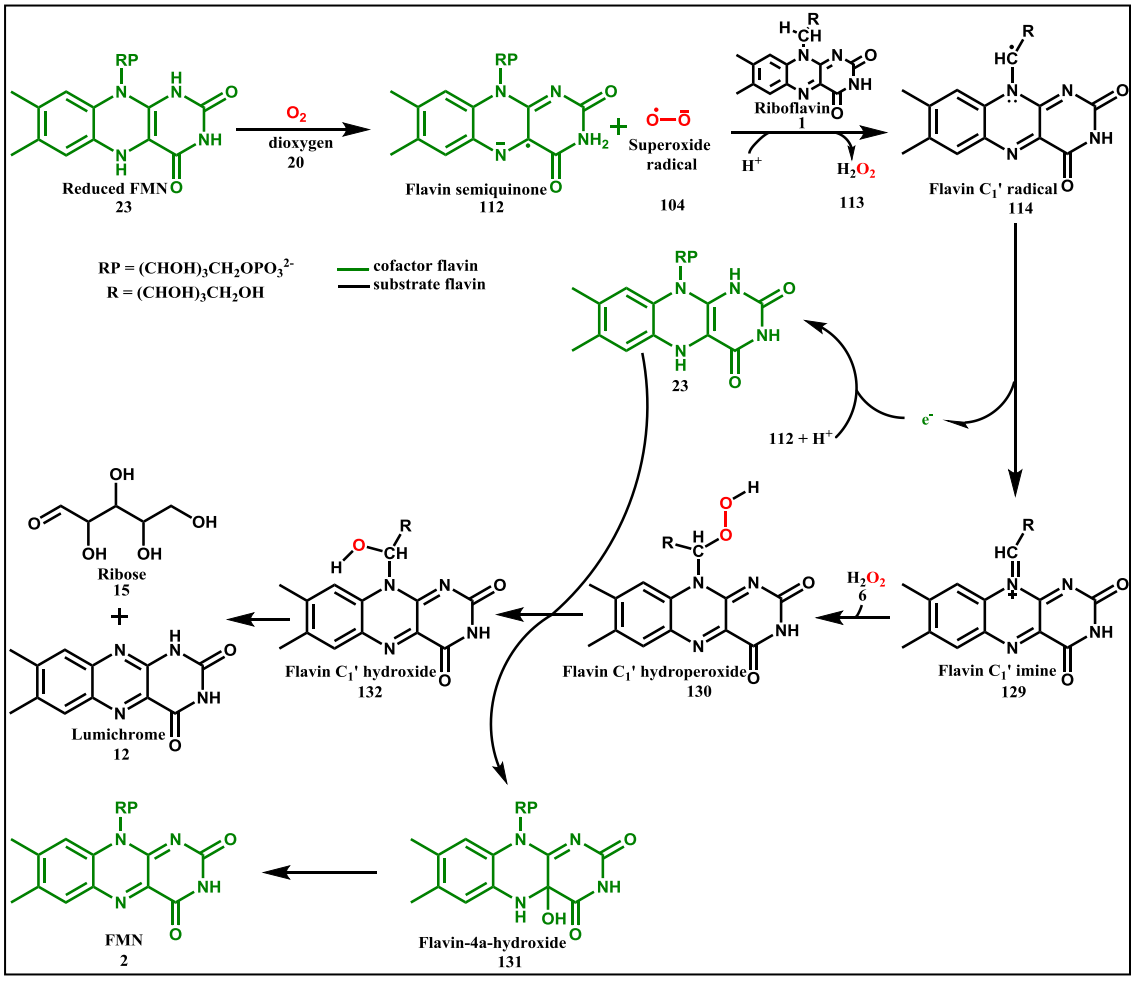

Figure 55: Flavin derived superoxide radical mediated degradation of riboflavin by RcaE.

Figure 56: Two consecutive one-electron transfers between reduced flavin cofactor (23) and oxygen (20) to generate superoxide (104) in ErV family Sulfhydryl oxidases.

molecule. In general, to limit the concentrations of superoxide **(104)** in vivo the two superoxide degrading enzymes superoxide reductase and superoxide dismutase uptake superoxide **(104)** and convert it to less toxic species like hydrogen peroxide **(113)** and oxygen **(20)**.[81] Apart from the two superoxide degrading enzymes, RcaE now serves as the only other example of an enzyme which uptakes superoxide **(104)** directly as a substrate. Figure 55 presents the mechanistic proposal for RcaE consistent with the experimental evidences that we have obtained on the intermediacy of a flavin-semiquinone-superoxide anion radical pair **(112-104)** in riboflavin **(1)** degradation by RcaE.

Formation of riboflavin-C_1' radical (114)

In the next step we propose the participation of the FMN derived superoxide radical anion **(104)** in a subsequent one electron oxidation of the substrate riboflavin **(1)** by hydrogen atom abstraction at C_1' of the sugar side chain. This will result in the formation of riboflavin-C_1' radical **(114)** and hydrogen peroxide **(113)**. Derived on the results obtained for the enzymatic degradation of cyclopropylmethylflavin **(115)**, it is clear that the mechanism proceeds through the formation of a radical at C_1' of the substrate flavin **(114)** by superoxide radical anion **(104)**. In the ensuing steps along the mechanistic pathway we propose that the substrate radical **(114)** formed is subsequently oxidized to riboflavin-C_1'-imine **(129)**, donating an electron back to the reduced cofactor FMN-semiquinone-anion **(112)**. The cofactor, in the course, is reduced to $FMNH_2$ **(23)**.

CHAPTER VI

FATE OF MOLECULAR OXYGEN IN RIBOFLAVIN DEGRADATION BY RcaE

6.1 Introduction

In Chapter V we have provided evidence for the participation of an FMN derived superoxide radical anion **(104)** in a one-electron oxidation of the substrate riboflavin **(1)** by hydrogen atom abstraction at C_1' of the sugar side chain (Figure 55). This results in the formation of the riboflavin substrate radical **(114)** and hydrogen peroxide **(113)**. We propose that in a second one electron oxidation, an electron transfer from the riboflavin substrate radical **(114)** to the reduced cofactor FMN semiquinone **(112)** yields the reduced cofactor FMN **(23)** and the riboflavin substrate imine **(129)** which then reacts with the hydrogen peroxide **(113)** at the active site to give the substrate flavin-C_1'-hydroperoxide **(130)**. The substrate hydroperoxide **(130)** in the consequent steps is converted to lumichrome **(12)** and ribose **(15)**. Derived on our experimental evidence it is likely that the reduction of the substrate hydroperoxide **(130)** to hydroxide **(132)** is brought about by the reduced cofactor FMN **(23)** at the active site.

The next step in the mechanism of riboflavin degradation by RcaE was to figure out the fate of the oxygen molecule **(20)** in the reaction. According to the experimental evidence obtained so far, it is clear that initially the oxygen molecule **(20)** gets converted to a superoxide radical anion **(104)** on reaction with the reduced cofactor FMN **(23)**. The radical anion is then converted to a hydroperoxide anion which on protonation gives hydrogen peroxide **(113)**. To figure out the fate of the hydroperoxide in the active site, the determination of the source of the oxygen atom in the ribose **(15)** formed was

necessary. In this chapter, we have established that the oxygen in the ribose **(15)** formed originates from molecular oxygen **(20)**.

6.2 Results and Discussions

Test for the release of hydrogen peroxide by oxygen electrode experiments

According to the experimental evidences obtained so far, it is clear that initially a superoxide radical anion **(104)** is formed when molecular oxygen reacts with the reduced cofactor FMN **(23)**. The radical anion **(104)** is then converted to a hydroperoxide anion which on protonation gives hydrogen peroxide **(113)**. The release of **113** in turn, can be analyzed by Clarke electrode after treatment of the reaction mixture with catalase.[82] In order to test the calibration of the oxygen electrode instrument, aerobic buffer with a dissolved oxygen **(20)** concentration of 260 µM was diluted 1.2 times with anaerobic buffer to get a corresponding 44 µM decrease in the oxygen concentration (Figure 57).

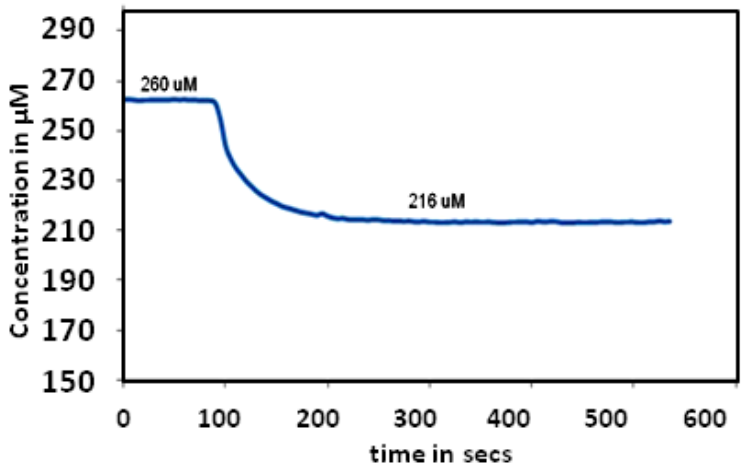

Figure 57: Calibration of the oxygen electrode instrument.

In order to figure out if any hydrogen peroxide **(113)** is released from the reaction, the reaction mixture was treated with catalase and oxygen electrode was used to detect the formation of any oxygen **(20)**. Figure 58 shows the results of the oxygen electrode experiments, where stoichiometric amounts of photo-reduced FMN **(23)** was added to a mixture of riboflavin **(1)** and the enzyme in an oxygenated buffer containing 260 µM oxygen **(20)** (Segment A) to get an equivalent amount of oxygen **(20)** consumption (C_{O2} Segment [A – B]). On addition of catalase to the system, no oxygen **(20)** production was observed (C_{O2} Segment [C-B]) indicating that hydrogen peroxide **(113)** is not a product of the reaction. (C_{O2} Segment [D-C]) is the control that shows the production of oxygen **(20)** on addition of external hydrogen peroxide **(113)** solution to the system.

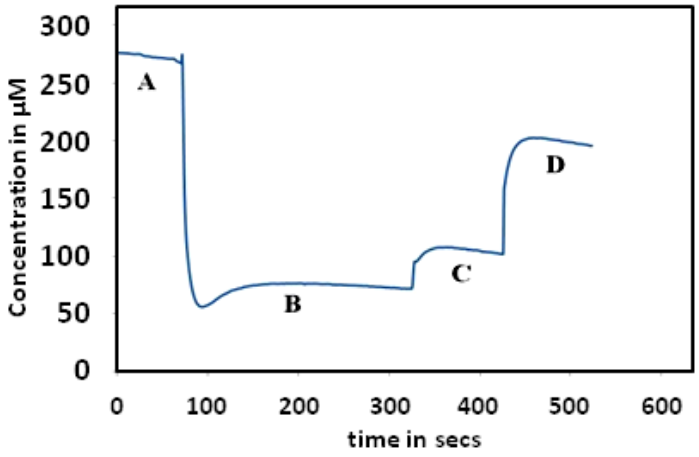

Figure 58: Oxygen Electrode analysis of RcaE reaction with the native substrate under single turnover conditions. Segment A represents the oxygen **(20)** concentration in air-saturated buffer in the presence of enzyme and riboflavin **(1)**. The decrease in the concentration of oxygen **(20)** from Segment A to Segment B corresponds to the stoichiometric consumption of oxygen **(20)** with respect to the concentration of reduced FMN **(23)** added in Segment A. Segment B corresponds to the oxygen **(20)** concentration in the system after the consumption of oxygen **(20)** by RcaE to convert riboflavin **(1)** to lumichrome **(12)** in the presence of reduced FMN **(23)**. The slight increase in the oxygen **(20)** concentration in Segment C compared to Segment B is due to the concentration factor when 50 µL of catalase in buffer with an oxygen **(20)** concentration of 260 µM is added to 550 µL of the reaction mixture in Segment B with an oxygen **(20)** concentration of 62 µM. Segment C corresponds to the oxygen **(20)** concentration in the system after catalase addition. The increase in oxygen **(20)** concentration in Segment D compared to Segment C is due to the generation of half equivalent of oxygen **(20)** when 50 µL of 150 µM external hydrogen peroxide **(113)** is added to Segment C. Segment D corresponds to the oxygen **(20)** concentration in the system after external hydrogen peroxide **(113)** addition.

Figure 59 shows the graph for the enzymatic reaction where the catalase was added from the beginning. It shows the similar results as in Figure 58. As control experiment, the oxidation of reduced FMN **(23)** in the presence of the enzyme was studied (Figure 60). In Segment B, a release of hydrogen peroxide **(113)** was detected by the increase in oxygen **(20)** concentration in the presence of catalase added in Segment A. Segment C shows that the catalase in the reaction mixture is active to the externally added hydrogen peroxide **(113)**.

Fate of molecular oxygen (20) in the enzymatic transformation

The detection of the source of the oxygen in the ribose **(15)** was technically demanding. Firstly, the oxygen in the ribose is lost when trapping agents like hydroxylamine or hydrazine are used to trap the ribose. Finally, as the oxygen is incorporated as an aldehyde, it is easily exchangeable with the solvent. Hence, in order to trap the oxygen in the ribose in a form that it can be identified, a coupled reaction was devised (Figure 61) where the released ribose **(15)** was first converted to ribose-5-phosphate **(24)** by ribose kinase (Rbks) followed by the conversion of the **24** to ribulose-5-phosphate **(133)** by ribose-5-phosphate isomerase (Rpi).[83] **133** can be trapped with PFBHA **(65)** to form ribulose-5-phosphate-PFBHA oxime **(134)**. Due to the reversibility of ribose-phosphate isomerase, ribose-5-phosphate-PFBHA oxime **(67)** was also expected to be formed as one of the products. In ribulose-5-phosphate-PFBHA oxime **(134),** the oxygen at the 5' position will be trapped in the form of a non-exchangeable hydroxyl group and can thus be analyzed for ^{18}O incorporation by LCMS in a reaction using ^{18}O labeled molecular

oxygen **(20)**. In contrast, there will be no incorporation of the ^{18}O label in ribose-5-phosphate-PFBHA oxime **(67)**.

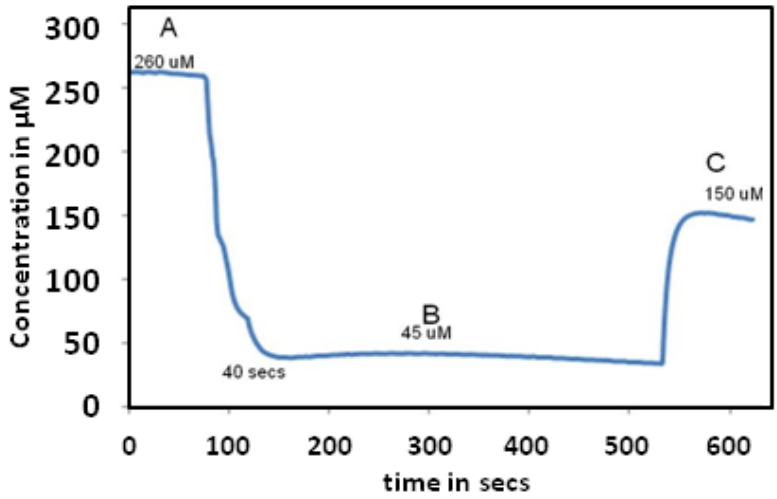

Figure 59: Oxygen Electrode analysis of RcaE reaction with the native substrate under single turnover conditions. Segment A represents the oxygen **(20)** concentration in air saturated buffer where enzyme, riboflavin **(1)** and catalase are present. The decrease in the concentration of oxygen **(20)** from Segment A to Segment B corresponds to the stoichiometric consumption of oxygen **(20)** with respect to the concentration of reduced FMN **(23)** added in Segment A. Segment B corresponds to the oxygen **(20)** concentration in the system after the consumption of oxygen by RcaE to convert riboflavin **(1)** to lumichrome **(12)** in the presence of reduced FMN **(23)**. The increase in oxygen **(20)** concentration in Segment C compared to Segment B is due to the generation of half equivalent of oxygen **(20)** when 50 µL of 150 µM external hydrogen peroxide **(113)** is added to Segment B. Segment C corresponds to the oxygen **(20)** concentration in the system after external hydrogen peroxide **(113)** addition.

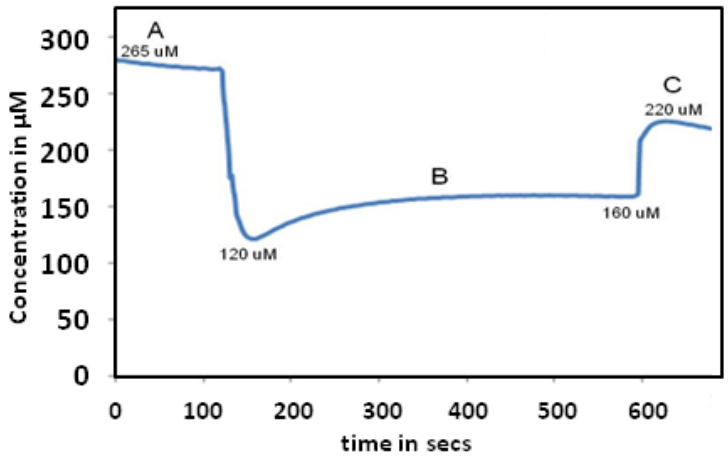

Figure 60: Oxygen Electrode analysis of RcaE reaction in the absence of the substrate riboflavin (1). Segment A represents the oxygen **(20)** concentration in air saturated buffer where enzyme and catalase are present. Segment B corresponds to the oxygen **(20)** concentration in the system after the consumption of oxygen **(20)** by reduced FMN **(23)** to form oxidized FMN **(2)**. Segment C corresponds to the oxygen **(20)** concentration in the system after the evolution of oxygen **(20)** from catalase in the presence of added external hydrogen peroxide **(113)**.

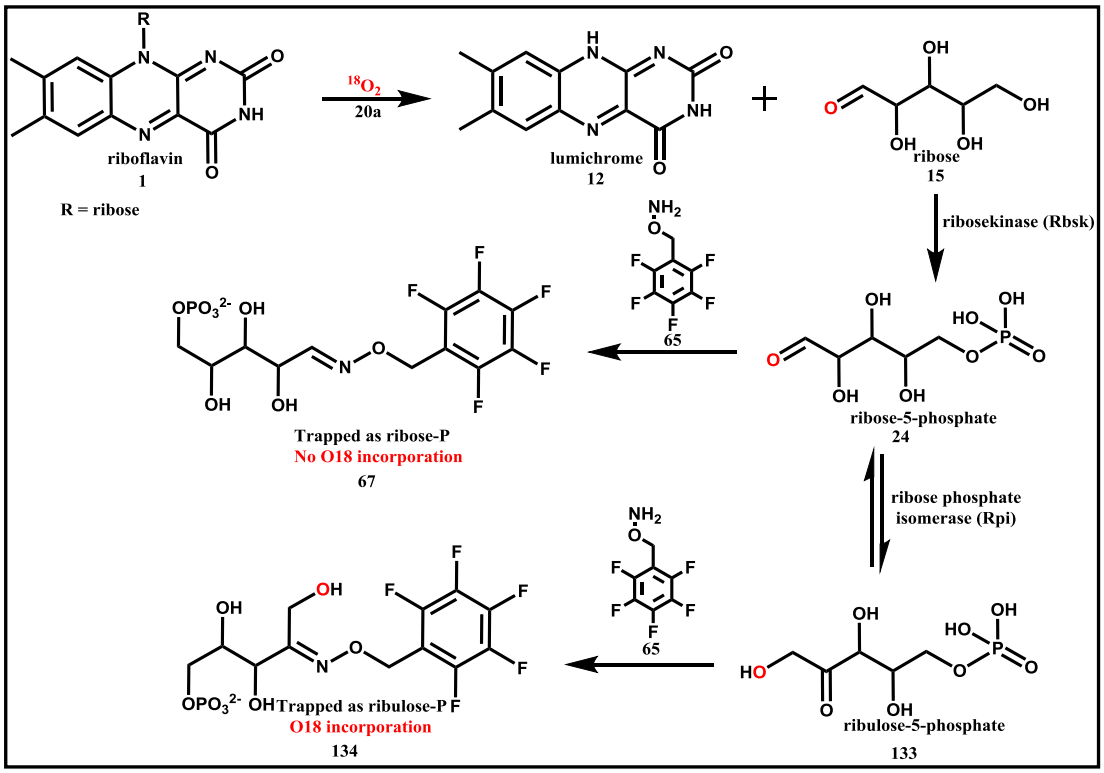

Figure 61: Scheme for the coupled reaction to show incorporation of ^{18}O in ribose released from the RcaE reaction.

Reaction in $^{18}O_2$ (20a) to look for incorporation of molecular oxygen in the ribose (15) formed

Coupled reactions of RcaE with ribose kinase and ribose phosphate isomerase were carried out in $^{18}O_2$ **(20a)** with riboflavin **(1)** as the substrate. The product of the coupled reaction ribulose-5-phosphate **(133)** was trapped with PFBHA **(65)** to give ribulose-5-phosphate-PFBHA oxime **(134),** which stayed in equilibrium with the ribose-5-phosphate-PFBHA oxime **(67)**. From the LCMS analysis (Figure 62), the peak for EIC at 426 corresponding to the exact mass of both ribose-5-phosphate-PFBHA oxime **(67)** and ribulose-5-phosphate-PFBHA oxime **(134)** also had a mass at m/z 428 when

analyzed by ESI-Mass spectrometry in the positive mode, thereby indicating the incorporation of an oxygen molecule from $^{18}O_2$ into the 5-membered sugar (Figure 62A). From the mass mass spectrometric analysis, no ^{18}O incorporation was found in ribose-5-phosphate-PFBHA oxime **(67)** (Figure 62B) whereas ~60% ^{18}O incorporation was found in the ribulose-5-phosphate-PFBHA oxime **(134)** (Figure 62C). This experiment provided evidence for the incorporation of molecular oxygen at the C_1' of riboflavin to give lumichrome **(12)** and the sugar aldehyde.

Stoichiometric formation of lumichrome (12) with reduced FMN (23)

The graph in Figure 63 represents an equivalent formation of lumichrome **(12)** with the addition of reduced FMN **(23)** to the reaction in the presence of excess substrate riboflavin **(1)** and enzyme. A crystal structure of the substrate and cofactor bound enzyme will reveal the active site conformations of the substrate, cofactor, and oxygen, which is currently under way.

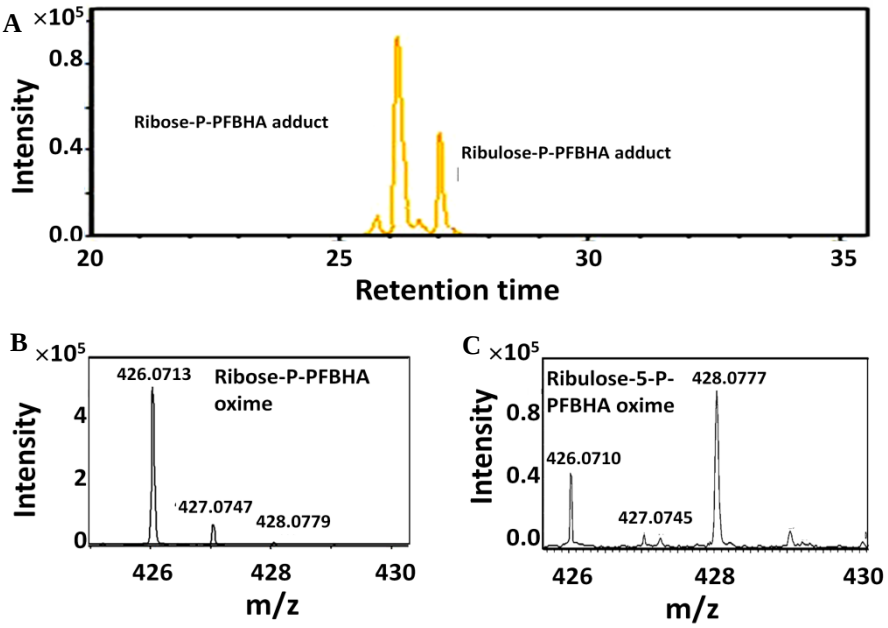

Figure 62: LCMS analysis of the coupled reaction of RcaE, Ribokinase, Ribosephosphate isomerase with riboflavin (1) as the substrate and reduced FMN (23) as the cofactor in $^{18}O_2$ (20a) in the presence of PFBHA (65). A: Extracted Ion Chromatogram (EIC) at m/z 426.04 corresponding to $M+H^+$ of both ribose-5-phosphate-PFBHA oxime **(67)** (left peak) and ribulose-5-phosphate-PFBHA oxime **(134)** (right peak) to look for the formation of both the species in the coupled reaction. B: ESI-MS analysis in the positive mode for **67** showing no ^{18}O incorporation. C: ESI-MS analysis in the positive mode for **134** showing 60% ^{18}O incorporation.

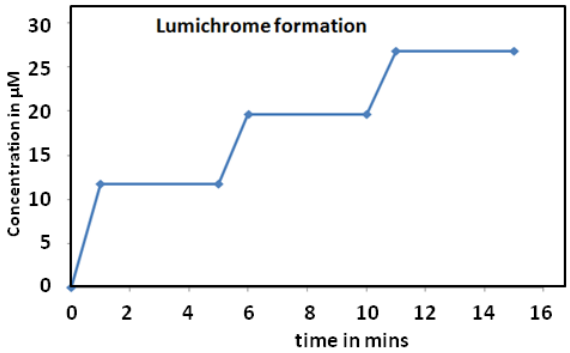

Figure 63: Stoichiometry of the formation of lumichrome (12) with added reduced FMN (23). Stoichiometric formation of lumichrome **(12)** (Y-axis) with each addition of 10 µM photoreduced FMN **(23)** after an interval of 5 mins in the presence of excess RcaE and riboflavin **(1)**. The amount of lumichrome **(12)** formed decreases with the addition of increasing amounts of photoreduced FMN **(23)** due to the competing auto-oxidation reaction of reduced FMN **(23)**.

6.3 Experimental

Oxygen electrode experiment

For the experiment presented in Figure 58, 150 µL of 150 µM photo-reduced FMN **(23)** in anaerobic buffer was added to 350 uL of aerobic buffer containing 150 µM of enzyme and 125 µM riboflavin **(1)** in Segment A. In the segment B the signal stabilized at 62 µM. This was followed by the addition of 50 µL of 20 units of catalase to achieve a final concentration of 91 µM oxygen in Segment C. 50 µL of 150 µM H_2O_2 **(113)** was added to the reaction mixture to get a final concentration of 190 µM oxygen **(20)** in Segment D. For the experiment in Figure 59, similar conditions as in Figure 58 were used with the difference that the 20 units of catalase was added in the start at Segment A. In the next experiment (Figure 60), to 150 µM of enzyme in the presence of 20 units of catalase (Segment A), 150 µM of photoreduced FMN **(23)** was added to get

an oxygen **(20)** concentration of 120 μM in Segment B. To this 50 μL of 100 μM hydrogen peroxide **(113)** was added to get an oxygen **(20)** concentration of 220 μM in Segment C.

Cloning, overproduction, and reconstitution of recombined His-tagged ribose-phosphate isomerase (RpiA)

The *rpiA* gene was amplified by PCR using genomic DNA of *E.coli K12* as the template (F primer: 5'-AA *CATATG* ACGCAGGATGAATTG-3', R primer: 5'-AA *GAATTC* AGA TTTCACAATGGTTTTGACAC-3', engineered NdeI and EcoRI site are in italics). The PCR product was digested with NdeI and EcoRI and ligated into pET28b (NdeI/EcoRI digested backbone) to generate the plasmid pXH-2. The plasmid was transformed into BL21 (DE3). Resulting transformants were grown in 3 L of LB medium with 40 μg/mL of kanamycin at 37 °C to an OD_{600} of 0.5 IPTG was added to a final concentration of 0.4 mM and incubation was continued at 15 °C for 18 hours. The His-tagged RpiA was purified on a HisTrap HP column (GE) and buffer-exchanged into 50 mM KH_2PO_4, 300 mM NaCl, 10% glycerol, pH 7.5 by passing through an Econo-Pac 10DG desalting column (Bio-rad). The protein was flash-frozen in liquid nitrogen and stored at -80 °C. For enzyme reconstitution, a reaction mixture (100 μL) of 20 μM RpiA and 250 μM ribose-5-phosphate was incubated at 37 °C for 15 mins. Protein was removed by ultrafiltration (10 kDa cut-off filter) and the reaction mixture was analyzed by HPLC followed by LC-MS.

Coupled reaction with $^{18}O_2$

A 100 uL reaction containing 250 µM riboflavin **(1)**, 200 µM photoreduced FMN **(23)** and 10 mM ATP **(21)** was mixed with an enzyme cocktail containing 10 µM RcaE, 20 µM ribokinase, 20 µM ribosephosphate isomerase in an eppendorf tube. The eppendorf tube was placed in a 10 mL round-bottom flask and was made anaerobic by incubation in the glove box for 2 hours. Then the mouth of the flask was sealed with a rubber stopper and parafilm and the setup was brought outside the glove box. To start the reaction, a balloon containing $^{18}O_2$ **(20a)** was purged into the flask. The setup was incubated for 10 mins at 37 ^{o}C. The enzymes in the reaction were removed by filtration through a cut-off filter, and the reaction was incubated with PFBHA **(65)** at 37 ^{o}C for 1 hour. The resulting reactions were analyzed by LCMS to look for ^{18}O incorporation in the ribulose-5-phosphate oxime **(134)**. The different sets of reactions including the control reactions carried out are shown in Table 4.

Table 4: Reaction conditions for the coupled reaction with RcaE, RcaD and RpiA

	Riboflavin 500 uM	FMN 1mM	NADH 5mM	ATP 5mM	$MgCl_2$ 5mM	NaCl 50mM	Ribose 1mM	RcaE 20 uM	RcaD 20uM	RpiA 50uM
Assay 1 Full reaction	+	+	+	+	+	+	-	+	+	+
Assay 3 Full reaction in $^{18}O_2$	+	+	+	+	+	+	-	+	+	+
Assay 4 Full reaction with ribose in $^{18}O_2$	-	+	+	+	+	+	+	+	+	+
Assay 5 No RcaE in $^{18}O_2$	+	+	+	+	+	+	-	-	+	+
Assay 6 No RpiA in $^{18}O_2$	+	+	+	+	+	+	-	+	+	-

6.4 Conclusion

No detection of released hydrogen peroxide **(113)** in the reaction mixture by Clark electrode (Figure 58) was suggestive of the involvement of the hydrogen peroxide **(113)** in the later steps of the mechanism. A likely fate of the hydroperoxide ion at the active site can be its incorporation at the C_1' of the substrate flavin imine **(129)** (Figure 55). For this possibility to hold true, the oxygen atom in the ribose **(15)** released had to come from molecular oxygen **(20)**. Indeed, in the coupled reactions with $^{18}O_2$ **(20a)**, a 60% incorporation of ^{18}O into the released ribose **(15)** was observed.

As discussed in the previous chapter (Chapter V), the formation of the flavin imine **(129)** was attributed to the reaction between the flavin derived superoxide radical **(104)** with the C_1' position of riboflavin **(1)**. Here, we propose that in next step, the flavin imine **(129)** reacts with the hydrogen peroxide **(113)** in the active site to give the corresponding flavin-hydroperoxide **(130)** (Figure 55). Further conversion of the **130** to the flavin hydroxide **(132)** is proposed to be mediated by the reduced cofactor $FMNH_2$ **(23)** at the active site. According to our mechanistic hypothesis, **23** steps in and reduces the substrate flavin-hydroperoxide **(130)** to the corresponding hydroxide **132** via the intermediacy of flavin-4α-hydroxide **(131)**. Finally the flavin-4α-hydroxide **(131)** releases a water molecule to get converted to oxidized flavin **(2)**. This makes FMN **(2)** the end product of the reaction and hence the reduced cofactor is not regenerated in the enzymatic transformation. Thus the requirement of FMN in the reaction must be stoichiometric. Indeed, the degradation of riboflavin by RcaE was found to be stoichiometric with respect to the concentration of photoreduced FMN **(23)** (Figure 63).

The other possible route for the reduction of **130** to **132** is via the intermediacy of the recently discovered flavin N_5-oxide species.[84-86] In this system, we propose the formation of a reduced FMN-N_5-oxide **(28)** which may then release a water molecule and get converted to oxidized flavin (FMN) **(2)** (Figure 64).

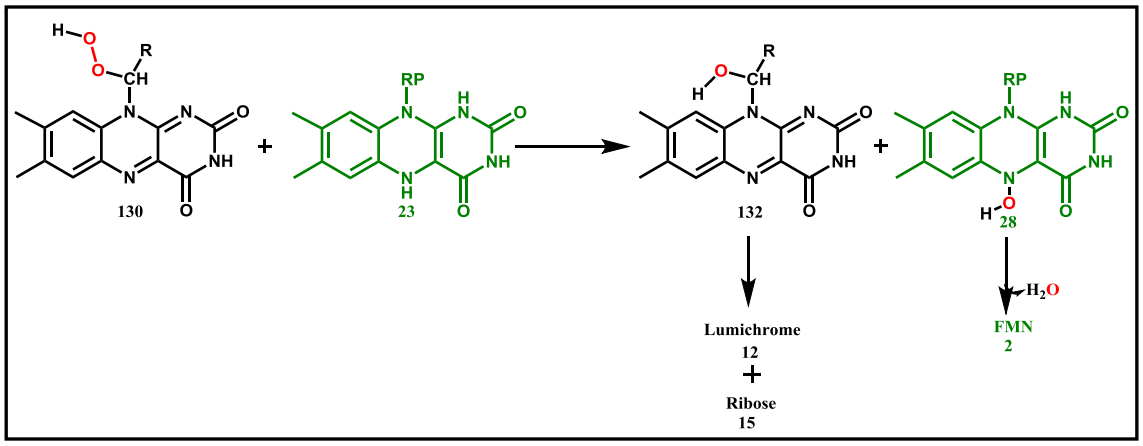

Figure 64: Scheme for reduced FMN-N_5-oxide mediated cleavage of flavin hydroperoxide intermediate (130).

CHAPTER VII

STEREOCHEMICAL STUDIES OF RcaE WITH ISOTOPICALLY ENRICHED DEUTERATED RIBOFLAVIN

7.1 Introduction

The stereochemistry of hydrogen abstraction at C_1' of riboflavin **(1)** can be predicted by either solving the crystal structure of RcaE bound to the substrate or from stereochemical studies with isotopically labeled riboflavin analogs. In the event of a low resolution crystal structure, knowing the stereochemistry of the hydrogen abstraction by biochemical studies will help us predict the relative orientation of the substrate and cofactor at the active site. The stereochemistry of the hydrogen abstraction can be determined from the ratio of the unlabeled vs. the monodeuterated ribose formed when the C_1'-deuterated riboflavin **(135)** analog enriched at the R or S is incubated with the enzyme (Figure 65).

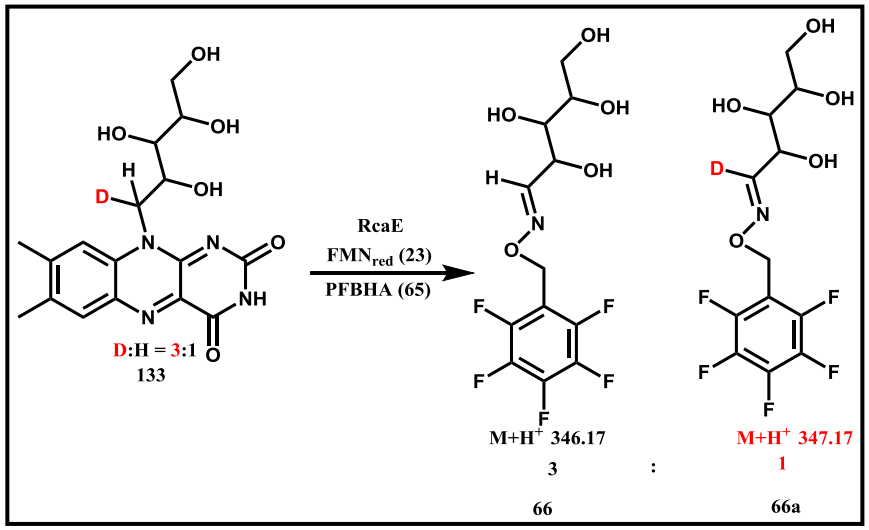

Figure 65: Fate of the D label in the oxime formed from D-labeled riboflavin (135).

Also, the residues responsible for binding the two flavins at the active site have been predicted by bioinformatic analysis of the conserved domains for RcaE using the Uniprot database (Figure 66).

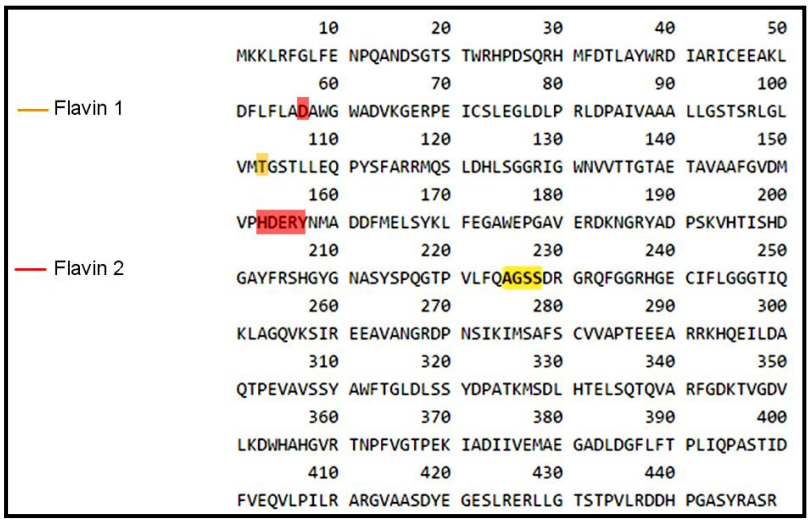

Figure 66: Predicted residues responsible for binding the two flavins at the active site of RcaE.

7.2 Abstraction of pro-R hydrogen from C_1' position of riboflavin

When a 3:1 mixture of C_1'-S-D-riboflavin : C_1'-R-D-riboflavin was incubated with the enzyme in the presence of PFBHA **(65)**, formation of the unlabeled ribose-PFBHA oxime **(66)** : D-ribose-PFBHA oxime **(66a)**was observed in ~ 1 : 3 ratio (Figure 67). This clearly suggested that the enzyme preferentially picks up the pro-R hydrogen from the C_1' position of D-riboflavin. To re-establish the results, a 3:1 mixture of C_1'-R-D-riboflavin : C_1'-S-D-riboflavin was incubated with the enzyme in the presence of **65**. In this case the ratio of unlabeled ribose-PFBHA oxime **(66)** : D-ribose-PFBHA oxime **(66a)** formed was ~ 3 : 1. This established that the pro-S hydrogen is not abstracted in

the transformation. A clear picture of the stereochemical orientation of the substrate in the protein active site will be obtained with a crystal structure having the substrate bound to the active site.

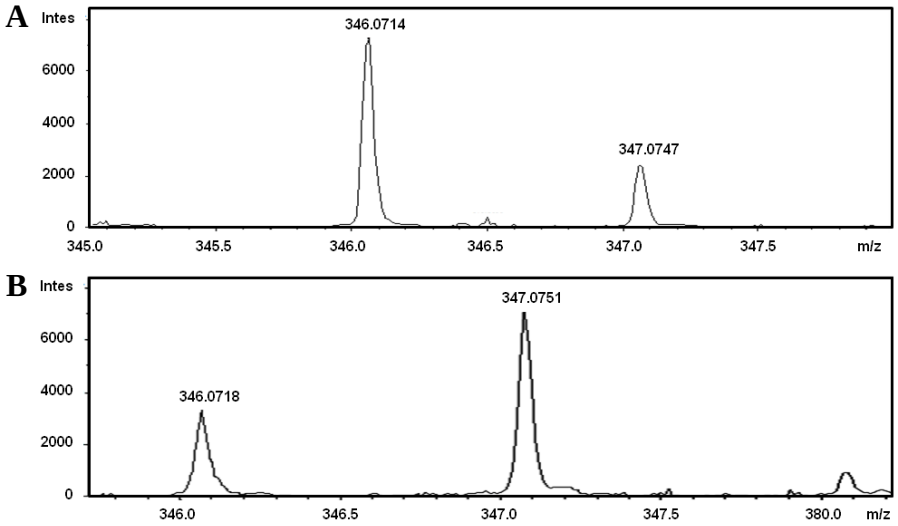

Figure 67: Detection of the formation of both non-labeled and D-labeled ribose-PFBHA from the S and R isomers of C1'-D-riboflavin (135). A: Formation of unlabeled : D-labeled ribose-PFBHA in ~ 3 : 1 ratio from C1'-D-riboflavin using 75% of C1'-R-D-riboflavin. B: Formation of unlabeled : D-labeled ribose-PFBHA in ~1 : 3 ratio from C1'-D-riboflavin using 75% of C1'-S-D-riboflavin.

7.3 Enzymatic reaction with R and S C_1'-D riboflavin (133)

In two different sets of enzymatic reactions, 250 µM R/S C_1'-D riboflavin was incubated with 20 µM FMN in the presence of 5 mM NADH and 50 µM RcaE. The reactions were incubated for 10 mins followed by incubation with 2 mM PFBHA **(65)** at

65°C for 1 hour. The resulting solution was analyzed by LCMS to analyze for D-incorporation in the ribose-PFBHA oxime formed in the reaction mixture.

CHAPTER VIII

CRYSTAL STRUCTURE DETERMINATION OF RcaE

8.1 Introduction

The biochemical evidences obtained on the mechanism of RcaE indicate the participation of a flavin derived semiquinone radical **(104)** in the abstraction of hydrogen from the C_1' of riboflavin **(1)**. Also, stereochemical experiments indicate that the pro-R hydrogen at C_1' is abstracted in the transformation. In order to get a better idea of the stereochemistry of the reaction, a crystal structure determination of the enzyme will be helpful. Also, it will show us the relative orientations of the substrates at the active site thereby validating our previous biochemical studies. Initial attempts to obtain a crystal structure with RcaE with the bound reduced cofactor FMN **(23)** were unsuccessful. Since the enzyme binds to reduced FMN **(23)** it was challenging to obtain protein crystals under aerobic conditions. Hence, an FMN analog, 5-deazaFMN **(72)** was designed to use for co-crystallization with RcaE. Due to the replacement of nitrogen with a carbon at the 5 position, reduced 5-deazaflavin is incapable of aerial oxidation involving an SET mechanism with molecular oxygen. Further approaches adopted to obtain the crystal structure was to use orthologs of RcaE, and also try out the truncated version of the protein developed by alignment to the nearest neighbor with a crystal structure, LadA – the long chain alkane monooxygenase which in *Geobacillus thermodenitrificans* converts long-chain alkane to corresponding primary alcohols.[87]

8.2 Results and Discussions

Purification of RcaE for crystal screen experiments

RcaE was purified using the regular purification procedure for His-tagged proteins. Next, the histidine tag was cleaved from the protein using TEV protease that cleaved at the TEV cleavage site located between the protein sequence and the His-tag sequence. This was followed by a round of purification through a Ni-NTA column to get rid of the histidine tag and the His-tagged TEV. Figure 68A shows the pure band of His-tag cleaved RcaE after purification. The eluent from the column consisted of the pure His-tag cleaved RcaE. For further purification, the tag cleaved protein was passed through a size exclusion column to obtain a predominant single band at 12.5 mins corresponding to the monomer of RcaE (Figure 68B).

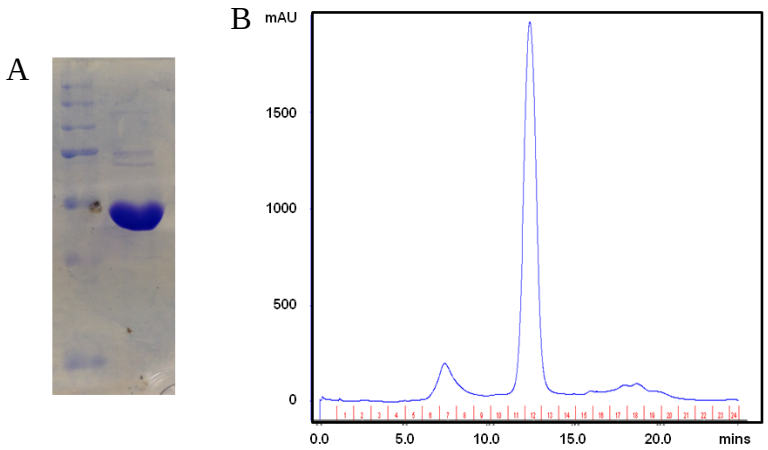

Figure 68: Purification of RcaE for crystallization. A: Purified RcaE after His-tag cleavage. B: RcaE after elution through a size-exclusion column.

Crystallization of RcaE

From binding studies reported in Chapter III it is evident that the cofactor FMN binds to the enzyme only in its reduced form. This activates the enzyme for binding with the oxidized substrate riboflavin **(1)**. However, in order to get a crystal structure of RcaE bound to the cofactor, reduced FMN **(23)** cannot be used due to its fast rate of oxidation under aerobic conditions. To circumvent the problem, 5-deazaFMN **(72)** was chemically synthesized and reduced with dithionite **(44)**. Due to the absence of the pyrazine ring this reduced form of 5-deazaFMN **(72)** would not undergo aerial oxidation and would thus remain bound to the enzyme in its reduced form throughout the entire duration of crystallization. Four different set ups were used for crystallization (Table 5). Set 1 and Set 2 were set up for crystallization of apo-protein in the absence and in the presence of the reducing agent dithionite, respectively. In Set 3, the enzyme incubated with reduced cofactor 5-deazaFMN **(72)** was set up for crystallization. Set 4 consisted of the enzyme bound to reduced cofactor 5-deazaFMN **(72)** and substrate riboflavin **(1)**. The crystallization was set in 96-well plates with different types and concentrations of precipitants and salts using the sitting-drop vapor diffusion method. Eleven 96-well plates were set up for the crystal screen that include 3 different salt screens (WIZARD and SRX) containing different salts and buffer at different pH; 6 lab screens (LS, CS, IMEX) containing salt, buffer and different types and concentrations of precipitants; 2 screens (PI and IND) containing different types of salt with different concentrations of the precipitant PEG. After 2-4 weeks, transparent crystals were obtained in some of the conditions, but all the crystals were found to be salt crystals. This indicated that the full

length RcaE from the *Microbacterium species* may not be suitable for crystallization. Thus, in anticipation of solving the problem, crystallization trials were set up using the truncated version of RcaE where the flexible N-terminal and C-terminal ends were predicted by the software Phyre2 using the already solved crystal structure of LadA bound to FMN (PDB - 3B9O).[87] Also 5 different orthologs of RcaE from 5 organisms were tested for crystallization.

Table 5: Conditions for crystallization of RcaE.

	Enzyme	Cofactor	Riboflavin	Ditionite	Total volume
Set 1	10 mg/mL	-	-	-	450 µL
Set 1	10 mg/mL	-	-	2 mM	450 µL
Set 3	10 mg/mL	2 mM	2 00 µM	2 mM	450 µL
Set 4	10 mg/mL	2 mM	2 00 µM	2 mM	450 µL

Crystallization of the truncated enzyme

LadA is the closest member to RcaE with a 40% sequence similarity for which the crystal structure has been solved. The sequence of RcaE was aligned to the sequence of LadA and using the software Phyre2, the flexible regions of RcaE were predicted. These regions form hanging loops, hence likely to hinder protein crystallization. Phyre2 uses the alignment of hidden Markov models via HHsearch[1] to significantly improve accuracy of alignment and detection rate. Next, it incorporates a new *ab initio* folding

simulation called Poing[2] to model regions of the protein of interest with no detectable homology to known structures. From the results, the flexible regions were at the N-terminal and C-terminal regions of RcaE (Figure 69). This made the truncation easier as the core of the protein would remain intact after truncation. The truncation was achieved by a subcloning strategy where the gene was cloned from pTHT by designing primers with restriction site absent in pTHT but present in a second vector pGEM7. Then, restriction digestion of the gene of interest was carried from pGEM7 using restriction sites common to both pTHT and pGEM7 followed by re-cloning into pTHT vector. The resulting plasmid was then isolated, purified and sequenced to confirm the truncation. Crystallization screens were set with the truncated protein following the same conditions as the native protein.

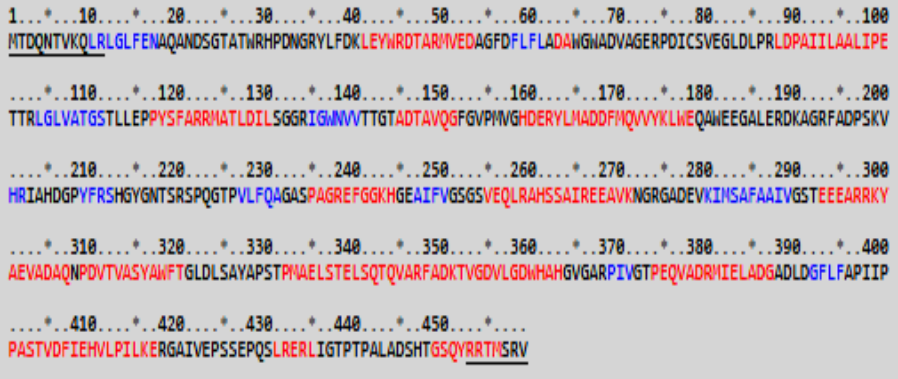

Figure 69: The sequence of RcaE with the underlined flexible N and C terminal sequences.

The red sequences constitute parts of α-helix and the blue sequences constitute parts of β-sheets.

Design, overexpression and purification of RcaE orthologs for protein crystallization

The sequence similarity network for RcaE was obtained by NCBI protein psiBLAST. Orthologs of RcaE were initially selected derived on > 95 % sequence coverage and a high (> 60 %) sequence identity (Table 6). The next criterion used to shortlist suitable targets was to check if the orthologs had neighboring functional genes similar to RcaE responsible for riboflavin catabolism (Table 7). Such a comparison for the neighboring genes of the orthologs from *Kitasatospora setae* is shown in Figure 70. Finally, five orthologs from *Herbiconiux sp., Marine actinobacterium, Devosia riboflavin, Leifsonia aquatic and Kitasatospora setae* were selected as targets for crystallization.

Table 6: Bioinformatic analysis of the RcaE orthologs

Description	Max Score	Total Score	Query Coverage	E value	Identity
Hypothetical protein [*Herbiconiux sp.* YR403]	673	673	97 %	0.0	71 %
Hypothetical protein [*Marine actinobacterium* PHSC20C1]	669	669	97 %	0.0	70 %
Hypothetical protein [*Devosia riboflavina*]	649	649	98 %	0.0	67 %
Hypothetical protein [*Leifsonia aquatica*]	648	648	96 %	0.0	72 %
Hypothetical protein [*Kitasatospora setae*]	639	639	97 %	0.0	68 %

Table 7: List of functional genes (marked in red) in the gene cluster containing RcaE

gene	start	stop	Amino acid	Protein homolog	Identity (%)
ORF21	2106	1585	174	Flavin reductase Marine actinobacterium PHSC20C1	87/159 55%
ORF22	2209	2811	201	PadR family transcriptional regulator Salinibacterium sp. PAMC 21357	120/186 65%
ORF23	3671	2820	284	Ribokinase Llyobacter polytropus DSM 2926	105/287 37%
ORF24	5073	3697	459	N5,N10-methylene tetrahydromethanopterin reductase Bacillus sp. 10403023	139/340 41%
ORF25	6036	5191	282	Transporter Marine actinobacterium PHSC20C1	202/269 75%
ORF26	6826	6032	265	ABC transporter ATP-binding protein marine actinobacterium PHSC20C1	189/258 73%
ORF27	5924	6859	312	Phenol hydroxylase Natronorubrum tibetense	53/165 32%

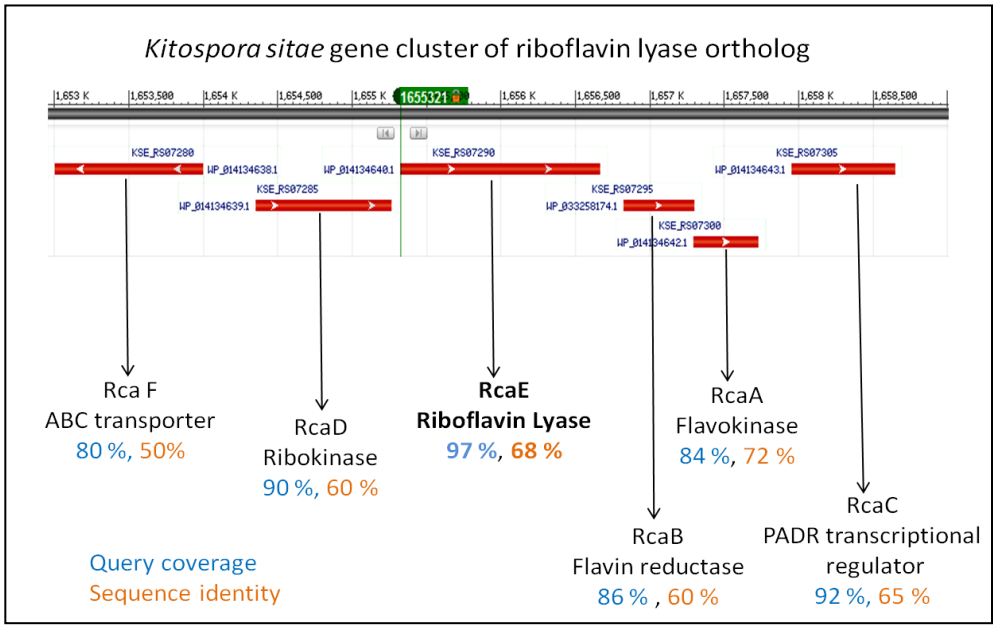

Figure 70: The genes neighboring RcaE ortholog in *Kitasatospora setae* and their similarity genes in the RcaE gene cluster.

The five orthologs of RcaE were gene synthesized from Genscript, cloned into pTHT vector, overexpressed in BL21-DE3 cells and purified by Ni-NTA column chromatography as described earlier (Figure 71A). For the His-tag cleavage the proteins were treated with TEV protease and purified by NI-NTA column chromatography. The tag cleavage and purification of the orthologs from *Kitasatospora setae* (Ortholog 2) is shown in Figure 71B.

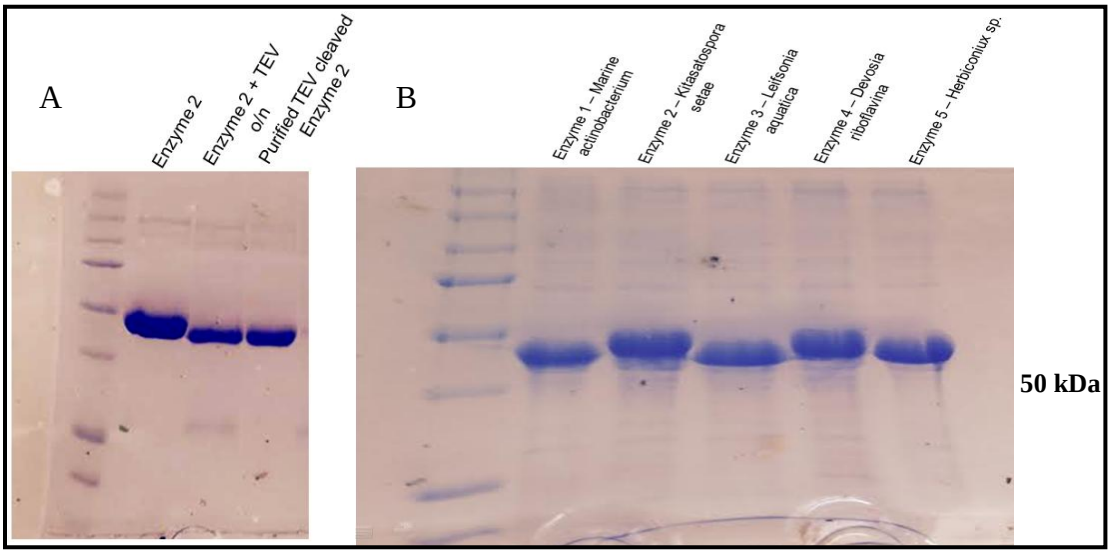

Figure 71: Purification of the five RcaE orthologs for crystallization. A: SDS-PAGE gel analysis of purified RcaE orthologs from five different microorganisms. B: SDS-PAGE gel analysis of RcaE ortholog from *Kitasatospora setae* after his-tag cleavage and further purification.

Test for enzyme activity of the purified RcaE orthologs and truncated RcaE

The following experiments were done to test the riboflavin lyase activity of the RcaE orthologs.

- Enzyme converts riboflavin **(1)** to lumichrome **(12)** and ribose **(15)** (Figure 72)
- Lumiflavin **(86)** acts as the substrate to indicate radical chemistry (Figure 73)
- FMN is used as the cofactor (Figure 74)
- Reduced 5-deazaFMN **(72)** binds to the enzyme to make sure that the analog is suitable for crystallization experiments
- Same studies with the truncated protein

Enzymatic reactions were set up using the different substrates and cofactors listed in Table 8.

Table 8: The list of the different substrates and cofactors used for the enzymatic reactions of RcaE orthologs.

substrate	Reducing agent	cofactor
riboflavin	NADH	FMN
lumiflavin	dithionite	deazaFMN
deazariboflavin		

Figure 72A shows the HPLC trace for the reconstitution of the 5 orthologs of RcaE and the truncated RcaE with riboflavin as the substrate and reduced FMN **(23)** as the cofactor. All the orthologs give almost complete conversion of riboflavin **(1)** to lumichrome **(12)** in 30 minutes. Figure 72B is the representative for the control reactions performed with the orthologs. It includes the reaction results in the absence of individual reaction components for the Ortholog 2. The release of ribose **(15)** as the other reaction product was tested for the orthologs by LC-MS.

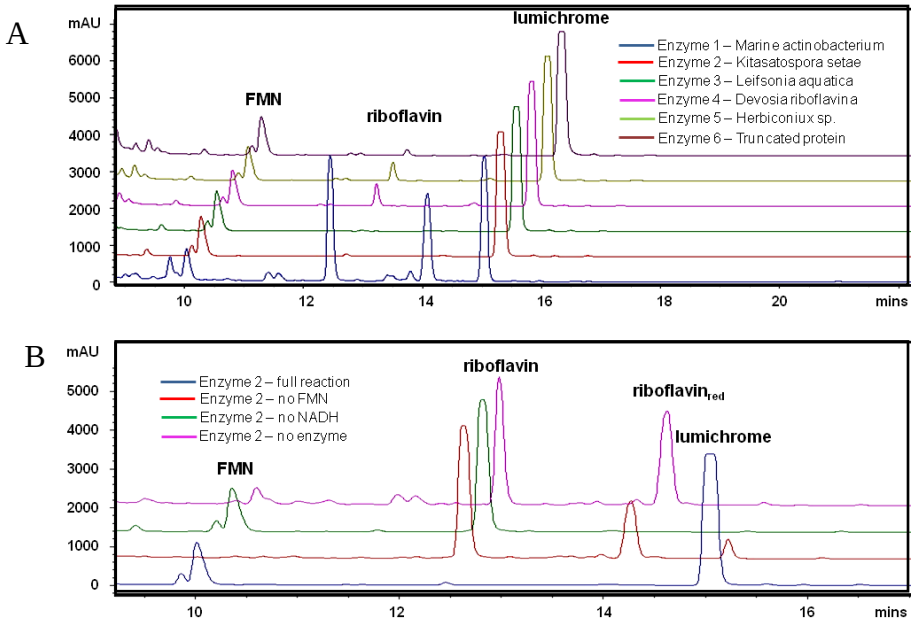

Figure 72: Reconstitution of RcaE orthologs. A: HPLC trace for the formation of lumichrome (13) for the 1 RcaE orthologs and truncated RcaE. B: The control reactions for the Ortholog 2 whre FMN, enzyme and NADH are absent in three different reactions.

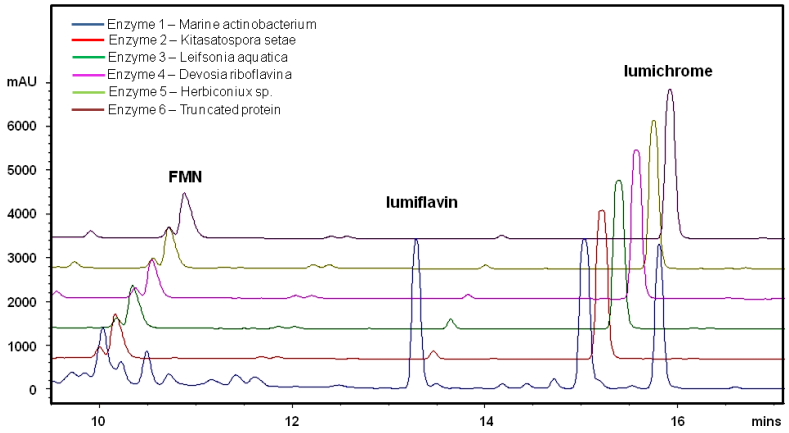

Figure 73: Reconstitution of RcaE orthologs and truncated RcaE with lumiflavin as the substrate and reduced FMN as the cofactor.

The next set of experiments was carried out to establish the role of FMN as the cofactor. As discussed in Chapter III 5-deazaFMN **(72)** and 5-deazariboflavin **(73)** were used in the reactions. As expected no lumichrome **(12)** formation was observed when 5-deazaFMN **(72)** and riboflavin **(1)** were incubated with the enzymes in the presence of dithionite **(44)**. In contrast, 5-deazariboflavin **(73)** was converted to 5-deazalumichrome **(74)** in the enzymatic reaction in the presence of FMN **(2)** and dithionite **(44)** (Figure 74). The reaction was much slower for Ortholog 4 and required incubation for 4 hrs.

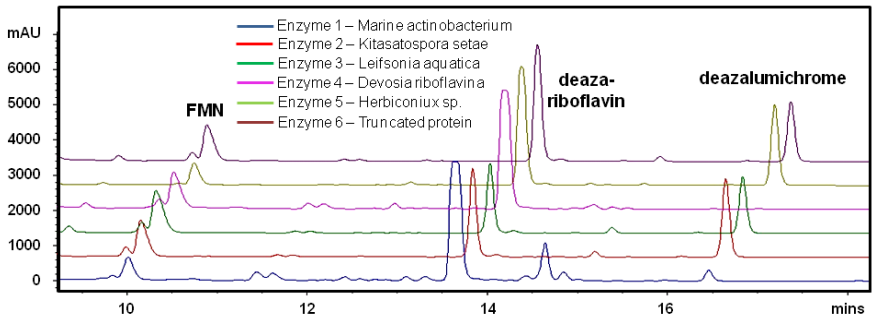

Figure 74: Reconstitution of RcaE orthologs with reduced FMN (23) as the cofactor and 5-deazariboflavin (73) as the substrate.

8.3 Experimental

Crystal screen set-up for the RcaE orthologs

Crystallization plates were set up in 96-well plate format for the five orthologs of RcaE and the truncated RcaE using sitting-drop vapor diffusion method. The crystallization solutions were used as described before. Bright yellow crystals were obtained for Ortholog 5 (*Herbiconiux sp.)* in 8 different crystal solutions (Table 9). The

conditions marked in red in the table were used for further optimization of the crystals. Initial X-ray diffraction with the crystals provided diffraction patterns consistent with protein crystals. But, the resolution of the diffraction data was extremely poor (Figure 75).

Table 9: The mother liquor composition for crystal formation with Ortholog 5.

Solution	Condition	pH
INDEX A3	2 M ammonium sulfate, 0.1 M Bis-Tris	5.5
INDEX A4	2 M ammonium sulfate, 0.1 M Bis-Tris	6.5
INDEX A6	2 M ammonium sulfate, 0.1 M Tris	8.5
INDEX C3	2.4 M sodium malonate	7.0
Crystal Screen B6	1 M ammonium sulfate, 0.1 M HEPES 0.5 % w/v PEG8000	7.0
Crystal Screen D2	1 M sodium cacodylate, 0.1 M HEPES	6.5
Lab Screen G 12	0.1 M HEPES, 4.3 M NaCl	7.5
Salt Screen E4	2.4 M ammonium phosphate dibasic, 0.1 M Tris	8.5

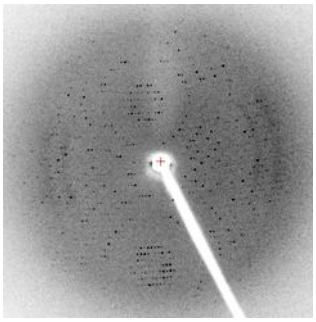

Figure 75: Diffraction pattern obtained from the crystal of RcaE ortholog from *Herbiconiux sp.*

Optimization for conditions for crystallization of RcaE orthologs from Herbiconiux sp.

The crystals were further refined using hanging drop method in 24-well plates. Taking the initial solution composition as the starting point, both pH and concentration of the salts were varied along the X and Y axes of the 24-well plate. The modified solvent compositions for the two different screening solutions selected are shown in Figure 76. For each screening solution, four 24-well plates were used for optimization with different concentrations of the components and different pH.

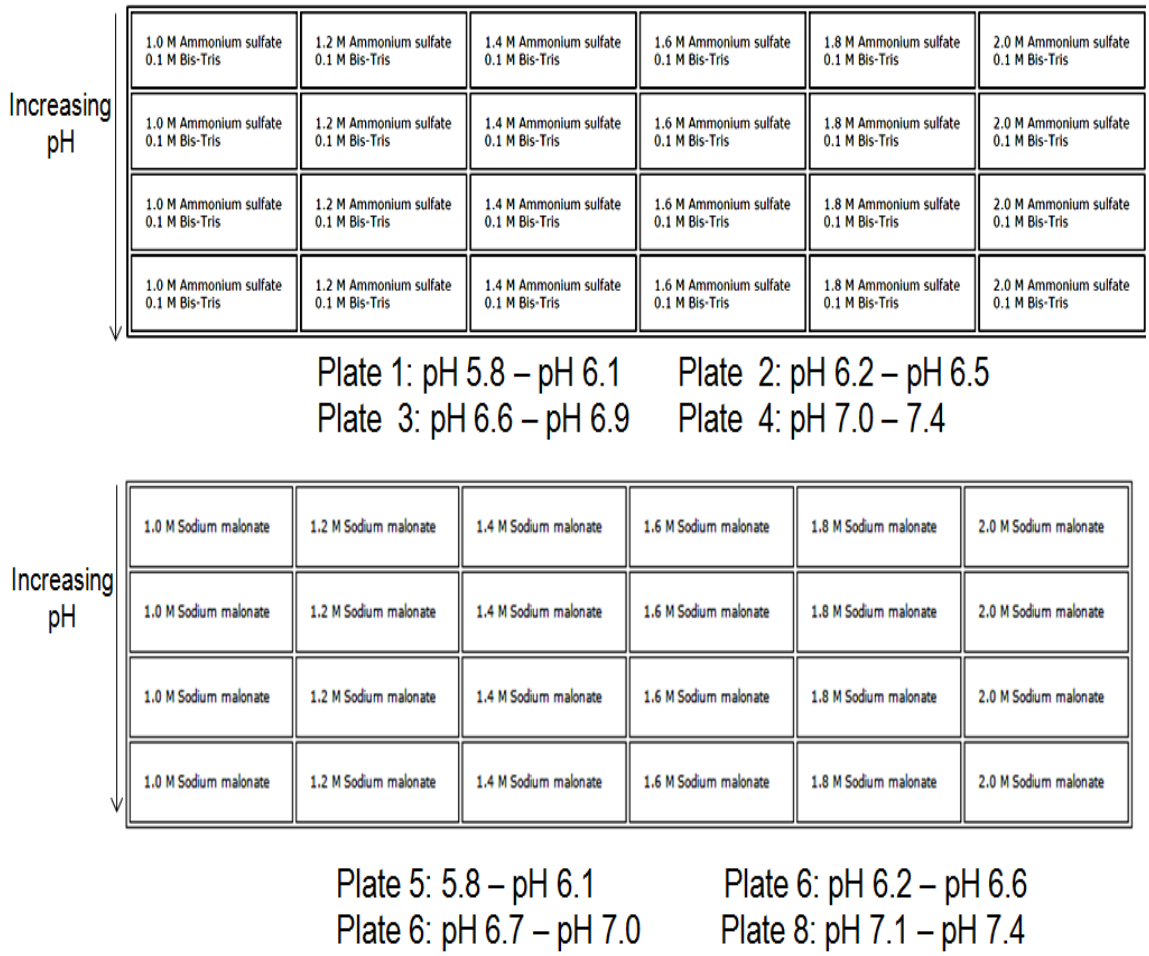

Figure 76: Crystal screen solutions selected for the optimization of RcaE orthologs crystals.

Within 3 weeks of setting up the crystals, long, beautiful rod shaped bright yellow crystals were obtained in the solution with 1.8 – 2.0 M ammonium sulfate and 0.1 (M) Bis-Tris at pH 5.8 – 6.2.

Enzyme purification by TEV protease cleavage followed by size-exclusion chromatography

The enzyme RcaE (and its orthologs) obtained after desalting was incubated with TEV enzyme. The concentration of TEV is maintained such that it undergoes 5 turnovers to cleave the tag in the enzyme. The enzyme was incubated with TEV at room temperature for 4 hours followed by incubation at 4˚C for overnight. The mixture was then passed through a Ni-NTA column and the pure enzyme was eluted with 100 mM phosphate buffer at pH 8.0. The TEV and the histidine tag remained bound to the column. Small aliquots of samples from before and after TEV cleavage, as well as from the following purification process were run on an SDS-PAGE gel and compared for analysis of cleavage-efficiency and purity.

Cloning and overexpression of truncated RcaE

The protocol followed to clone the truncated RcaE is shown in Figure 77. The primers used for the cloning are also listed in the figure.

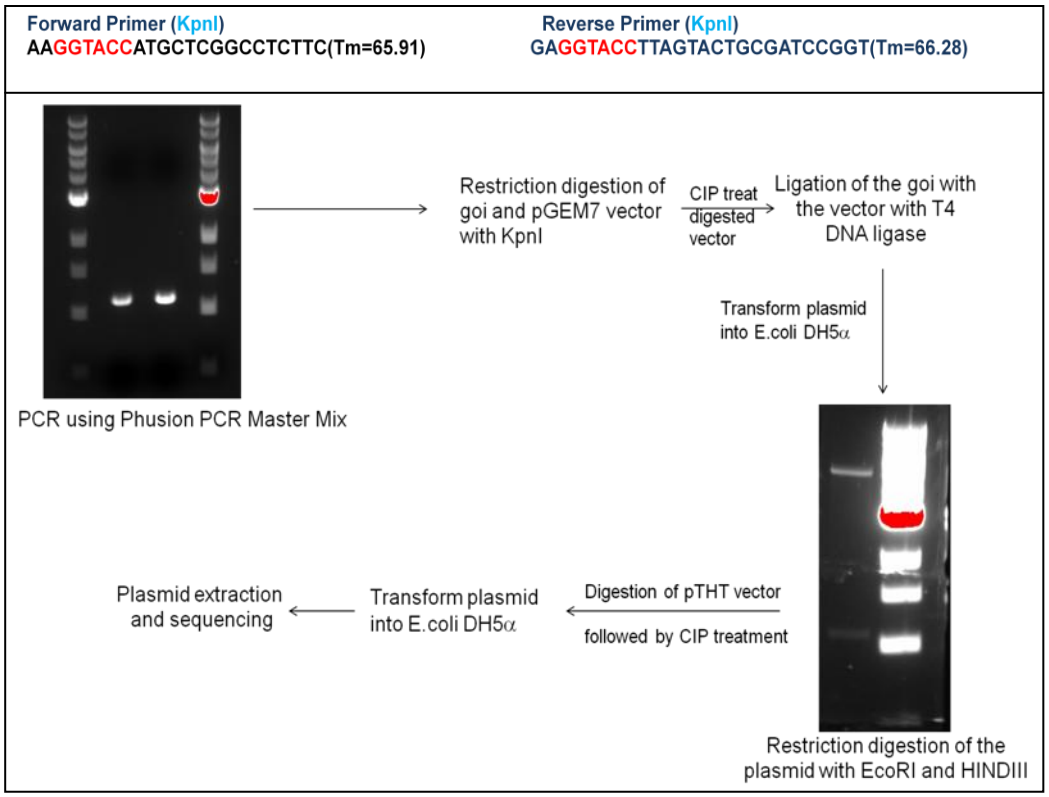

Figure 77: The forward and reverse primers for cloning truncated RcaE into pTHT vector (top). The protocol followed to obtain the truncated truncated RcaE (bottom).

Enzymatic reactions of the RcaE orthologs

250 µM of the substrate was incubated with 20 µM enzyme in the presence of 20 µM cofactor and 2 mM NADH **(22)**. All reactions were incubated at 37°C for 30 mins.

8.4 X-ray diffraction data for the crystal of RcaE ortholog

The X-ray diffraction data will be obtained for the crystals of RcaE ortholog from *Herbiconiux sp.* Data was collected at the Advanced Photon Source (Argonne, Illinois, USA)-1 Å (wavelength) a at beamline 24ID-C using a Pilatus 6 M pixel detector at a temperature of 100 K. X-ray Diffraction data were collected for 360 frames. Data

sets were integrated in HKL2000 to obtain the unit cell dimensions. Next, the space group was determined from the systematic absences by Xtriage (PHENIX) to be P_{212121} (orthorhombic space group). Phasing was achieved by PHENIX software using Molecular Replacement method. The crystal structure of LadA bound to FMN (PDB 3B9O) with a 40 % sequence similarity with RcaE was used for homology modeling. Following this, an electron density map was generated and fit to individual residues. Further rounds of refinements revealed a positive density corresponding to 5-deazaFMN **(72)**. A faint density for the other flavin ring was observed but the density was not enough to build a structure. This might have been due to the poor solubility of riboflavin **(1)** in comparison to the phosphorylated flavin 5-deazaFMN **(72)**.

8.5 X-ray crystal structure of RcaE ortholog from *Herbiconiux sp.*

A crystal structure of the RcaE ortholog with a resolution of 2.12 Å was obtained. The R_{work} was 0.22 whereas the R_{free} was 0.25. The protein crystallized as a dimer (Figure 78). The active site on each monomer is present near the surface. One of the monomers had 5-deazaFMN **(72)** bound to the active site. Figure 79 shows the Rossmann fold with 6 alternate α-helices and β-sheets at the active site of the monomer housing the 5-deazaFMN **(72)**.

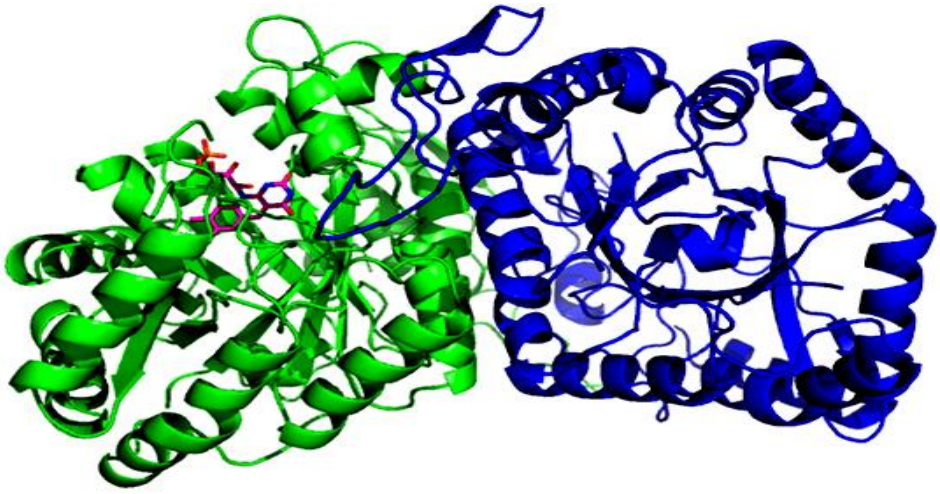

Figure 78: Crystal structure of the dimer of RcaE ortholog from Herbiconiux sp. with 5-deazaFMN (72) bound at the active site

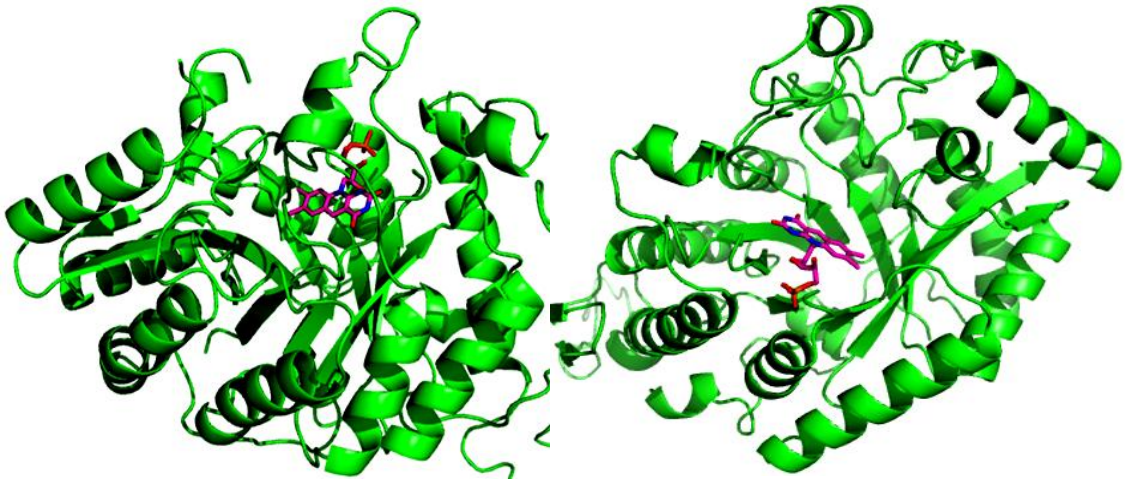

Figure 79: Rossmann fold in the crystal structure of the monomer of RcaE ortholog A: 6 alternate a-helices and b-sheets forming the Rossmann fold. B: Top view of the Rossmann fold housing the cofactor 5-deazaFMN **(72)**

A zoom in to the active site reveals the active site residues responsible for the binding of the cofactor (Figure 80A). His155, Ser230 and Try159 stabilize the phosphate group of the 5-deazaFMN **(72)**. One of the oxygen from the phosphate group stabilizes the C_3'-hydroxyl group by hydrogen bonding. Also, the N_1 of the flavin ring interacts with the C_2'-hydroxyl group. Hence, there is a stabilized tight binding pocket for the ribose-phosphate group of the cofactor at the active site. The other interactions are Asp59 with N_3 and Asn134 with the C_5 (originally a nitrogen in the cofactor FMN **(2)**). A π-stacking interaction of the flavin ring with Phe245 is observed (Figure 80B). There are two conspicuously placed Phe residues (Phe11 and Phe56) that might orient themselves once the substrate is bound to intercalate the flavin ring.

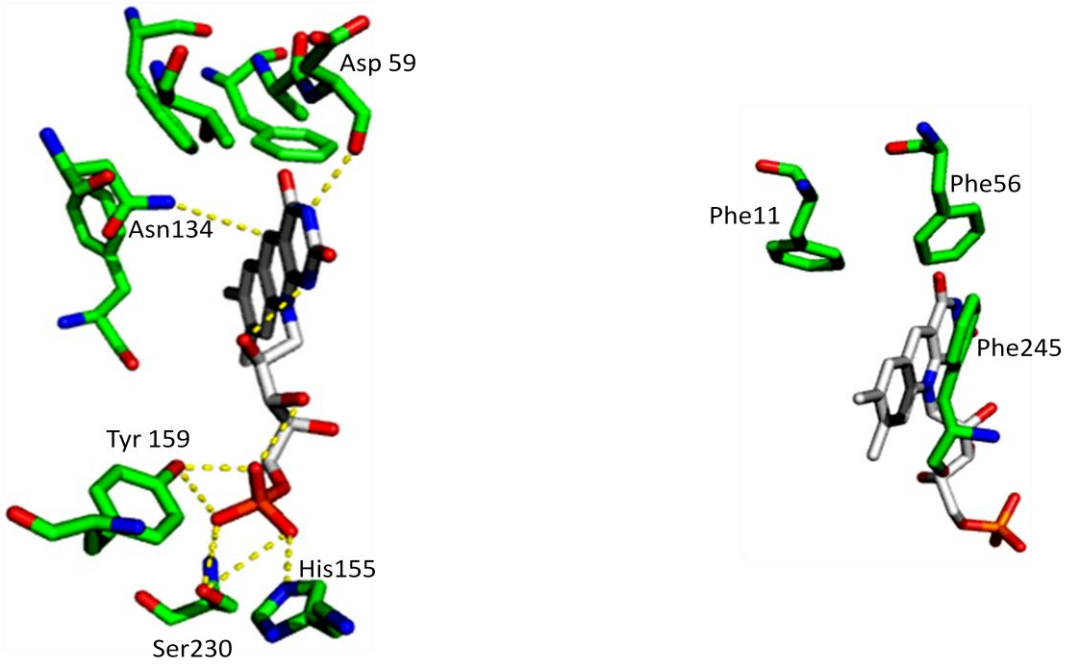

Figure 80: Interaction of the active site residues with the cofactor

CHAPTER IX

SUMMARY, CONCLUSION AND FUTURE PERSPECTIVE

9.1 Summary

In this thesis, a mechanistic proposal for the oxidative degradation of riboflavin by riboflavin lyase consistent with the experimental results obtained from substrate analog and isotope labeling experiments has been proposed (Figure 55 reproduced).

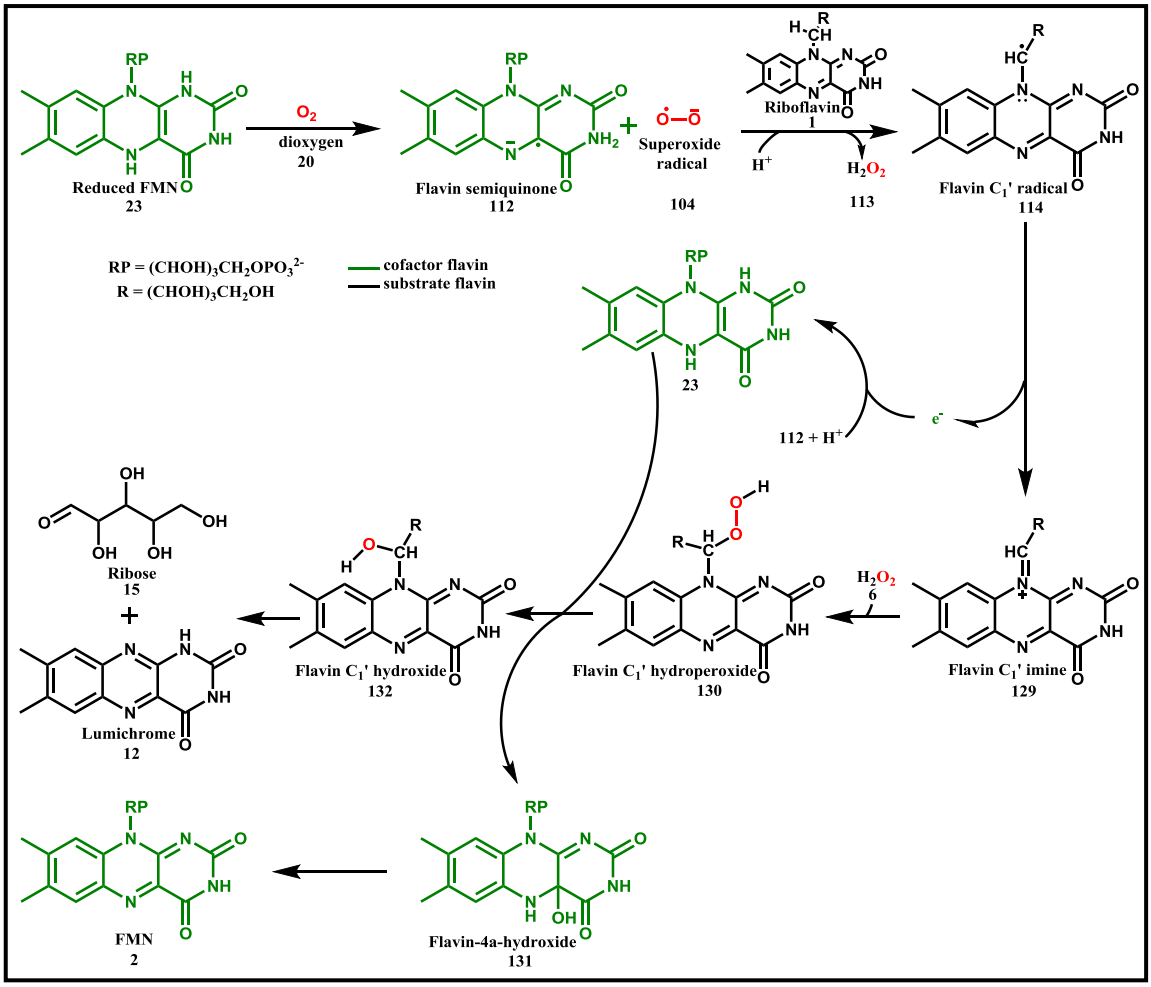

Figure 55 (reproduced): Mechanistic scheme for riboflavin degradation by riboflavin lyase.

Riboflavin lyase is a flavoenzyme which utilizes reduced flavin (FMN) **(23)** as the cofactor to cleave a second flavin molecule riboflavin **(1)**. The enzyme first binds to reduced FMN **(23)** followed by riboflavin **(1)**. Reduced FMN **(23)** at the active site then reacts with molecular oxygen **(20)** to give the corresponding flavin semiquinone **(112)** and superoxide radical anion **(104)**. Superoxide radical anion **(104)** then abstracts a hydrogen from the C_1' position of the substrate riboflavin generating the riboflavin-C_1'-radical **(114)** and hydrogen peroxide **(113)**. **114** in the next step transfers an electron to the cofactor, FMN semiquinone **(112)** at the active site and is converted to the flavin-C_1'-imine **(129)**. In the subsequent step, the hydrogen peroxide **(113)** at the active site combines with the imine **(129)** to produce the flavin-C_1'-hydroperoxide **(130)**. After this, the reduced cofactor FMN **(23)** at the active site reduces **130** to the corresponding flavin-C1'-hydroxide **(132)**. During this step, the reduced FMN **(23)** is converted to the oxidized FMN **(2)** via the formation of the flavin-4α-hydroxide **(131)**. Flavin-C_1'-hydroxide **(132)** in the next step is hydrolyzed to generate lumichrome **(12)** and ribose **(15)**.

The generation of lumichrome **(12)** when riboflavin lyase is incubated with potassium superoxide **(111)** and riboflavin **(1)** provides direct evidence for the formation of the superoxide radical **(104)** as an intermediate in the enzymatic reaction. Analog studies with lumiflavin **(86)** indicated that the reaction indeed proceeds through a radical mechanism. To confirm the intermediacy of the riboflavin C_1' radical **(114)** in the reaction mechanism, the radical trap cyclopropylmethylflavin **(115)** has been used. With cyclopropylmethylflavin **(115)** as the substrate, a ring cleavage chemistry due to β-bond

scission after the formation of the radical at C_1' generated butanal **(117)** as one of the reaction products confirming the formation of the riboflavin C_1'-radical **(114)**. Absence of any release of hydrogen peroxide **(113)** by oxygen electrode experiments, followed by ^{18}O incorporation experiments confirming the incorporation of oxygen atom into the ribose **(15)** from molecular oxygen **(20)** led to the proposal for the formation of the flavin-C1'-hydroperoxide **(130)** from its preceding imine **(129).** Finally the stoichiometric formation of lumichrome **(12)** with externally added reduced FMN **(23)** indicates that the oxidized FMN **(2)** is the final product of the reaction. From these results we propose that the reduced cofactor FMN **(23)** at the active site reduces **130** to the flavin-C_1'-hydroxide **(132)** followed by hydrolysis to lumichrome **(12**) and ribose **(15)**.

9.2 Conclusion

RcaE serves as the first example where the reduced cofactor FMN **(23)** is required to catalyze the breakdown of a second flavin molecule, riboflavin **(1)**. This novel transformation is brought about by a flavin derived superoxide radical **(104)** system. Mixed function amine oxidase (MFAO) is the only reported example speculated to proceed via a similar flavin derived superoxide radical intermediate. Riboflavin lyase (RcaE) is the first example of a flavoenzyme where conclusive evidence for the actual participation of a superoxide radical is shown. The fact that a superoxide radical mediated enzymatic conversion of riboflavin **(1)** to lumichrome **(12)** is observed even in the absence of the reduced cofactor FMN **(23)** points to the fact that the superoxide radical **(104)** is the active oxidizing species in the transformation (Figure 78). The role of

the cofactor, reduced FMN **(23)** is the generation of this superoxide radical **(104)** from oxygen **(20)**.

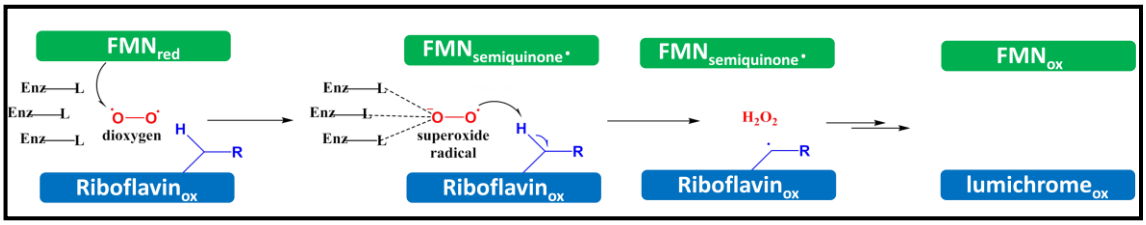

Figure 79: Scheme for hydrogen abstraction from the substrate by flavin derived superoxide radical (104) to give the substrate radical.

9.3 Future Perspective

Further degradation of the isoalloxazine ring

In the Microbacterium marytipicum G10 strain isolated from a riboflavin rich environment, lumichrome is not further degraded and is precipitated out into the medium. This interesting observation indicates that the purpose of riboflavin degradation in this strain and some other rhizobia (as evident from the phylogenetic distribution of RcaE) is the production of the alloxazine ring, lumichrome **(2)** which can then act as an important signaling molecule. Hence, the catabolism stops at this stage.

In contrast, there might be other strains present in riboflavin rich environment which may be able to cleave the alloxazine ring of the flavin all the way to use this molecule as a potential carbon and/or nitrogen source. Such an example was reported by the Stadtman group in 1965 where a *Pseudomonas RF* strain was shown to degrade riboflavin all the way to the lactone **(18)** and oxalimide **(19)** (Figure 4).[28,31] But the strain

could not be recovered for further studies. The future goal of the riboflavin catabolism project will be to focus on the isoalloxazine catabolism. The group of bacterial strains that have been collected from DSM Nutritional Products, Germany, might contain an individual strains responsible for isoalloxazine catabolism. The soil and dust samples recovered from DSM will be grown on riboflavin using an enrichment method to identify the strains growing on riboflavin as the carbon/nitrogen source. This will be followed by isolation of the individual strains that can grow on riboflavin.

Crystal structure determination with the cofactor and the substrate/product bound

A crystal structure of the enzyme will throw light on the active site conformations of the enzyme and the binding pockets for the two flavins along with molecular oxygen. We have obtained protein crystals for an ortholog of riboflavin lyase from *Herbiconiux species* at 2.1 Å resolution with the cofactor 5-deazaFMN **(72)** bound. The insolubility of the substrate riboflavin **(1)** in aqueous medium might play a role in its inability to co-crystallize with the protein. Currently we are working on obtaining a RcaE orthologs crystal bound to both the cofactor 5-deazaFMN **(72)** and a relatively water-soluble substrate analog such as 6,7-dimethyl-8-ribityllumazine **(136) (Appendix A)** to get a deeper insight into the active site structure. This may also help to identify the oxyanion hole responsible for binding to molecular oxygen and also the superoxide radical intermediate.

REFERENCES

(1) Powers, H. J. Riboflavin (vitamin B-2) and health. *The American Journal of Clinical Nutrition* **2003,** *77* (6), 1352.

(2) John T. Pinto, R. S. R. *Handbook of Vitamins* 2013.

(3) Shi, Z.; Zachara, J. M.; Shi, L.; Wang, Z.; Moore, D. A.; Kennedy, D. W.; Fredrickson, J. K. Redox reactions of reduced flavin mononucleotide (FMN), riboflavin (RBF), and anthraquinone-2,6-disulfonate (AQDS) with ferrihydrite and lepidocrocite. *Environmental Science & Technology* **2012,** *46* (21), 11644.

(4) Ashoori, M.; Saedisomeolia, A. Riboflavin (vitamin B2) and oxidative stress: a review. *The British Journal of Nutrition* **2014,** *111* (11), 1985.

(5) Buehler, B. A. Vitamin B2: Riboflavin. *Journal of Evidence-Based Complementary & Alternative Medicine* **2011,** *16* (2), 88.

(6) Bacher, A.; Eberhardt, S.; Fischer, M.; Kis, K.; Richter, G. Biosynthesis of vitamin B2 (riboflavin). *Annu Rev Nutr* **2000,** *20*, 153.

(7) Richter, G.; Fischer, M.; Krieger, C.; Eberhardt, S.; Lüttgen, H.; Gerstenschläger, I.; Bacher, A. Biosynthesis of riboflavin: characterization of the bifunctional deaminase-reductase of Escherichia coli and Bacillus subtilis. *Journal of Bacteriology* **1997,** *179* (6), 2022.

(8) Keller, P. J.; Le Van, Q.; Kim, S. U.; Bown, D. H.; Chen, H. C.; Kohnle, A.; Bacher, A.; Floss, H. G. Biosynthesis of riboflavin: mechanism of formation of the ribitylamino linkage. *Biochemistry* **1988,** *27* (4), 1117.

(9) Gerhardt, S.; Schott, A.-K.; Kairies, N.; Cushman, M.; Illarionov, B.; Eisenreich, W.; Bacher, A.; Huber, R.; Steinbacher, S.; Fischer, M. Studies on the Reaction Mechanism of Riboflavin Synthase: X-Ray Crystal Structure of a Complex with 6-Carboxyethyl-7-Oxo-8-Ribityllumazine. *Structure* **2002,** *10* (10), 1371.

(10) Hustad, S.; McKinley, M. C.; McNulty, H.; Schneede, J.; Strain, J. J.; Scott, J. M.; Ueland, P. M. Riboflavin, Flavin Mononucleotide, and Flavin Adenine Dinucleotide in human plasma and erythrocytes at baseline and after low-dose riboflavin supplementation. *Clinical Chemistry* **2002,** *48* (9), 1571.

(11) Kitzing, K.; Auweter, S.; Amrhein, N.; Macheroux, P. Mechanism of Chorismate Synthase: Role of the two invariant histidine residues in the active site. *Journal of Biological Chemistry* **2004,** *279* (10), 9451.

(12) In Class 1 Oxidoreductases XI: EC 1.14.11–1.14.14; S*pringer Berlin Heidelberg: Berlin, Heidelberg*, 2006, DOI:10.1007/3-540-37708-5_123

(13) Wang, Z.; Chernyshev, A.; Koehn, E. M.; Manuel, A.; Lesley, S. A.; Kohen, A. Oxidase Activity of a Flavin-Dependent Thymidylate Synthase. *The FEBS Journal* **2009,** *276* (10), 2801.

(14) Ghisla, S.; Edmondson, D. E. Flavin Coenzymes. *In eLS; John Wiley & Sons, Ltd*, 2001, DOI:10.1002/9780470015902.a0000654.pub3

(15) A H Neims, a.; Hellerman, L. Flavoenzyme catalysis. *Annual Review of Biochemistry* **1970,** *39* (1), 867.

(16) Mewies, M.; McIntire, W. S.; Scrutton, N. S. Covalent attachment of flavin adenine dinucleotide (FAD) and flavin mononucleotide (FMN) to enzymes: the current state of affairs. *Protein science : a publication of the Protein Society* **1998,** *7* (1), 7.

(17) Daithankar, V. N.; Wang, W.; Trujillo, J. R.; Thorpe, C. Flavin-linked Erv-family sulfhydryl oxidases release superoxide anion during catalytic turnover. *Biochemistry* **2012,** *51* (1), 265.

(18) Bender, D. A.; Bender, D. A. Vitamin B2 – Riboflavin. *Nutritional Biochemistry of the Vitamins*; Cambridge University Press, 2003.

(19) Zempleni, J.; Galloway, J. R.; McCormick, D. B. The identification and kinetics of 7 alpha-hydroxyriboflavin (7-hydroxymethylriboflavin) in blood plasma from humans following oral administration of riboflavin supplements. *Int J Vitam Nutr Res* **1996,** *66* (2), 151.

(20) Combs Jr, G. F. In The Vitamins (Fourth Edition); *Academic Press: San Diego*, 2012, DOI:http://dx.doi.org/10.1016/B978-0-12-381980-2.00011-6.

(21) Begley, T. P.; Chatterjee, A.; Hanes, J. W.; Hazra, A.; Ealick, S. E. Cofactor biosynthesis – still yielding fascinating new biological chemistry. *Current Opinion in Chemical Biology* **2008,** *12* (2), 118.

(22) Daniel, A.; Snider, M. Elucidating the Nicotinic Acid Degradation Pathway in Bacillus niacini. *The FASEB Journal* **2015,** *29*.

(23) Unno, M.; Matsui, T.; Ikeda-Saito, M. Structure and catalytic mechanism of heme oxygenase. *Natural Product Reports* **2007,** *24* (3), 553.

(24) Mukherjee, T.; Hanes, J.; Tews, I.; Ealick, S. E.; Begley, T. P. Pyridoxal phosphate: Biosynthesis and catabolism. *Biochimica et Biophysica Acta (BBA) - Proteins and Proteomics* **2011,** *1814* (11), 1585.

(25) Neal, R. A. Bacterial metabolism of thiamine. I. The isolation and characterization of the initial intermediates in the oxidation of thiamine. *The Journal of Biological Chemistry* **1968,** *243* (17), 4634.

(26) Bacher, A.; Rappold, H. Bacterial degradation of folic acid. *Methods in enzymology* **1980,** *66*, 652.

(27) Im, W. B.; Roth, J. A.; McCormick, D. B.; Wright, L. D. Bacterial Degradation of Biotin: V. Metabolism of 14c-carbonyl-labeled biotin d-sulfoxide. *Journal of Biological Chemistry* **1970,** *245* (23), 6269.

(28) Harkness, D. R.; Stadtman, E. R. Bacterial degradation of riboflavin. VI. Enzymatic conversion of riboflavin to 1-ribityl-2,3-diketo-1,2,3,4-tetrahydro-6, 7-dimethylquinoxaline, urea, and carbon dioxide. *The Journal of Biological Chemistry* **1965,** *240* (10), 4089.

(29) Foster, J. W. Microbiological aspects of riboflavin: I. Introduction. II. Bacterial oxidation of riboflavin to lumichrome. *Journal of Bacteriology* **1944,** *47* (1), 27.

(30) Yang, C. S.; McCormick, D. B. Substrate specificity of riboflavin hydrolase from Pseudomonas riboflavina. *Biochimica et Biophysica Acta* **1967,** *132* (2), 511.

(31) Barz, W.; Stadtman, E. R. Bacterial degradation of riboflavin. VII. Studies on the bacterial decomposition of 6,7-dimethylquinoxaline-2,3-diol. *Archiv fur Mikrobiologie* **1969,** *67* (2), 128.

(32) Foster, J. W.; Yanagita, T. A bacterial riboflavin hydrolase. *The Journal of Biological Chemistry* **1956,** *221* (2), 593.

(33) Huang, R.; Kim, H. J.; Min, D. B. Photosensitizing effect of riboflavin, lumiflavin, and lumichrome on the generation of volatiles in soy milk. *Journal of Agricultural and Food Chemistry* **2006,** *54* (6), 2359.

(34) Chaiyen, P.; Fraaije, M. W.; Mattevi, A. The enigmatic reaction of flavins with oxygen. *Trends in Biochemical Sciences 37* (9), 373.

(35) Palfey, B. A.; Ballou, D. P.; Massey, V. Oxygen activation by flavins and pterins. *Active Oxygen in Biochemistry*; *Springer Netherlands: Dordrecht,* 1995, DOI:10.1007/978-94-011-0609-2_2 10.1007/978-94-011-0609-2_2.

(36) Walsh, C. T.; Wencewicz, T. A. Flavoenzymes: versatile catalysts in biosynthetic pathways. *Natural Product Reports* **2013,** *30* (1), 175.

(37) Dijkman, W. P.; de Gonzalo, G.; Mattevi, A.; Fraaije, M. W. Flavoprotein oxidases: classification and applications. *Applied Microbiology and Biotechnology* **2013,** *97* (12), 5177.

(38) Huijbers, M. M. E.; Montersino, S.; Westphal, A. H.; Tischler, D.; van Berkel, W. J. H. Flavin dependent monooxygenases. *Archives of Biochemistry and Biophysics* **2014,** *544*, 2.

(39) Entsch, B.; van Berkel, W. J. Structure and mechanism of para-hydroxybenzoate hydroxylase. *FASEB journal : official publication of the Federation of American Societies for Experimental Biology* **1995,** *9* (7), 476.

(40) Ellis, H. R. The FMN-dependent two-component monooxygenase systems. *Archives of Biochemistry and Biophysics* **2010,** *497* (1–2), 1.

(41) Baldwin, T. O.; Christopher, J. A.; Raushel, F. M.; Sinclair, J. F.; Ziegler, M. M.; Fisher, A. J.; Rayment, I. Structure of bacterial luciferase. *Current Opinion in Structural Biology* **1995,** *5* (6), 798.

(42) Fraaije, M. W.; Mattevi, A. Flavoenzymes: diverse catalysts with recurrent features. *Trends in Biochemical Sciences 25* (3), 126.

(43) Joosten, V.; van Berkel, W. J. H. Flavoenzymes. *Current Opinion in Chemical Biology* **2007,** *11* (2), 195.

(44) Fieschi, F.; Nivière, V.; Frier, C.; Décout, J.-L.; Fontecave, M. The Mechanism and Substrate Specificity of the NADPH:Flavin Oxidoreductase from Escherichia coli. *Journal of Biological Chemistry* **1995,** *270* (51), 30392.

(45) Fox, J. L. Sodium dithionite reduction of flavin. *FEBS Letters* **1974,** *39* (1), 53.

(46) Burn, G. P.; O'Brien, J. R. P. The kinetics of the reduction of riboflavin by dithionite. *Biochimica et Biophysica Acta* **1959,** *31* (2), 328.

(47) Murthy, A. S. N.; Bhargava, R.; Reddy, K. S. Flavin mononucleotide (FMN)-ethylenediaminetetraacetic acid (EDTA) photogalvanic cell. *International Journal of Energy Research* **1982,** *6* (4), 389.

(48) Heelis, P. F.; Parsons, B. J.; Phillips, G. O.; McKellar, J. F. The photoreduction of flavins by amino acids and EDTA. A continuous and flash photolysis study. *Photochemistry and Photobiology* **1979,** *30* (3), 343.

(49) Mukherjee T., McCulloch. K. M., Ealick S. E., Begley. T. P. Cofactor catabolism. *Comprehensive Natural Products II* Elsevier, Oxford., 2010.

(50) Sikowitz, M. D.; Shome, B.; Zhang, Y.; Begley, T. P.; Ealick, S. E. Structure of a Clostridium botulinum C143S thiaminase I/thiamin complex reveals active site architecture. *Biochemistry* **2013,** *52* (44), 7830.

(51) Mueller, I. B.; Bergmann, B.; Groves, M. R.; Couto, I.; Amaral, L.; Begley, T. P.; Walter, R. D.; Wrenger, C. The vitamin B1 metabolism of Staphylococcus aureus is controlled at enzymatic and transcriptional levels. *PLoS One* **2009,** *4* (11), e7656.

(52) Kincaid, V. A.; Sullivan, E. D.; Klein, R. D.; Noel, J. W.; Rowlett, R. S.; Snider, M. J. Structure and catalytic mechanism of nicotinate (vitamin B3) degradative enzyme maleamate amidohydrolase from Bordetella bronchiseptica RB50. *Biochemistry* **2012,** *51* (1), 545.

(53) Begley, T. P. The biosynthesis and degradation of thiamin (vitamin B1). *Natural Product Reports* **1996,** *13* (3), 177.

(54) Neal, R. A. Bacterial metabolism of thiamine. II. The isolation and characterization of 3-(2'-methyl-4'-amino-5'-pyrimidylmethyl)-4-methylthiazole-5-acetic acid (thiamine acetic acid) as an intermediate in the oxidation of thiamine. *The Journal of Biological Chemistry* **1969,** *244* (19), 5201.

(55) Neal, R. A. Bacterial metabolism of thiamine. 3. Metabolism of thiamine to 3-(2'-methyl-4'-amino-5'-pyrimidylmethyl)-4-methyl-thiazole-5-acetic acid (thiamine acetic acid) by a flavoprotein isolated from a soil microorganism. *The Journal of Biological Chemistry* **1970,** *245* (10), 2599.

(56) Foster, J. W. Microbiological Aspects of Riboflavin: III. Oxidation studies with Pseudomonas riboflavina. *Journal of Bacteriology* **1944,** *48* (1), 97.

(57) Yang, C. S.; McCormick, D. B. In *Methods in Enzymology*; Academic Press, 1971; Vol. Volume 18, Part B.

(58) Kieser, T.; Bibb, M. J.; Buttner, M. J.; Chater, K. F.; Hopwood, D. A. Practical Streptomyces genetics; *The John Innes Foundation: Norwich*, 2000.

(59) Cheng, L.; Chen, W.; Zhai, L.; Xu, D.; Huang, T.; Lin, S.; Zhou, X.; Deng, Z. Identification of the gene cluster involved in muraymycin biosynthesis from Streptomyces sp. NRRL 30471. *Molecular BioSystems* **2011,** *7* (3), 920.

(60) Luzhetskii, A. N.; Ostash, B. E.; Fedorenko, V. A. [Interspecies conjugation of Escherichia coli-Streptomyces globisporus 1912 using integrative plasmid pSET152 and its derivatives]. *Genetika* **2001,** *37* (10), 1340.

(61) Weisburg, W. G.; Barns, S. M.; Pelletier, D. A.; Lane, D. J. 16S ribosomal DNA amplification for phylogenetic study. *J. Bacteriol* **1991,** *173* (2), 697.

(62) Marchena, M.; Gil, M.; Martin, C.; Organero, J. A.; Sanchez, F.; Douhal, A. Stability and photodynamics of lumichrome structures in water at different pHs and in chemical and biological caging media. *The Journal of Physical Chemistry. B* **2011,** *115* (10), 2424.

(63) Mazodier, P.; Petter, R.; Thompson, C. Intergeneric conjugation between Escherichia coli and Streptomyces species. *Journal of Bacteriology* **1989,** *171* (6), 3583.

(64) Yamamoto, K.; Asano, Y. Efficient production of lumichrome by Microbacterium sp. strain TPU 3598. *Applied and Environmental Microbiology* **2015,** *81* (21), 7360.

(65) Rajamani, S.; Bauer, W. D.; Robinson, J. B.; Farrow, J. M., 3rd; Pesci, E. C.; Teplitski, M.; Gao, M.; Sayre, R. T.; Phillips, D. A. The vitamin riboflavin and its derivative lumichrome activate the LasR bacterial quorum-sensing receptor. *Molecular Plant-Microbe Interactions : MPMI* **2008,** *21* (9), 1184.

(66) Phillips, D. A.; Joseph, C. M.; Yang, G.-P.; Martínez-Romero, E.; Sanborn, J. R.; Volpin, H. Identification of lumichrome as a Sinorhizobium enhancer of alfalfa root respiration and shoot growth. *Proceedings of the National Academy of Sciences of the United States of America* **1999,** *96* (22), 12275.

(67) Walsh, C. Naturally occurring 5-deazaflavin coenzymes: biological redox roles. *Accounts of Chemical Research* **1986,** *19* (7), 216.

(68) Miliszkiewicz, N.; Walas, S.; Tobiasz, A. Current approaches to calibration of LA-ICP-MS analysis. *Journal of Analytical Atomic Spectrometry* **2015,** *30* (2), 327.

(69) Murahashi, S.-I.; Zhang, D.; Iida, H.; Miyawaki, T.; Uenaka, M.; Murano, K.; Meguro, K. Flavin-catalyzed aerobic oxidation of sulfides and thiols with formic acid/triethylamine. *Chemical Communications* **2014,** *50* (71), 10295.

(70) Karasulu, B.; Thiel, W. Photoinduced intramolecular charge transfer in an electronically modified flavin derivative: roseoflavin. *J Phys Chem B* **2015,** *119* (3), 928.

(71) Muller, F. A two-step chemical synthesis of lumiflavin. *Methods in Enzymology* **1980,** *66*, 265.

(72) Bender, D. A. Nutritional Biochemistry of the Vitamins; *Cambridge University Press*, 2003.

(73) Kuppusamy, P.; Zweier, J. L. Characterization of free radical generation by xanthine oxidase. Evidence for hydroxyl radical generation. *The Journal of Biological Chemistry* **1989,** *264* (17), 9880.

(74) Muller, P.; Ahmad, M. Light-activated cryptochrome reacts with molecular oxygen to form a flavin-superoxide radical pair consistent with magnetoreception. *The Journal of Biological Chemistry* **2011,** *286* (24), 21033.

(75) Fetzner, S.; Steiner, R. A. Cofactor-independent oxidases and oxygenases. *Applied Microbiology and Biotechnology* **2010,** *86* (3), 791.

(76) Rauckman, E. J.; Rosen, G. M.; Kitchell, B. B. Superoxide radical as an intermediate in the oxidation of hydroxylamines by mixed function amine oxidase. *Molecular Pharmacology* **1979,** *15* (1), 131.

(77) Fukuto, J. M.; Di Stefano, E. W.; Burstyn, J. N.; Valentine, J. S.; Cho, A. K. Mechanism of oxidation of N-hydroxyphentermine by superoxide. *Biochemistry* **1985,** *24* (15), 4161.

(78) Remucal, C. K.; McNeill, K. Photosensitized amino acid degradation in the presence of riboflavin and its derivatives. *Environmental Science & Technology* **2011,** *45* (12), 5230.

(79) Segura-Aguilar, J. A new direct method for determining superoxide dismutase activity by measuring hydrogen peroxide formation. *Chemico-Biological Interactions* **1993,** *86* (1), 69.

(80) Benov, L. How superoxide radical damages the cell. *Protoplasma 217* (1), 33.

(81) Sheng, Y.; Abreu, I. A.; Cabelli, D. E.; Maroney, M. J.; Miller, A.-F.; Teixeira, M.; Valentine, J. S. Superoxide Dismutases and Superoxide Reductases. *Chemical Reviews* **2014,** *114* (7), 3854.

(82) Escobar, L.; Salvador, C.; Contreras, M.; Escamilla, J. E. On the application of the Clark oxygen electrode to the study of enzyme kinetics in apolar solvents: the catalase reaction. *Analytical Biochemistry* **1990,** *184* (1), 139.

(83) Zhang, R.-g.; Andersson, C. E.; Savchenko, A.; Skarina, T.; Evdokimova, E.; Beasley, S.; Arrowsmith, C. H.; Edwards, A. M.; Joachimiak, A.; Mowbray, S. L. Structure of Escherichia coli ribose-5-phosphate isomerase: A ubiquitous enzyme of the pentose phosphate pathway and the calvin cycle. *Structure (London, England : 1993)* **2003,** *11* (1), 31.

(84) Teufel, R.; Miyanaga, A.; Michaudel, Q.; Stull, F.; Louie, G.; Noel, J. P.; Baran, P. S.; Palfey, B.; Moore, B. S. Flavin-mediated dual oxidation controls an enzymatic Favorskii-type rearrangement. *Nature* **2013,** *503* (7477), 552.

(85) Teufel, R.; Stull, F.; Meehan, M. J.; Michaudel, Q.; Dorrestein, P. C.; Palfey, B.; Moore, B. S. Biochemical establishment and characterization of EncM's flavin-N5-oxide Cofactor. *Journal of the American Chemical Society* **2015,** *137* (25), 8078.

(86) Adak, S.; Begley, T. P. dibenzothiophene catabolism proceeds via a flavin-N5-oxide intermediate. *Journal of the American Chemical Society* **2016**, DOI:10.1021/jacs.6b00583 10.1021/jacs.6b00583.

(87) Li, L.; Liu, X.; Yang, W.; Xu, F.; Wang, W.; Feng, L.; Bartlam, M.; Wang, L.; Rao, Z. Crystal structure of long-chain alkane monooxygenase (LadA) in complex with coenzyme FMN: unveiling the long-chain alkane hydroxylase. *Journal of Molecular Biology* **2008,** *376* (2), 453.

APPENDIX

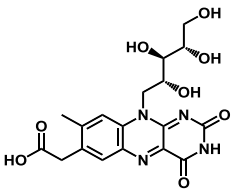

7α-carboxymethylriboflavin
10

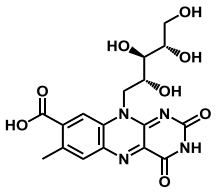

8α-carboxymethylriboflavin
11

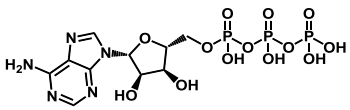

Adenosine triphosphate
21

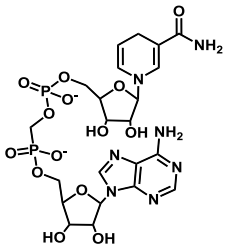

NADH
22

dithionite
44

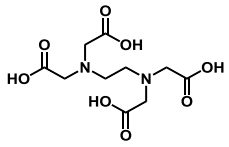

EDTA
45

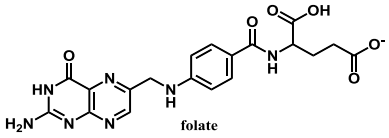

folate
60

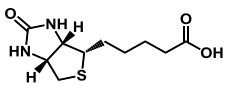

biotin
61

pentafluorobenzylhydroxylamine
65

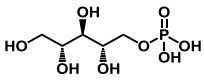

ribitol phosphate
70

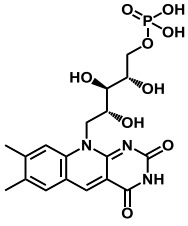

5-deazaFMN
72

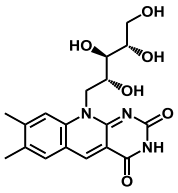

5-deazariboflavin
73

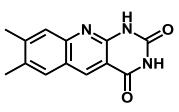

deazalumichrome
74

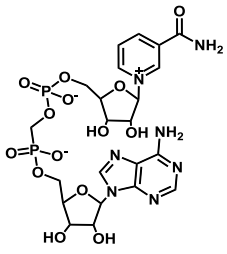

NAD+
75

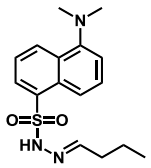

(*E*)-*N*'-butylidene-ansylhydrazide

120

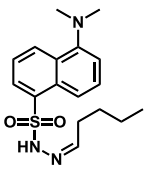

(*Z*)-*N*'-butylidene-dansylhydrazide

120

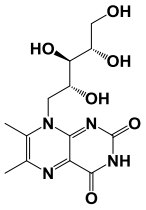

6,7-Dimethyl-8-ribityllumazine

136

Appendix A: Structures of the analogs and their derivatives for flavin and the sugar chain

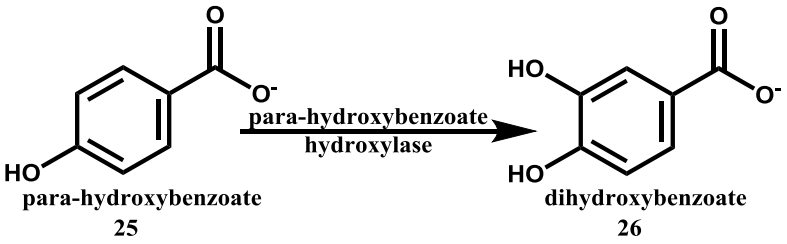

para-hydroxybenzoate
25

dihydroxybenzoate
26

Appendix B: Reaction catalyzed by para-hydroxybenzoate hydroxylase

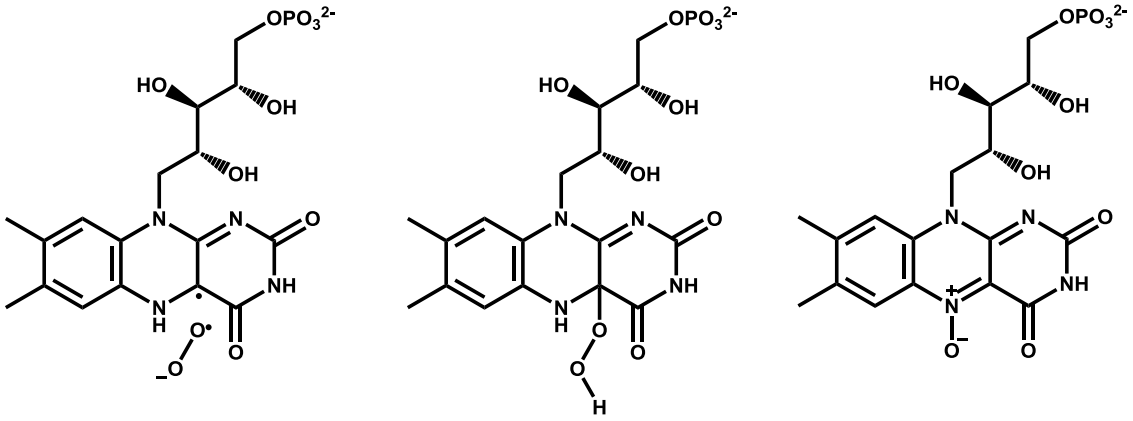

flavin semiquinone-superoxide anion radical pair

$C_4\alpha$-(hydro)peroxyflavin
27

flavin-N_5-oxide
28

Appendix C: Active flavin oxygenating species

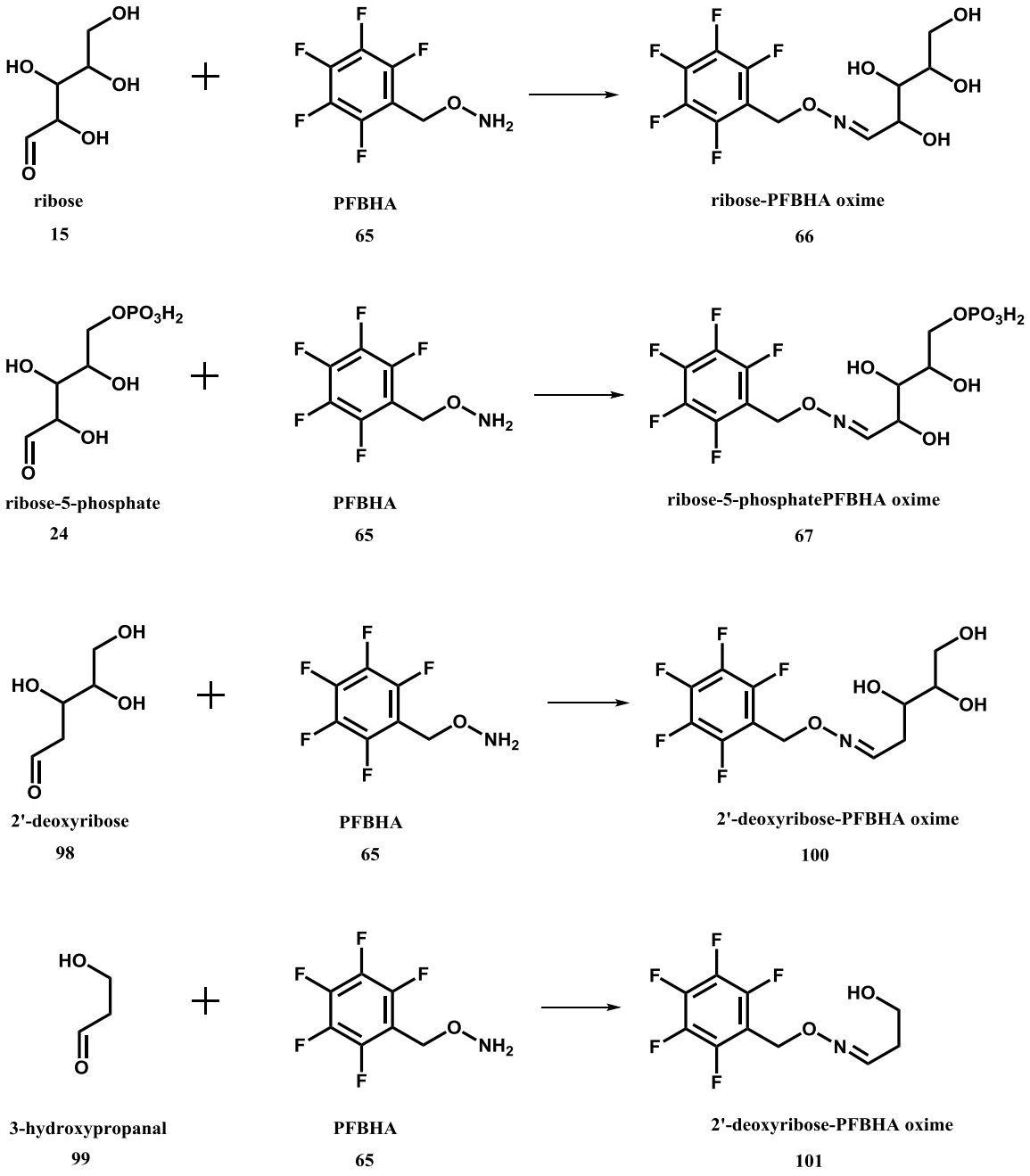

Appendix D: Formation of the corresponding oximes for different flavin substrates after treatment with PFBHA

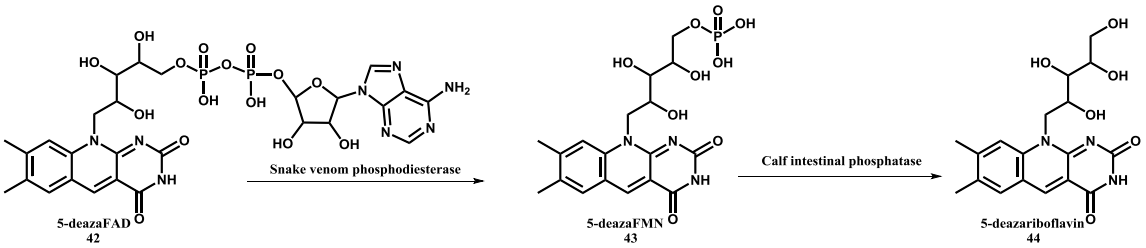

Appendix E: Synthesis of 5-deazaFMN **(72)** and 5-deazariboflavin **(73)** from 5-deazaFAD **(71)**

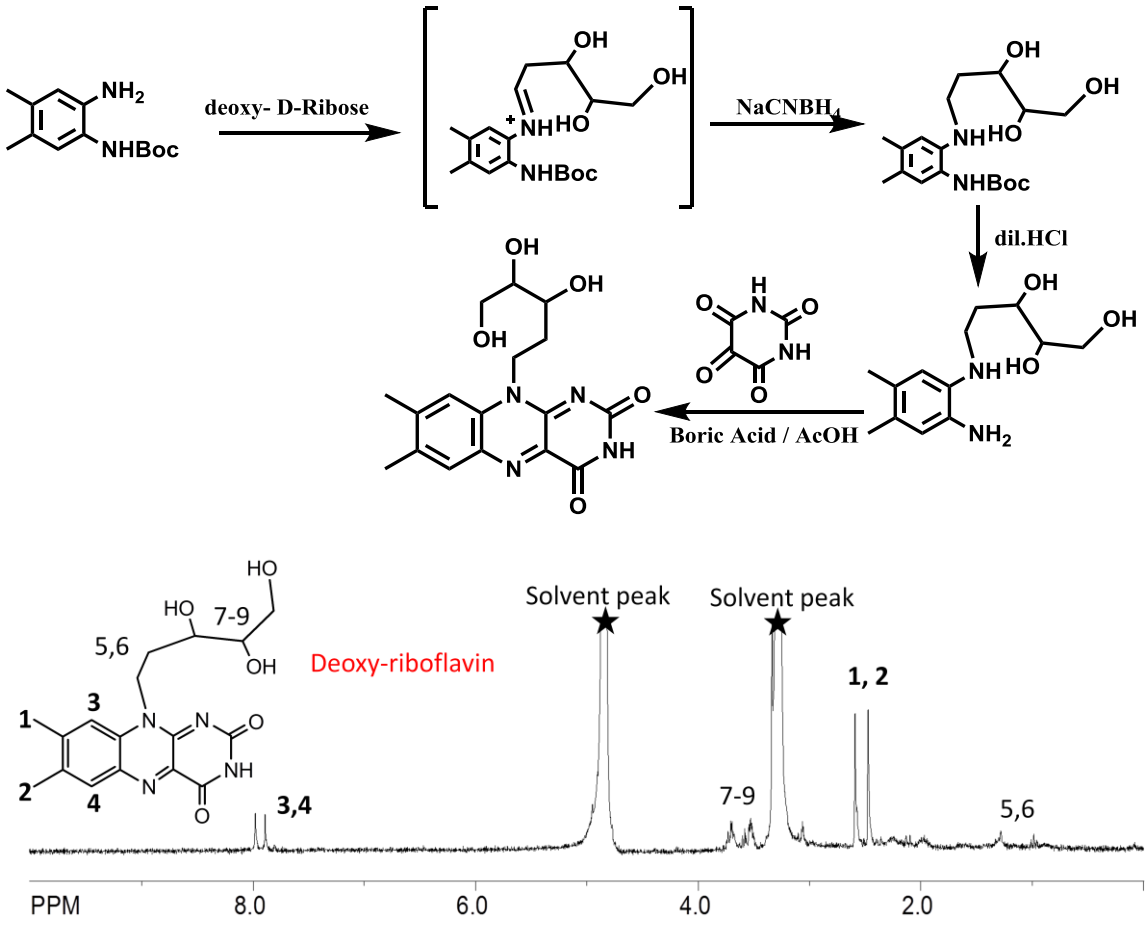

Appendix F: Scheme for the synthesis of 2'-deoxyriboflavin **(84)** and its NMR characterization

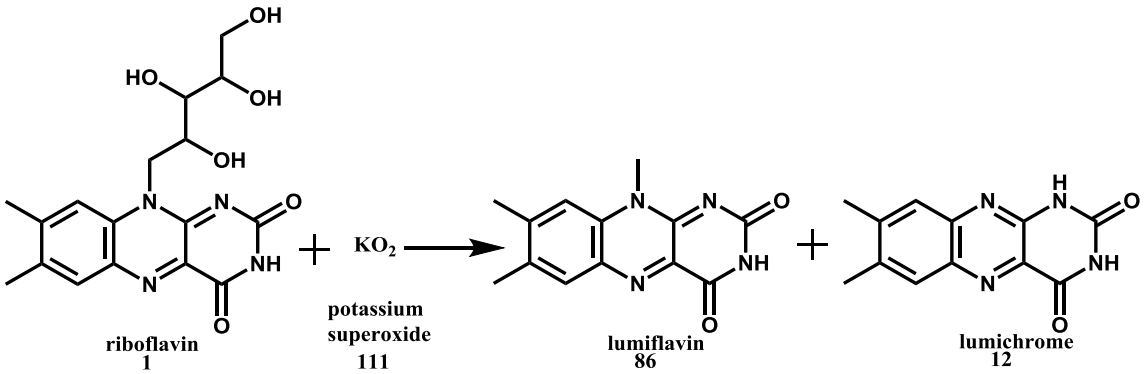

Appendix G: Scheme for the chemical degradation of riboflavin **(1)** with potassium superoxide **(111)**

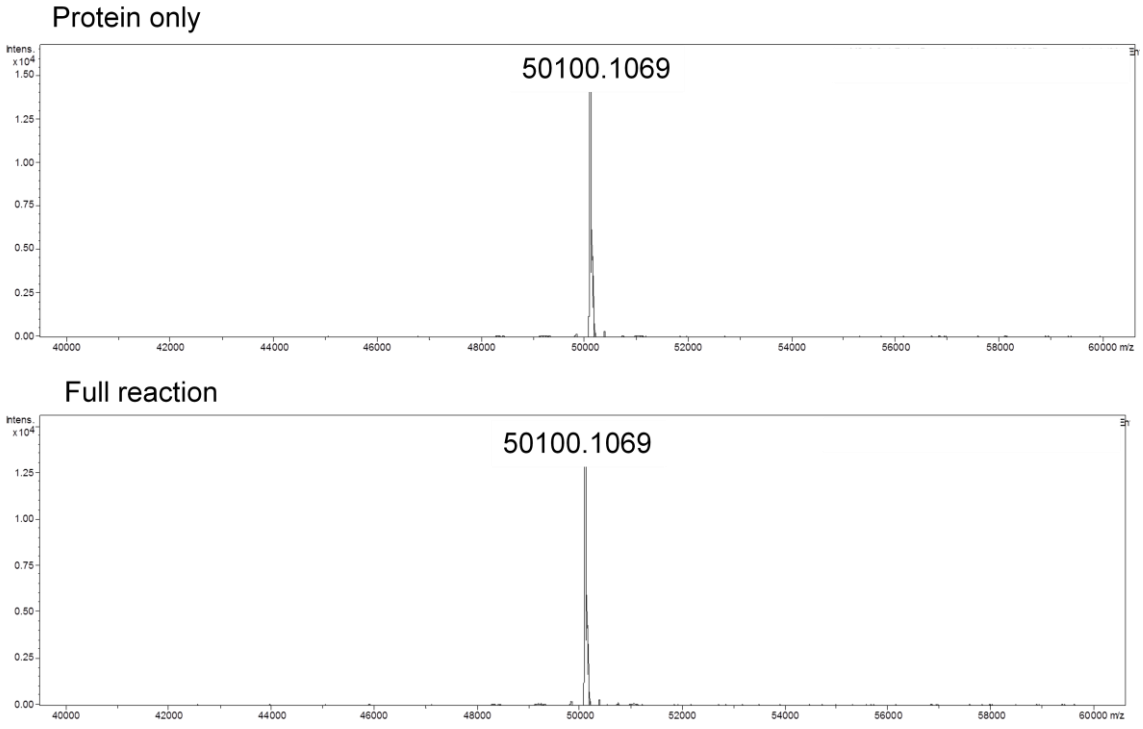

Appendix H: Whole protein mass spectroscopy of RcaE as is and RcaE after reaction with cyclopropylflavin **(115).** No change in mass is observed

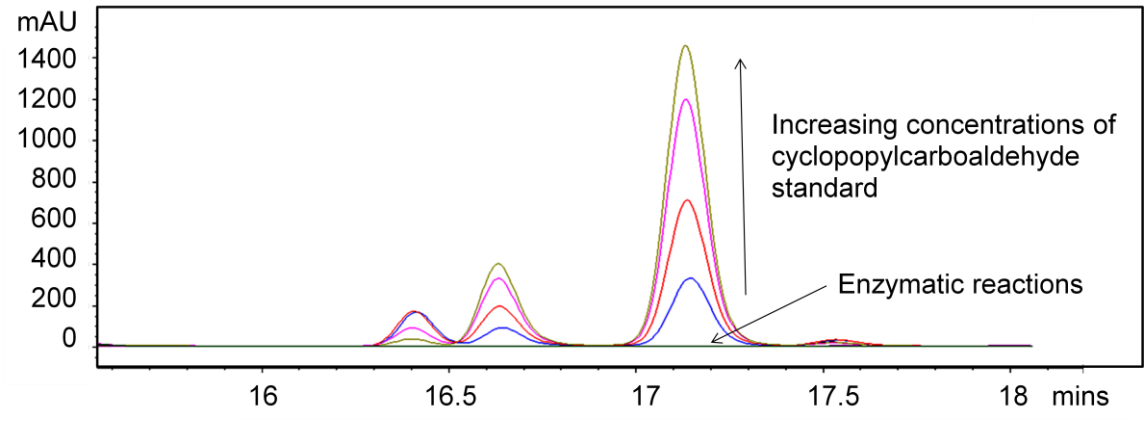

Appendix I: Cyclopropylmethylene-dansylhydrazone **80** not detected in the reaction of RcaE with cyclopropylmethylflavin **(115)**.

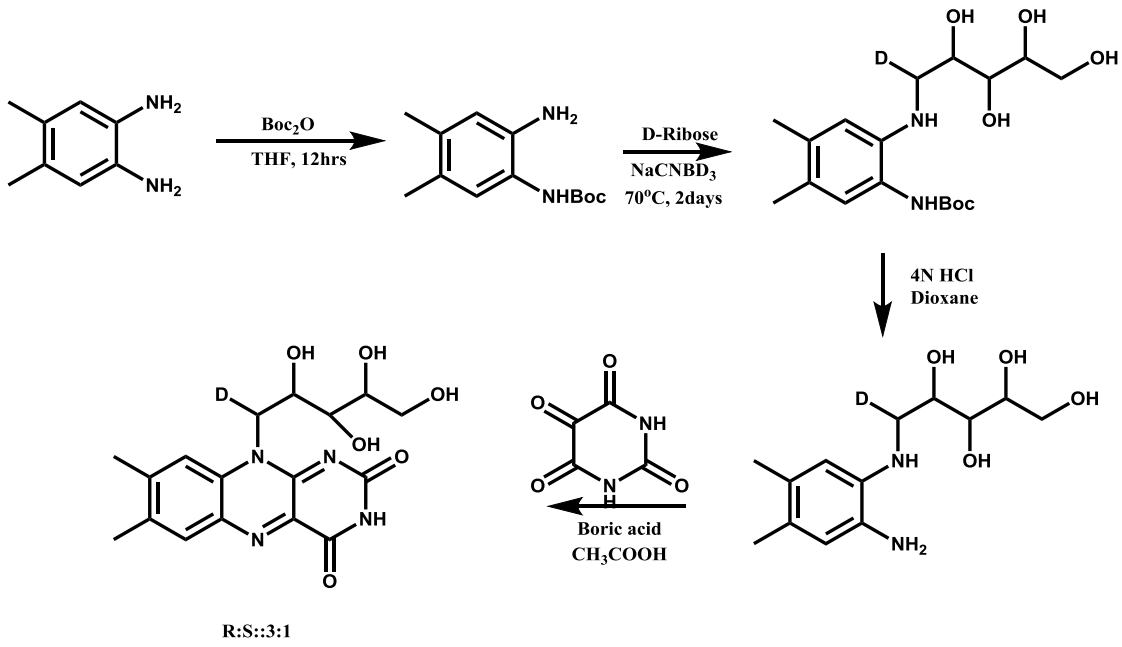

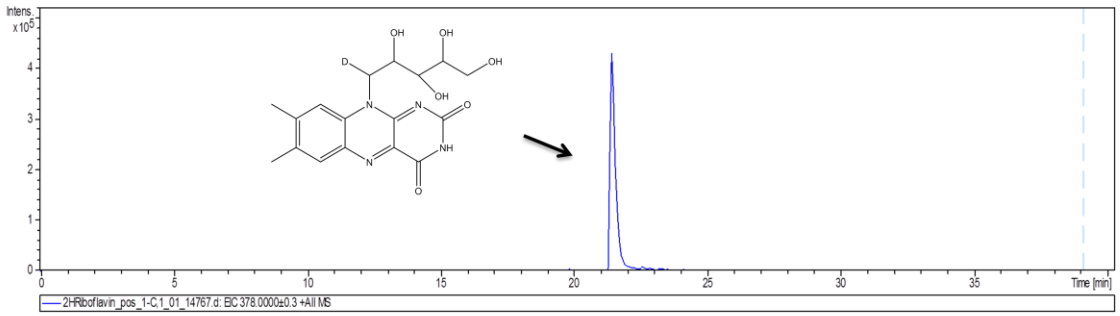

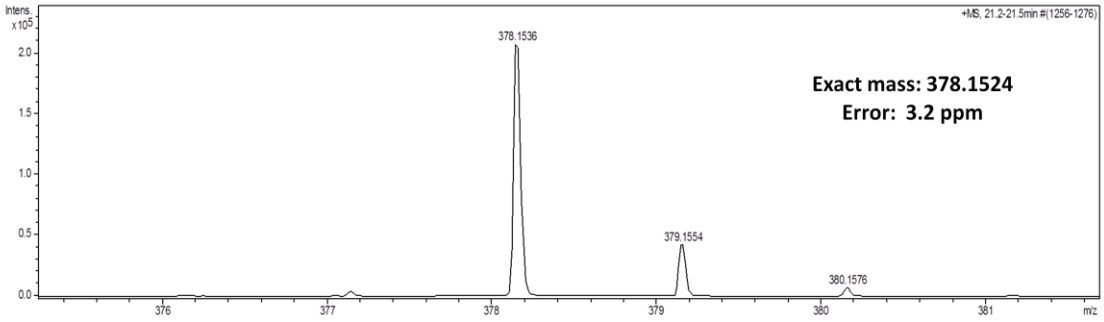

Appendix J: Scheme for the synthesis of 3 : 1 (R : S) 1'-D-riboflavin **(84)** and its LCMS characterization

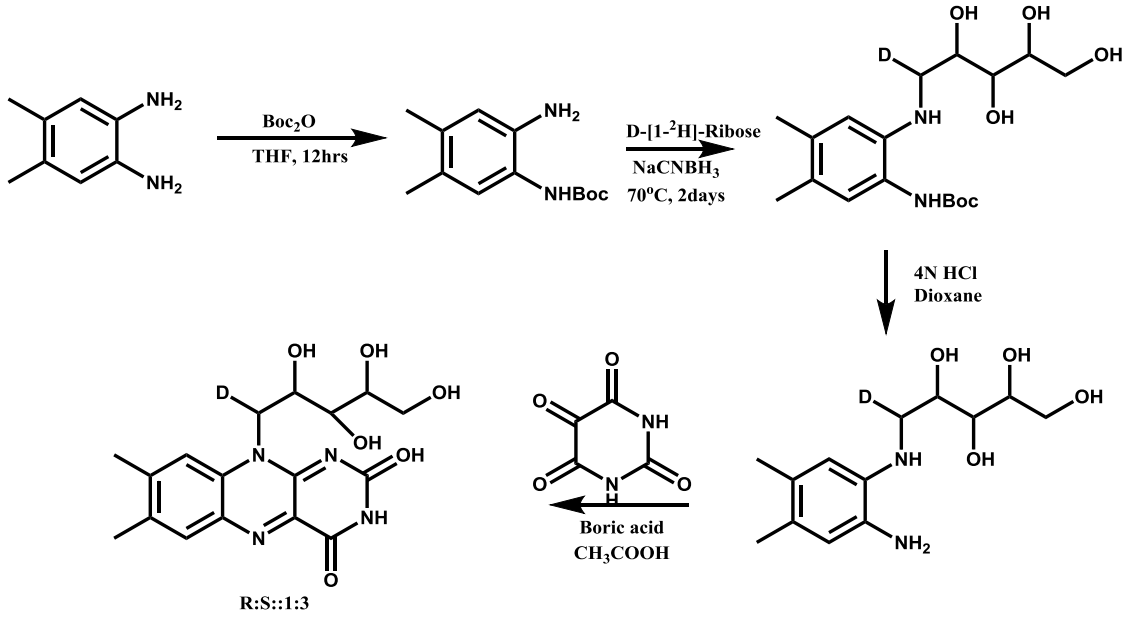

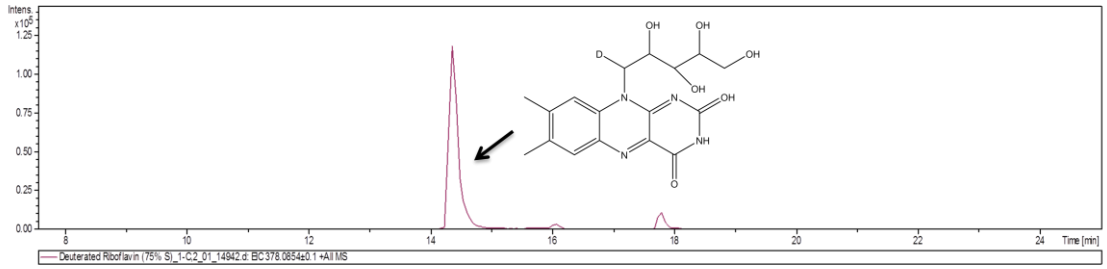

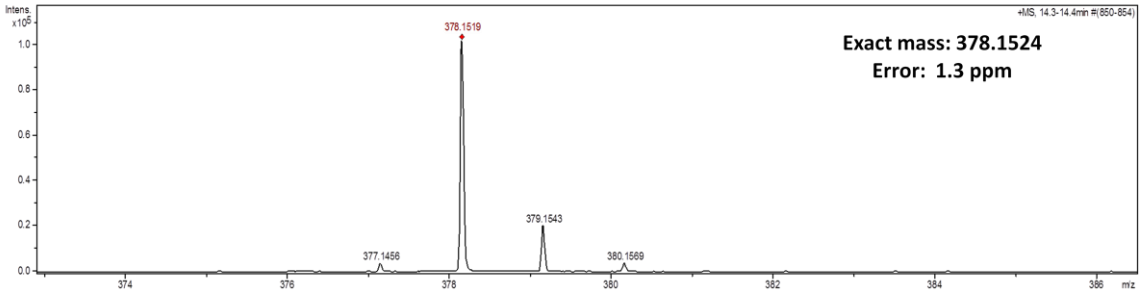

Appendix K: Scheme for the synthesis of 1 : 3 (R : S) 1'-D-riboflavin **(84)** and its LCMS characterization